

**Using Vehicle Dynamics Simulation and Meta-models to
Understand Factors and Mechanisms Affecting Roll Angle:
An Initial Assessment**

Report: ATLAS-2018-22

Akram Abu-Odeh

Melissa Marisol Martinez

Tristan Fletcher

Lindsay Harris

Maysam Kiani

Texas A&M Transportation Institute



**University of Michigan
2901 Baxter Rd. Room 124
Ann Arbor, MI 48109-2150**

**Texas A&M University
Texas A&M Transportation Institute
College Station, TX 77843-3135**

July 2018

DISCLAIMER

The contents of this report reflect the views of the authors, who are responsible for the facts and the accuracy of the information presented herein. This document is disseminated under the sponsorship of the U.S. Department of Transportation's University Transportation Centers Program, in the interest of information exchange. The U.S. Government assumes no liability for the contents or use thereof.

ACKNOWLEDGMENT

This research project was supported by the Center for Advancing Transportation Leadership and Safety (ATLAS Center). The ATLAS Center is supported by a grant from the U.S. Department of Transportation, Office of the Assistant Secretary for Research and Transportation, University Transportation Centers Program (DTRT13-G-UTC54). The ATLAS Center is a collaboration between the University of Michigan Transportation Research Institute (UMTRI) and the Texas A&M Transportation Institute (TTI). The authors acknowledge the computational support provided by the Texas A&M High Performance Research Computing (HPRC) (<http://hprc.tamu.edu/>). The authors appreciate the HPRC facility assistance. The researchers appreciate the support of Mechanical Simulation for providing CarSim and Livermore Software Technology Corporation (LSTC) for providing LS-DYNA and LS-OPT.

1. Report No. ATLAS-602761-00022-1		2. Government Accession No.		3. Recipient's Catalog No.	
4. Title and Subtitle Using Vehicle Dynamics Simulation and Meta-models to Understand Factors and Mechanisms Affecting Roll Angle: An Initial Assessment				5. Report Date July 2018	
				6. Performing Organization Code	
7. Author(s) Akram Abu-Odeh, Melissa Martinez, Lindsay Harris, Maysam Kiani				8. Performing Organization Report No.	
9. Performing Organization Name and Address Texas A&M Transportation Institute Texas A&M REELLIS Campus 3100 State Highway 47, Bldg. 7091 Bryan, TX 77807				10. Work Unit no. (TRAIS)	
				11. Contract or Grant No. DTRT13-G-UTC54	
12. Sponsoring Agency Name and Address Advancing Transportation Leadership and Safety (ATLAS) Center 2901 Baxter Rd., Room 124, Ann Arbor, MI 48109-2150 USA				13. Type of Report and Period Covered	
				14. Sponsoring Agency Code	
15. Supplementary Notes Supported by a grant from the U.S. Department of Transportation, OST-R, University Transportation Centers Program					
16. Abstract A rollover is defined as any vehicle rotation of 90 degrees or more about any true longitudinal or lateral axis, according to NASS CDS. Rollover crashes are still represented highly in terms of frequency and fatalities among other crash categories. Even though there are various vehicular technical innovations that act as a preventative or protective improvement, rollover crashes and subsequent loss of life and injuries are still highly represented in crash statistics. In 2015, rollovers represented 33 percent of occupant fatalities. Existing research on rollover as it relates to highway safety is often based on crash data analysis. Limited studies have investigated the initiating mechanisms contributing to vehicular propensity to rollover. Hence, there is a gap in knowledge to understand initiation factors that affect rollover events. Vehicle dynamics simulations (not crash data) were utilized to create several vehicle rollover crashes. Using vehicle models from the vehicle dynamics code (CarSim), several vehicle rollover crashes were created. A second aspect of this research is to develop a meta-model of vehicle roll angle as a function of initiation/influencing factors. Monte Carlo analyses was performed on the response surface generated. The surface meta-model, accuracy model, and global sensitivities were analyzed. These models showed that for both vehicles, speed had the greatest influence on the vehicle's propensity to rollover. Encroachment angle had the second largest influence for both vehicles.					
17. Key Words Rollover, Data Analytics, Meta-models, Vehicle Dynamics Simulations				18. Distribution Statement Unlimited	
19. Security Classification (of this report) Unclassified		20. Security Classification (of this page) Unclassified		21. No. of Pages 90	22. Price

TABLE OF CONTENTS

	Page
List of Figures	vi
List of Tables	viii
Chapter 1: Background and Objective	1
Background.....	1
Research Objective	5
Chapter 2: Literature Review	7
Fundamentals of Vehicle Dynamics	7
Rotational Systems.....	11
Driver Behavior	15
Vehicle Dynamics Code	16
Data Analytics.....	17
NCHRP 16-05 Guidelines for Cost-Effective Safety Treatment of Roadside Ditches	18
Vehicle Dynamics Simulations.....	20
NCHRP 17-22 Identification of Vehicular Impact Conditions Associated with Serious Ran-Off-Road Crashes.....	21
Chapter 3: Approach and Methods	23
Approach.....	23
Vehicle Dynamics Simulations.....	23
Data Analytics—Methods.....	23
Chapter 4: Results and Discussion	33
Results.....	33
Vehicle Dynamics Simulations.....	33
Data Analytics.....	38
Discussion.....	39
Meta-modeling (Response Surface).....	41
Monte Carlo Simulation.....	42
Chapter 5: Verification and Comparison of Vehicle Dynamics Simulations Using Finite Element Analysis	51
Vehicle, Terrain, and Interactions.....	51
Computational Time and Accuracy	52
Chapter 6: Conclusions and Recommendations	69
References	73
Supplemental Sources Consulted.....	74
Appendix: Meta-models Cases	77

LIST OF FIGURES

	Page
Figure 1. SAE vehicle axis system.	9
Figure 2. Arbitrary forces acting on a vehicle.	11
Figure 3. Forces acting to roll a vehicle.	13
Figure 4. CarSim simulation flowchart.	24
Figure 5. CarSim Run Control screen.	25
Figure 6. CarSim Procedures screen.	26
Figure 7. Class C hatchback.	26
Figure 8. Full-size SUV.	27
Figure 9. Full size pickup truck, 5.5 ft bed.	27
Figure 10. Class E sedan.	27
Figure 11. 621.79 m radius road with a 3:1 side-slope.	28
Figure 12. Straight road with a 3:1 side-slope.	28
Figure 13. Road profile of the 3:1 side-slope.	29
Figure 14. Road Profile of 4:1 side-slope.	29
Figure 15. LS-OPT user interface.	30
Figure 16. Data analytics.	31
Figure 17. LS-OPT categories.	32
Figure 18. Response surface and global sensitivities for a full-size SUV.	40
Figure 19. Neural network.	41
Figure 20. Data analytics.	43
Figure 21. Maximum roll angle response surface as a function of the encroachment angle and friction coefficient.	45
Figure 22. Lateral vehicular travel response surface as a function of encroachment angle and friction coefficient.	46
Figure 23. Quality of maximum roll angle response surface.	47
Figure 24. Quality of the lateral travel response surface.	48
Figure 25. ANOVA bars for maximum roll angle.	49
Figure 26. ANOVA value with 100(1-alpha)% confidence level.	49
Figure 27. Sensitivity of the response on the design variables and encroachment conditions.	50
Figure 28. Comparisons of two codes, CarSim and LS-DYNA, in simulating vehicle encroachment events on slope (a) pickup truck encroachment and (b) passenger car encroachment.	53
Figure 29. Pickup truck encroaching at a 15° angle at a speed of 110 km/h (CarSim).	55
Figure 30. Pickup truck encroaching at a 15° angle at a speed of 110 km/h (FEA).	55
Figure 31. Roll angle results—Case 1 (CarSim).	56
Figure 32. Roll angle results—Case 1 (FEA).	56
Figure 33. Lateral displacement—Case 1 (CarSim).	57
Figure 34. Lateral displacement—Case 1 (FEA).	57
Figure 35. Pickup truck encroaching at a 25° angle at a speed of 80 km/h.	58
Figure 36. Pickup truck encroaching at a 25° angle at a speed of 80 km/h.	59
Figure 37. Roll angle results—Case 2 (FEA).	59

Figure 38. Roll angle results—Case 2 (CarSim).	60
Figure 39. Lateral displacement—Case 2 (CarSim).	60
Figure 40. Lateral displacement—Case 2 (FEA).	61
Figure 41. Class C hatchback departing at a 15° encroachment angle at a speed of 110 km/h.	62
Figure 42. Toyota Yaris encroaching at a 15° angle at a speed of 110 km/h.	62
Figure 43. Roll angle results—Case 3 (CarSim).	63
Figure 44. Roll angle results—Case 3 (FEA).	63
Figure 45. Lateral displacement results—Case 3 (CarSim).	64
Figure 46. Lateral displacement results—Case 3 (FEA).	64
Figure 47. Class C hatchback encroaching at a 25° angle at a speed of 120 km/h.	65
Figure 48. Toyota Yaris encroaching at a 25° angle at a speed of 120 km/h.	66
Figure 49. Roll angle results—Case 4 (Carsim).	66
Figure 50. Roll angle results—Case 4 (FEA).	67
Figure 51. Lateral displacement results—Case 4 (CarSim).	67
Figure 52. Lateral displacement results—Case 4 (FEA).	68
Figure 53. Data analytics: Recommended future work.	71

LIST OF TABLES

	Page
Table 1. Texas fatalities by crash type.....	1
Table 2. Passenger vehicle occupant deaths in rollover vs. no rollover crashes	1
Table 3. Passenger vehicle occupant deaths in single-vehicle rollover crashes, 1978-2015.....	2
Table 4. Deaths in single-vehicle rollover crashes as a percent of all occupant deaths, 2015.....	3
Table 5. Specified minimum design radius.....	5
Table 6. Center of gravity height (inches).	14
Table 7.	20
Table 8. Vehicle characteristics.	24
Table 9. Vehicle dynamics simulation matrix.	29
Table 10. Summary of vehicle dynamics simulations.	34
Table 11. Summary of vehicle dynamics simulations: Driver perception reaction time.....	35
Table 12. General trends.	38
Table 13. Design variables for data analytics.	39
Table 14. Range of variables.	44
Table 15. Summary of simulation cases used in FEA.	54

CHAPTER 1: BACKGROUND AND OBJECTIVE

BACKGROUND

The rollover crash is one of the most fatal forms of crashes among passenger vehicles. These account for one third of all occupant fatalities in 2015. Table 1 summarizes crash data from 2012 to 2016 for the state of Texas.

Table 1. Texas fatalities by crash type.

Crash Type	2012	2013	2014	2015	2016
Total fatalities (all crashes)*	3,408	3,389	3,536	3,582	3,776
Single vehicle	55%	54%	54%	52%	52%
Involving a large truck	17%	16%	16%	16%	15%
Involving speeding	37%	35%	36%	31%	28%
Involving a rollover	30%	30%	31%	27%	27%
Involving a roadway departure	53%	54%	54%	50%	49%
Involving an intersection (or intersection related)	19%	20%	19%	20%	19%

Table 2. Passenger vehicle occupant deaths in rollover vs. no rollover crashes

Year	Car Occupants				Pickup Occupants				SUV Occupants			
	Rollover		No Rollover		Rollover		No Rollover		Rollover		No Rollover	
	No.	%	No.	%	No.	%	No.	%	No.	%	No.	%
1997	5,143	22	18,019	78	2,479	42	3,443	58	1,516	63	900	37
1998	5,122	23	17,235	77	2,537	43	3,367	57	1,703	63	1,008	37
1999	5,174	23	16,945	77	2,699	44	3,396	56	1,901	63	1,118	37
2000	4,997	23	16,988	77	2,529	42	3,467	58	2,067	62	1,270	38
2001	5,028	23	16,576	77	2,636	43	3,485	57	2,159	61	1,362	39
2002	5,243	24	16,764	76	2,715	45	3,343	55	2,474	62	1,548	38
2003	4,916	23	16,137	77	2,509	43	3,324	57	2,658	60	1,805	40
2004	4,781	23	15,779	77	2,519	44	3,197	56	2,949	62	1,823	38
2005	4,830	24	15,062	76	2,773	46	3,267	54	2,909	60	1,938	40
2006	4,739	25	14,295	75	2,781	47	3,096	53	2,919	59	2,054	41
2007	4,400	25	13,363	75	2,660	46	3,098	54	2,929	59	2,046	41
2008	3,982	25	11,709	75	2,368	47	2,653	53	2,510	58	1,840	42
2009	3,509	25	10,593	75	2,246	48	2,473	52	2,388	56	1,866	44
2010	3,194	24	10,210	76	2,057	46	2,386	54	2,340	57	1,790	43
2011	3,058	24	9,653	76	1,973	46	2,272	54	2,259	55	1,836	45
2012	3,200	24	9,889	76	1,987	46	2,352	54	2,287	55	1,884	45
2013	2,984	23	9,720	77	1,916	45	2,299	55	2,057	50	2,041	50
2014	2,815	22	9,714	78	1,871	44	2,352	56	2,070	50	2,033	50
2015	2,965	23	10,192	77	1,909	43	2,558	57	2,203	48	2,342	52

Table 3. Passenger vehicle occupant deaths in single-vehicle rollover crashes, 1978-2015.

Year	Car Drivers	Pickup Drivers	SUV Drivers	All passenger Vehicle Drivers	All Passenger Vehicle Occupants
1997	2,818	1,469	754	5,178	7,712
1998	2,857	1,545	808	5,328	7,848
1999	2,866	1,667	999	5,644	8,255
2000	2,795	1,526	1,035	5,466	8,112
2001	2,836	1,651	1,063	5,654	8,375
2002	2,977	1,668	1,224	5,967	8,724
2003	2,755	1,595	1,331	5,789	8,462
2004	2,706	1,540	1,490	5,853	8,525
2005	2,761	1,711	1,478	6,074	8,730
2006	2,764	1,754	1,555	6,198	8,790
2007	2,634	1,683	1,516	5,934	8,429
2008	2,354	1,537	1,398	5,380	7,541
2009	2,101	1,478	1,273	4,913	6,868
2010	1,946	1,324	1,226	4,548	6,375
2011	1,848	1,297	1,218	4,430	6,148
2012	1,951	1,288	1,287	4,567	6,273
2013	1,805	1,219	1,112	4,181	5,825
2014	1,673	1,195	1,185	4,100	5,570
2015	1,775	1,202	1,205	4,243	5,766

Table 4. Deaths in single-vehicle rollover crashes as a percent of all occupant deaths, 2015.

		Drivers				All occupants			
		Single-Vehicle Rollover		All Crashes		Single-Vehicle Rollover		All Crashes	
		No.	%	No.	%	No.	%	No.	%
Cars	Mini	82	15	552	100	102	14	712	100
	Small	538	18	2,985	100	709	17	4,066	100
	Midsize	663	19	3,408	100	928	20	4,726	100
	Large	369	20	1,864	100	497	20	2,542	100
	Very large	100	16	626	100	146	15	989	100
	All cars	1,775	19	9,531	100	2,414	18	13,157	100
Pickups	Small	304	29	1,043	100	364	29	1,240	100
	Large	599	34	1,787	100	775	34	2,308	100
	Very large	253	44	569	100	330	44	748	100
	All pickups	1,202	34	3,523	100	1,532	34	4,467	100
SUVs	Small	246	29	855	100	322	29	1,122	100
	Midsize	648	40	1,633	100	934	40	2,354	100
	Large	226	45	504	100	340	44	766	100
	Very large	72	42	170	100	112	42	264	100
	All SUVs	1,205	38	3,192	100	1,724	38	4,545	100
All passenger vehicles	All	4,243	26	16,484	100	5,766	26	22,543	100

In 2015, there was a total of 32,166 fatal crashes in the United States. Of these 32,166 crashes, there was a total of 35,092 fatalities. Forty-eight percent of these crashes occurred in rural areas, 45 percent occurred in urban areas, and 8 percent of the crashes happened in unknown areas (1). Thirty-eight percent of rural crashes involved vehicle rollovers and 24 percent of crashes happened in urban areas. The percentage of fatalities in rollover crashes was highest for SUVs (36 percent), followed by pickup trucks (30 percent), vans (22 percent), and passenger cars (20 percent) (1). Fatal crashes have declined by 16.8 percent over the past decade, but have increased by 7 percent in the last year. Fatality rate per 100 million vehicle miles traveled was 2.6 times higher in rural areas than in urban areas. There is still a gap in knowledge to understand initiation factors that affect rollover events. Although much research has been done on the topic, there is still a gap in knowledge to understand initiation factors that

affect rollover events. Many factors contribute to a vehicle's roll angle. Vehicle type, vehicle center of gravity (CG), speed, roadway characteristics, and driving behaviors are just a few that influence roll angle.

The type of vehicle and its corresponding CG greatly influence the vehicle's propensity to rollover. A vehicle with a low CG is less likely to topple over as opposed to one with a higher CG.

The goal of roadside design is to limit if not eliminate serious injuries and fatalities associated with ran-off road crashes. Roadside geometrical design and safety features have a strong influence on the severity and frequency of crashes. To design optimum roadside geometrics and to determine which roadside safety features are adequate, it is vital to identify impact characteristics associated with serious injury and fatal crashes. It is important to have definitive data on whether there are real relationships between the selected test impact conditions and actual crashes involving serious injuries and fatalities. The safety performance of roadside features is evaluated primarily through full-scale crash testing. The purpose of this testing is to observe and evaluate the performance of safety features under impact conditions that are either similar or more severe than those associated with real world crashes resulting in serious injuries or fatalities. Even though full-scale crash test data provide a small window into the nature of ran-off-road crashes, it does not provide sufficient data to identify the impact conditions associated with serious injury and fatal crashes. The American Association of State Highway and Transportation Officials current policy states that shoulder slopes that drain away from the paved surface on the outside of a super-elevated horizontal curve should be designed to avoid too great a cross-slope break, calculated as the algebraic difference between the cross-slope of the traveled way and shoulder (2). To avoid large pavement/shoulder cross-slope breaks, it may be desirable that all or part of the shoulder be sloped upward at about the same or lesser that the super-elevated traveled way. The Roadside Design Guide (3) indicates the roadside should be rounded because it reduces the chances of an errant vehicle becoming airborne. This also affords the driver more control over the vehicle.

Side-slopes and ditches have been identified as the primary tripping mechanism in single vehicle ran-off-road (SVROR) rollovers (4). Side-slopes refer to the slopes of areas adjacent to the shoulder and located between the shoulder and the right-of-way line, according to the Texas Department of Transportation. A relatively flat area adjacent to the travel-way is desired so that

out-of-control vehicles are less likely to turn over, vault, or impact the side of a drainage channel. Steeper slope ratios (3:1) are negotiable by drivers. However, recovery on these steeper slopes is less likely. Where conditions are favorable, it is desirable to use flatter slopes to increase roadside safety. The front slope is the slope adjacent to the shoulder. The front slope should be 6:1 or flatter. Slope rates of 3:1 may be used in constrained conditions. Since recovery is less likely on 3:1 and 4:1 slopes, fixed objects should not be present near the toe of the slopes. The intersections of slope planes in the highway cross section should be well rounded for added safety, increased stability, and improved aesthetics.

Table 5. Specified minimum design radius.

Design Speed (mph)	Minimum Radius (m) for a Superelevation of		
	4%	6%	8%
30	250	231	214
50	926	833	758
60	1500	1330	1200
70	NA	2040	1810

Using the vehicle dynamics code, CarSim, several vehicle rollover scenarios were created to assess how roadway characteristics and driver inputs affect the vehicle's roll angle. Data from CarSim were the input into LS-OPT to create different meta-models. A meta-model is a model of a model. The meta-models were used to assess how different factors affect vehicle roll angle. A meta-model of vehicle roll angle as a function of speed, friction, curvature, encroachment angle, and ditch slope is to be developed as well.

RESEARCH OBJECTIVE

This research objectives are:

1. Enhancing our understanding of rollover propensity giving certain roadway designs, vehicle types, and maneuvers.
2. Using vehicle dynamics simulations (and not crash data) to create several vehicle rollover crashes.

CHAPTER 2: LITERATURE REVIEW

FUNDAMENTALS OF VEHICLE DYNAMICS

The first practical automobiles that were powered by gasoline engines came in 1886 by Karl Benz and Gottlieb Daimler. Over the following decade, automotive vehicles were developed by other pioneers with familiar names such as Henry Ford and Ransom Olds. By 1908, the automotive industry was well established in the United States of America with Henry Ford manufacturing the Model T. The General Motors Corporation was also founded around this time. By 1909, over 600 makes of American cars had been identified (5).

In the early 1900s, most of the engineering in the automotive industry went into invention and design that would yield faster, more comfortable, and more reliable vehicles. In general, motor vehicles achieved high speed capability well before good paved roads existed on which to use them. With higher speeds, the dynamics of vehicles assumed greater importance as an engineering concern. One of the first engineers to write on automotive dynamics was Frederick William Lanchester. Steering shimmy problems were prevalent at that time as well. The understanding of both turning behavior and the shimmy problems was hampered by a lack of knowledge about tire mechanics in these early years. In 1931, a test device was built, which could measure the necessary mechanical properties of the pneumatic tire for the understandings to be developed. Only then could engineers develop mechanistic explanations of the turning behavior of automobiles, which lays the groundwork for much of our understanding today. Engineers have achieved dramatic advancements in the technologies employed in automobiles from the Model T to the Taurus. More than ever, dynamics plays an important role in vehicle design and development.

A knowledge of the forces and moments generated by pneumatic rubber tires at the ground is essential to understanding highway vehicle dynamics. The motions accomplished in accelerating, braking, cornering, and ride is a response to forces imposed. The dominant forces acting on a vehicle to control performance are developed by the tire against the road. Therefore it becomes necessary to develop an intimate understanding of the behavior of tires, characterized by the forces and moments generated over the broad range of conditions over which they operate.

Understanding vehicle dynamics can be accomplished at two levels: the empirical and the analytical. The empirical understanding derives from trial and error by which one learns which factors influence vehicle performance, in which way, and under what conditions. However, the empirical method can often lead to failure. Without mechanistic understanding of how changes in vehicle design or properties affect performance, extrapolating past experience to new conditions may involve unknown factors, which may produce a new result, defying the prevailing rules of thumb. For this reason, engineers favor an analytical approach. The analytical approach attempts to describe the mechanics of interest based on the known laws of physics so that an analytical model can be established. In the more simple cases, the models can be represented by algebraic or differential equations that relate forces or motions of interest to control inputs and vehicle or tire properties. These equations then allow one to evaluate the role of each vehicle property. The existence of the model thereby provides a means to identify the important factors, the way in which they operate and under which conditions. The analytical methods also are not foolproof because they usually only approximate reality.

Before, many of the shortcomings of analytical methods were a consequence of the mathematical limitations in solving problems. Before computers, analysis was only considered successful if the problem could be reduced to a closed form solution. This limited the functionality of the analytical approach to solution of problems in vehicle dynamics. The existence of large numbers of components, systems, sub-systems, and nonlinearities in vehicles made comprehensive modeling virtually impossible, and the only utility obtained came from rather simplistic models of certain mechanical systems. The simplicity of the models can often constitute deficiencies that handicapped the engineering approach in vehicle development. Now, with the computational power available in desktop and mainframe computers, a major shortcoming of the analytical method has been overcome. It is now possible to assemble models for the behavior of individual components of a vehicle, allowing simulation and evaluation of its behavior before being rendered in hardware. These models can calculate performance that could not be solved for in the past. In cases where the engineer is uncertain of the importance of specific properties, those properties can be included in the model and their importance assessed by evaluating their influence on simulated behavior. This provides the engineer with a new tool as a means to test our understanding of a complex systems and investigate means of improving performance.

The subject of vehicle dynamics is concerned with the movements of vehicles on a road surface. The movements of interest are acceleration and braking, ride, and turning. Dynamic behavior is determined by the forces imposed on the vehicle from the tires, gravity, and aerodynamics. The vehicle and its components are studied to determine what forces will be produced by each of these sources at a particular maneuver and trim condition, and how the vehicle will respond to these forces. It is essential to establish an approach to modeling the systems and the conventions that will be used to describe motions.

A motor vehicle is made up of many components distributed within its exterior envelope. For many of the elementary analysis applied to it, all components move together. Under braking, the entire vehicle slows down as a unit. Thus, it can be represented as one lumped mass located at its CG. For acceleration, braking, and most turning analysis, one mass is sufficient. For single mass representation, the vehicle is treated as a mass concentrated at its CG as shown below. The point mass at the CG, with appropriate rotational moments of inertia, is dynamically equivalent to the vehicle itself for all motions in which it is reasonable to assume the vehicle to be rigid.

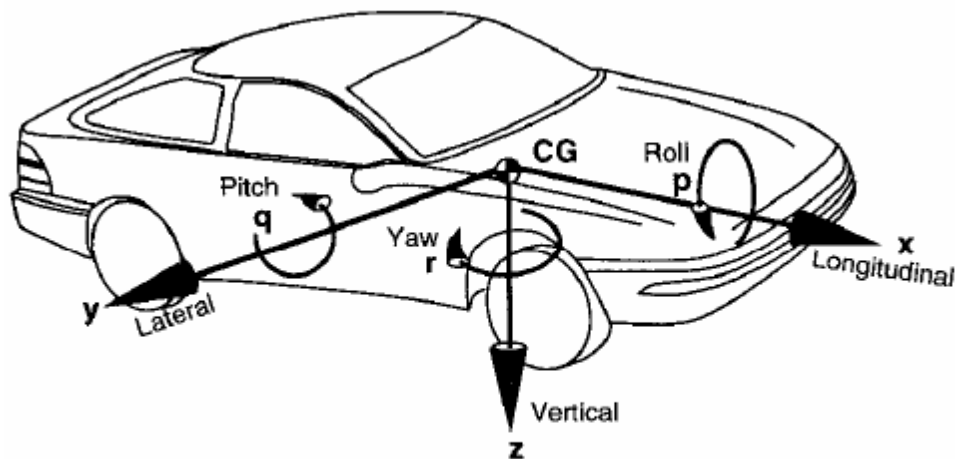


Figure 1. SAE vehicle axis system.

The vehicle motions are defined with reference to a right-hand orthogonal coordinate system, which originates at the CG and travels with the vehicle.

Where:

- X= forward and on the longitudinal plane of symmetry.
- Y= lateral out the right side of the vehicle.

- Z= downward with respect to the vehicle.
- P= roll velocity about the x-axis.
- Q= pitch velocity about the y-axis.
- R= yaw velocity about the z-axis.

Vehicle motion is usually described by the velocities for the vehicle fixed coordinate system, where the velocities are reference to the earth fixed coordinate system.

Vehicle attitude and trajectory through the course of a maneuver are defined with respect to a right-hand orthogonal axis system fixed on the earth. The coordinates are:

- X- forward travel.
- Y- travel to the right.
- Z- vertical travel (Positive downward).
- Ψ - heading angle (the angle between x and X in the ground).
- γ - Course angle (the angle between the vehicle's velocity vector and X-axis).
- β - sideslip angle (the angle between x-axis and the vehicle velocity vector).

Forces and moments are normally defined as they act on the vehicle. A positive force in the longitudinal direction on the vehicle is forward. The force corresponding to the load on the tire acts in the upward direction and is therefore negative in magnitude. The SAE J670e "vehicle dynamics terminology" gives the name normal force as that acting downward and the vertical force as the negative of the normal forces. Therefore, the vertical force is the equivalent of the tire load with a positive convention in the upward direction.

The fundamental law from which most vehicle dynamics analysis begin is the second law formulated by Sir Isaac Newton. The law applies to both translational and rotational systems.

Translational systems are the sum of the external forces acting on a body in a given direction is equal to the product of its mass and the acceleration in that direction (assuming the mass is fixed):

$$\sum F_x = M * a_x \quad [1]$$

Where:

- F_x = Forces in the x-direction.
- M = Mass of the body.
- A_x = Acceleration in the x-direction.

ROTATIONAL SYSTEMS

Rotational systems are the sum of the torques acting on a body about a given axis is equal to the product of its rotational moment of inertia and the rotational acceleration about that axis

$$\sum T_x = I_{xx} * \alpha_x \quad [2]$$

Where:

- T_{xx} = Torques about the x-axis.
- I_{xx} = Moment of inertia about the x-axis.
- α_x = Acceleration about the x-axis.

Determining the axle loading on a vehicle under arbitrary conditions is an application of Newton's Second Law.

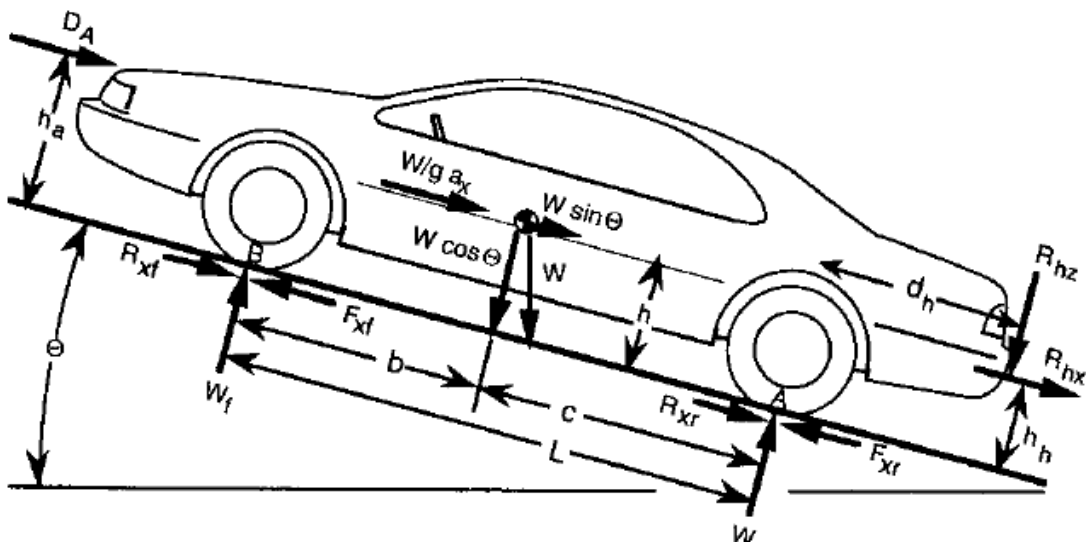


Figure 2. Arbitrary forces acting on a vehicle.

W is the weight of the vehicle acting at its CG with a magnitude equal to its mass times the acceleration of gravity. The weight of the vehicle would have two components on a sloped grade. If the vehicle is accelerating along the road, it is convenient to represent the effect by an equivalent inertial force known as a “d’Alembert force” acting at the CG opposite to the direction of the road. The tires will experience a force normal to the road representing the dynamic weights carried on the front and rear wheels. Tractive forces or rolling resistance forces may act in the ground plane in the tire contact patch. D_A is the aerodynamic force acting on the body of the vehicle. It may be represented as acting at a point above the ground indicated by the height or by a longitudinal force of the same magnitude in the ground with an associated moment equivalent to D_A times h_A .

The influence of grade on axle loads is also worth considering. Grade is defined as the rise over the run. The ratio is equal to the tangent of the grade angle. Common grades on interstate highways are limited to 4 percent wherever possible. Primary and secondary roads occasionally reach 10 to 12 percent grades.

Among the dynamic maneuvers a vehicle can experience, rollover is one of the most serious and threatening to the occupants. Rollover may be defined as any maneuver in which the vehicle rotates 90° or more about its longitudinal axis such that the body makes contact with the ground. Rollover may be precipitated from one or more combination of factors. It may occur on flat and level surfaces when the lateral accelerations on a vehicle reach a level beyond that which can be compensated by lateral weight shift on the tires. Cross-slope of the road surface may contribute along with disturbances to the lateral forces arising from curb impacts, soft ground, or other obstructions that may trip the vehicle. The vehicle rollover is one that involves a complex interaction of forces acting on and within the vehicle. The forces are influenced by the maneuver and roadway. This process has been investigated analytically and empirically using models that cover a range of complexities. The rollover process is most easily understood by starting with the fundamental mechanics involved in a quasi-static case and progressing to the more complex models.

The most rudimentary mechanics involved in rollovers can be seen by considering the balance of forces on a rigid vehicle in cornering. In a cornering maneuver, the lateral forces act in the ground plane to counterbalance the lateral acceleration acting at the CG of the vehicle. The

difference in the position at which these forces act creates a moment on the vehicle, which attempts to roll toward the outside of the turn.

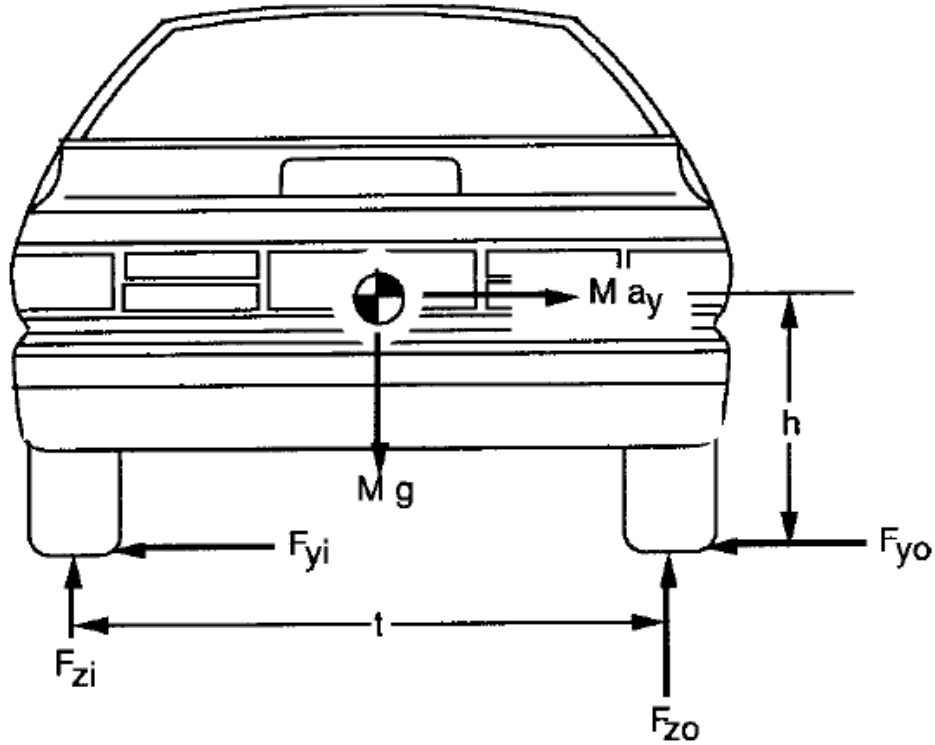


Figure 3. Forces acting to roll a vehicle.

Taking moments about the center of contact for the outside tires yields:

$$\frac{a_y}{g} = \frac{\frac{t}{2} + \phi h - \frac{F_{zi} t}{Mg}}{h} \quad [3]$$

On a level road, $\phi = 0$ with no lateral acceleration. In a highway design, cross-slope is used in curves exactly for this purpose. Given the radius of turn and an intended travel speed, the cross-slope will be chosen to produce a lateral acceleration in the range of 0 to 0.1 g's. As the lateral acceleration builds up, the load on the inside wheels must diminish. Through this process, the vehicle acts to resist or counterbalance the roll moment in cornering. The limit cornering condition will occur when the load on the inside wheels reaches zero. At that point, rollover will begin because the vehicle can no longer maintain equilibrium in the roll plane. The lateral acceleration at which rollover begins is the rollover threshold and is given by:

$$\frac{a_y}{g} = \frac{\frac{t}{2} + \phi h}{h} \quad [4]$$

With no cross-slope, the lateral acceleration that constitutes the rollover threshold is:

$$\frac{a_y}{g} = \frac{t}{2h} \quad [5]$$

This measure of rollover threshold is often used for a first-order estimate of a vehicle's resistance to rollover. The rollover threshold differs among the various types of vehicles on the road. Typical values fall in the following ranges.

Table 6. Center of gravity height (inches).

Vehicle Type	CG Height (Inches)	Tread (Inches)	Rollover Threshold (G)
Sports car	18–20	50–60	1.2–1.7
Compact car	20–23	50–60	1.1–1.5
Luxury car	20–24	60–65	1.2–1.6
Pickup truck	30–35	65–70	0.9–1.1
Passenger van	30–40	65–70	0.8–1.1
Medium truck	45–55	65–75	0.6–0.8
Heavy truck	60–85	70–72	0.4–1.6

The rigid-vehicle model suggests that the lateral acceleration necessary to reach the rollover of passenger cars and light trucks exceeds the cornering capabilities arising from the friction limits of the tires. It is possible for a car to spin out on a flat surface without rolling over. From this, one may conclude that rollover with these kinds of vehicles should be rare. However, accident statistics prove otherwise. This motivates a more in-depth analysis of the rollover phenomenon. In the case of heavy trucks, it is possible to reach the rollover threshold within the friction limits of the tires.

Rigid body rollover can be illustrated by plotting the lateral acceleration as a function of roll angle for the equilibrium of the vehicle. While at a zero roll angle, the lateral acceleration can be any value up to the rollover threshold. Once this threshold is reached, the inside wheel lifts. The vehicle then begins to roll and the equilibrium lateral acceleration decreases with angle because the CG is lifting and shifting toward the outside of the wheels. Consider a vehicle tipped on two wheels in a turn. The vehicle roll angle must be at the precise value on the above curve where the equilibrium lateral acceleration matches the actual in order to be in equilibrium. A

reduction of the equilibrium lateral acceleration can be caused by a slight disturbance that increases the roll angle. The excess lateral acceleration produces a roll acceleration that further increases that angle driving away from the equilibrium point. If this continues, the vehicle roll attitude accelerates rapidly to complete the rollover in a matter of a second or two.

It is appropriate to consider wheel lift-off as the beginning of rollover because of the inherent instability of the vehicle when the inside wheels leave the ground. However, it is possible for a driver to halt the action by quickly steering out of the turn, thereby reducing the lateral acceleration to a level that will return the vehicle to an upright position. A fast response is necessary because of the speed with which rollover proceeds. Rollover becomes irrecoverable only when the roll angle becomes so large that the CG of the vehicle passes outboard of the line of contact of the outside wheels. The limit corresponds to the point in the graph where the equilibrium lateral acceleration reaches zero. Stunt drivers can take a vehicle up to this point and drive on two wheels for extended distances despite the instability. But, it is a rare event for a typical motorist to avoid rollover if the vehicle should inadvertently roll to this position.

DRIVER BEHAVIOR

In 1977, the Society of Automotive Engineers conducted a study in which they observed a sedan traveling at 60 km/h faced with an emergency that is 1.3 seconds to collision. The severity of the emergency forced the driver to perform an emergency maneuver without braking. During the test, the drivers were told to avoid the emergency by performing a lane change through a 3.66 m lateral displacement. The common maximum steering angle of all the drivers was between 210° and 230° . Although the Society of Automotive Engineers' study was a useful reference, it did not provide guidance for the behavior of a driver returning to the travel lane. Braking was not applied during emergency avoidance situations (6).

With the use of a Computer Assisted Virtual Environment driving simulator, Kim et al. (7) recorded driver response to an emergency that is 1.3 seconds to collision. The driving simulator tested a sedan at 50 km/h driving behind a truck that suddenly stops. The simulation maneuver occurred on a straight urban road with a friction coefficient of 0.8. The braking was determined to be zero due to the severity of the emergency and the necessity for avoidance rather than stopping. This simulation scenario included data for the vehicle to return to the travel lane.

VEHICLE DYNAMICS CODE

Vehicle dynamics models serve a variety of purposes on simulations (8). A model must have sufficient complexity for the given application but should not be too complicated. In stability and handling simulations, various modes must be properly represented, including lateral/directional and longitudinal degrees of freedom. Limit performance effects of tire saturation that lead to plow out, spin out, and skidding require adequate tire force response models. Steering and braking subsystem characterization are necessary to represent important handling and stability requirements. A comprehensive set of vehicle dynamics model elements are:

- The basic inertial vehicle dynamics, including the interaction of sprung and unsprung masses and the wheel spin modes.
- A comprehensive tire model that includes lateral and longitudinal force response to normal load, slip, and camber.
- Power train including engine torque production and transmission and drive train components for transmitting the torque to the drive wheels.
- Steering system with power assist characteristics and compliance that produces understeer.
- Braking system including proportioning and antilock characteristics to minimize rear wheel lock up.
- Vehicle/road kinematics that compute vehicle position and orientation relative to the roadway and terrain.
- A driver or automatic controller for steering, throttle, and brake control.
- External forces and commands that produce system responses through vehicle motions and driver or automatic system control.

CarSim is a vehicle dynamics code that provides physical predictions of vehicle dynamical behavior in a form that can be used by most engineers and technical staff. It includes graphic user interface, database management, animation, and plotting.

DATA ANALYTICS

LS-OPT is a standalone design optimization and probabilistic analysis package that can be linked with several analyses programs or data sets of results of simulations or tests outcomes (9). LS-OPT allows the user to structure the design process, explore the design space, and compute optimal designs according to specified constraints and objectives. In the design approach, a design is improved by evaluating its response and making design changes based on experience or intuition. This approach does not always lead to the desired result since the design objectives are often in conflict. Therefore, it is not always clear how to change the design to achieve the best compromise of these objectives. A systematic approach can be obtained by using an inverse process of first specifying the criteria and then computing the best design according to a formulation. The improvement procedure that incorporates these design criteria into a mathematical framework is referred to as design optimization. This procedure is iterative and requires multiple simulations. Response surface methodology is a statistical method for constructing smooth approximations to functions in a multidimensional space. It is a methodology to address optimization. Response surface methodology selects designs that are optimally distributed throughout the design space to construct the approximate surfaces. To check the adequacy of the model, the equation for the residual sum of squares formula is used:

$$\varepsilon^2 = \sum_{i=1}^P (y_i - \hat{y}_i)^2 \quad [6]$$

Two sensitivity measures are implemented in LS-OPT: Linear ANOVA and GSA/Sobol. If a polynomial response surface method is selected, the analysis of variance (ANOVA) of the approximation to the experimental design is automatically performed. The ANOVA information can be used to screen variables during or at the start of the optimization process. The ANOVA method determines the significance of main and interaction effects. The ANOVA results are viewed in a bar/tornado chart form. The ANOVA bars show which design variable is important for the computation of the response. The ANOVA value is represented by the blue bar. The red bar indicates the confidence interval. When a red bar is too large, the value computed cannot be trusted. When the red bar is small, the confidence interval is small and the contribution of that variable is substantial. A global sensitivity analysis (GSA) is to be performed as well. Each bar represents a variable and its contribution of the variable to the variance of the respective response. The values sum to 100 percent. This measure is also known as the stochastic sensitivity

analysis or Sobol's analysis. The variance of the response may be written using the Sobol's indices approach:

$$f(x_1, \dots, x_n) = f_0 + \sum_{i=1}^n f_i(x_i) + \sum_{i=1}^n \sum_{j=i+1}^n f_{ij}(x_i, x_j) + \dots + f_{1,2,\dots,n}(x_1, \dots, x_n) \quad [7]$$

NCHRP 16-05 GUIDELINES FOR COST-EFFECTIVE SAFETY TREATMENT OF ROADSIDE DITCHES

The objective of this project was to conduct a cost-effectiveness evaluation of potential strategies for mitigating the severity of crashes on an identified set of high-risk ditch configurations. A literature review was performed to supply background information on the safety performance of roadside slopes and ditch designs. A survey was sent out to state agencies to establish the most commonly used practices concerning roadside slopes and ditch designs. An analysis of crash data was performed to:

- Identify trends in type and severity of ditch related crashes and their relationship with ditch geometry, roadway characteristics, vehicle type, presence of appurtenances, and other relevant characteristics.
- Obtain vehicle roadside encroachment characteristics for ran-off-road crashes and estimating injury severity and economic cost for ditch-initiated crashes.

The databases used for the analysis were:

- Fatal Analysis Reporting System (FARS), administered and maintained by the National Highway Traffic Safety Administration (NHTSA).
- NASS Crashworthiness Data System (NASS CDS), administered and maintained by NHTSA.
- NASS General Estimates System (NASS GES), administered and maintained by NHTSA.
- National Cooperative Highway Research Program (NCHRP) Project 17-22 database, developed by University of Nebraska at Lincoln.
- Highway Safety Information System, a nine-state database administered by the Federal Highway Administration (FHWA).

The final portion of the crash data analysis is a severity and cost analysis of ditch-initiated crashes the purpose of which was to:

- Understand the magnitude and severity of the ditch-initiated crashes, which the design guidelines and mitigation strategies developed in this project are intended to have an effect.
- Obtain good cost estimates of ditch-initiated crashes, which can be used to evaluate alternative ditch configurations and mitigation methods in a benefit-cost analysis.

A benefit-cost analysis was performed to determine which possible safety improvements would be most effective. The analysis comprised of five major component models:

1. Encroachment rate model—Encroachments per mile per year.
2. Encroachment characteristics model—Specifies relatively how often an encroachment that possesses certain characteristics (vehicle type, speed, angle, driver control, vehicle tracking, perception-reaction time) is expected to occur.
3. Ditch traversal and impact model.
 - a. Evaluated with CarSim.
 - b. Determines vehicle performance during ditch traversal given encroachment characteristics.
4. Impact-severity model.
 - a. Uses the outputs from CarSim models to specify the probability of injury severity.
 - b. Weakest link in the method.
 - c. Injury severity split into six categories.
 - i. No injury and no damage.
 - ii. Property damage only.
 - iii. Possible injury.
 - iv. Non-incapacitating injury.
 - v. Incapacitating injury.
 - vi. Fatal crash.
5. Crash cost model—The cost of each severity level is calculated using the data collected from the FARS and NASS GES data, and the cost of each encroachment is the sum of the

probability-weighted cost over all possible combinations of the encroachment characteristics.

VEHICLE DYNAMICS SIMULATIONS

A multi-rigid body vehicle dynamics code was used to perform vehicular trajectory simulations. There were three different code options considered for the simulation. CarSim was the simulation tool chosen for the study. CarSim has a built in antilock braking system (ABS), a library of tire models more advanced than other simulation tools, a better suspension system model that account for suspension compliance effects, a library of vehicle properties, and a subroutine was added to include body to terrain contact.

Table 7. Recommended design variables and encroachment investigated in NCHRP 16-05

Design Variable	Range of Variable
Foreslope ratio	10:1, 6:1, 4:1, 3:1
Foreslope width (ft)	0, 4, 10
Ditch bottom width (ft)	0, 4, 10
Backslope ratio	10:1, 6:1, 4:1, 3:1, 2:1
Backslope width (ft)	8, 16
Shoulder type and width	6% cross-slope
Pavement width (ft)	2, 6
Pavement width and turf (ft)	12 foot pavement and 7 foot turf
Vehicle type	Passenger car, passenger sedan, pickup truck, small SUV
Encroachment speed (mph)	45, 55, 65, 75
Encroachment angle (degrees)	10, 20, 30

Additionally the NCHRP 16-05 researchers investigated:

- Two Vehicle Orientations at Encroachment point, Tracking/Non-tracking.
 - Tracking.
 - Non-tracking with yaw rate of 15 degree/sec.
- Perception-Reaction Time—selected based on literature review.
- Driver Control Input.
 - Free-wheeling.
 - Panic return-to-road Steering.
 - Combined return-to-road steering and full ABS braking.

- Coefficient of Frictions for Tire-Terrain Friction—Selected based on literature review.
- Main-Lane Configurations.
 - Straight and Level.
 - Vertical grade.
 - 4 percent downgrade.
 - 6 percent downgrade.
 - Horizontal Curvature.
 - 0°.
 - 4.5°.
 - 6°.
- Impact Severity and Vehicle Stability Measures.
 - Maximum moving 50 ms acceleration severity index (ASI50ms) for unrestrained, lap-restrained, and lap and shoulder restrained occupants.
 - Maximum longitudinal and lateral extent of movements.
 - Maximum angular displacements: roll, pitch, and yaw.
 - Maximum 50-ms resultant vehicular acceleration (MRA50ms).
 - Vehicular Stability: stable, sideslip, spin out, rollover.

NCHRP 17-22 IDENTIFICATION OF VEHICULAR IMPACT CONDITIONS ASSOCIATED WITH SERIOUS RAN-OFF-ROAD CRASHES

The objectives of this study were to identify the vehicle types, impact conditions, and site characteristics associated with serious injury and fatal crashes involving roadside features and safety devices, create a robust relational database for future research, and develop an implementation plan for a long-term collection effort (*I0*). Data were collected under three different studies: FHWA Rollover, NCHRP 17-11, and NCHRP 17-22, using a retrospective data collection. Supplemental information was collected for roadway characteristics, roadside, and struck objects. Each crash was reconstructed to determine vehicle departure and impact conditions. Data could then be compiled into a database that could be used to analyze data. The database for SVROR crashes includes detailed characteristics of the vehicle, its trajectory, roadway, roadside, objects struck, and crash result for 877 crashes. The data are highly biased toward severe crashes. Speed limit provided the best discriminator for departure velocity and

angle. Normal distributions accurately represented departure velocities. Departure angles were best represented by gamma distributions. Dependency between departure angle and velocity was found to be insignificant for all individual speed limit classes, thus, they are independent of one another. However, the models of departure velocity and the square root of the departure angle can be used for distribution across all speed limit classes.

The findings also support the recommendation to reduce guardrail length. Differences in the database and Cooper's study can be explained by the differences in speed limit ranges. Modified runout length was shorter than the longitudinal travel distance on 60 mph roadways. Therefore, the suggestion is to use a design speed of 70 mph for all controlled access roadways, or implement an additional category for 60 mph with full access control.

The development of a long-term data collection plan was piloted using a continuous sampling subsystem (steady stream of new cases) and a special study subsystem (one particular type of crash). The data collection plan would provide the basis for determining important relationships such as impact severity and crash conditions, causation of injuries and fatalities, and a foundation for roadside safety features to reduce injuries and fatalities in the future.

CHAPTER 3: APPROACH AND METHODS

APPROACH

This research approach combines both vehicle dynamics simulations with meta-modeling to produce data analytics that presents actionable information.

VEHICLE DYNAMICS SIMULATIONS

Through simulation, combinations of key geometric design elements and other critical elements were evaluated to assess their impact on vehicle stability when encountering a range of frictions between the traveled way and shoulder. These include vehicle type, vehicle speed, vehicle path, slope ratio, roadway curvature, and friction of slope ratio. For this study, a fixed superelevation was assumed. After all vehicle rollover scenarios were created and data were collected, LS-OPT was used to create meta-models.

DATA ANALYTICS—METHODS

To run simulations on CarSim, several parameters must be specified. Figure 4 shows a flowchart on how simulations are created (11).

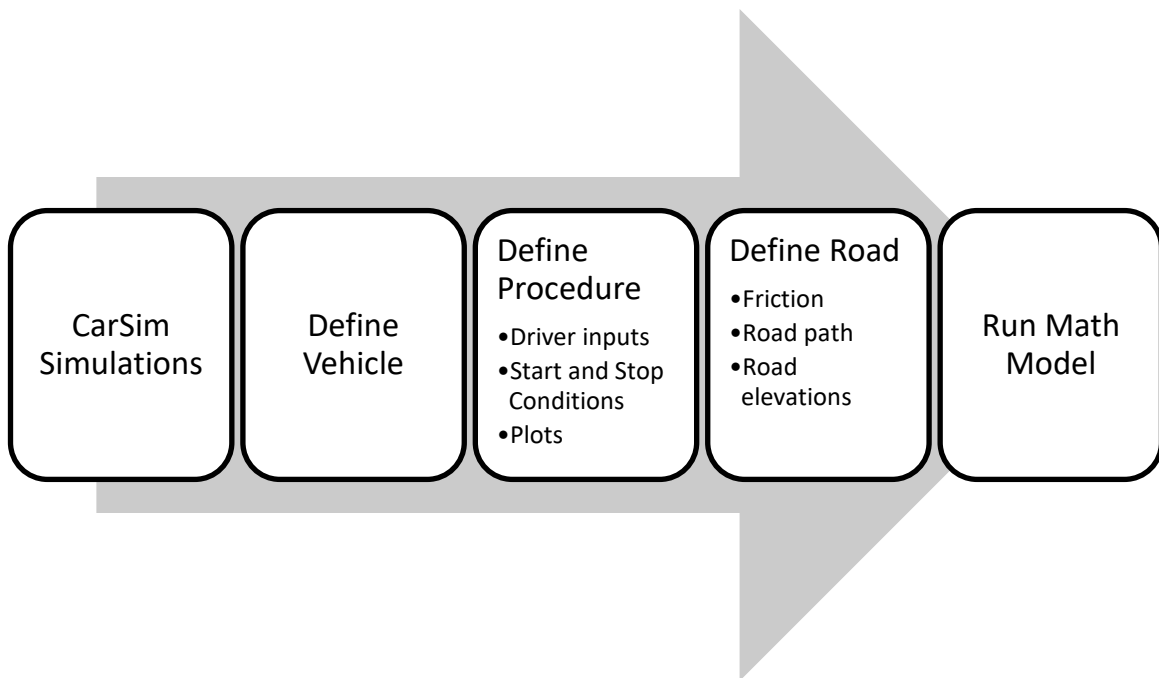


Figure 4. CarSim simulation flowchart.

Figure 5 is an image of the CarSim run control screen. From this screen, the vehicle used, the procedure, and the road must be specified. First, the vehicle is chosen. In this study, a Class C Hatchback vehicle and a Full-size SUV will be utilized. Figure 7–Figure 10 show images of the four vehicles used. The Class C Hatchback had a 1270 kg rigid sprung mass and the full-size SUV had a 2257 kg rigid sprung mass. The Full-size Pickup Truck had a rigid sprung mass of 1998 kg and the Class E Sedan had a mass of 1650 kg. These masses are preset in CarSim and were not changed. The SUV, pickup truck, and sedan had an ABS breaking system.

Table 8. Vehicle characteristics.

Vehicle Type	Mass (kg)	CG Height (mm)	Braking System
C-Class, hatchback 2012	1270	540	NO ABS
SUV, full size	2257	781	ABS
Pickup, full size, crew cab, 5.5 ft bed	1998	795	ABS
E-class sedan 2017	1650	530	ABS

Next, the procedure must be defined. Figure 6 shows an image of the graphic user interface on the procedure screen. The driving maneuver was specified in the procedures in CarSim. Plot definitions, driver controls, start, and stop conditions were also defined in the procedures. For this study, the vehicle has a set initial speed, no braking, and no steering. Eight

different speeds were also utilized. The encroachment angle is specified in the miscellaneous data field. The start and stop time of the runs is also specified here. After the procedure is defined, the roads must be built. Roads with varying slope ratio, and frictions were built in CarSim to run simulations. Slope ratio ranged from 1V:3H to 1V:4H. The friction of the slope ratio ranged from 0.9 to 1.5. The roads used also had two curvatures: a road with a 621.79-m radius and a road with an infinite radius. These were achieved using the Road segment builder in CarSim. Table 9 shows the variation in design variables utilized in the study. Figure 11 and Figure 12 show the two roads used in this study.

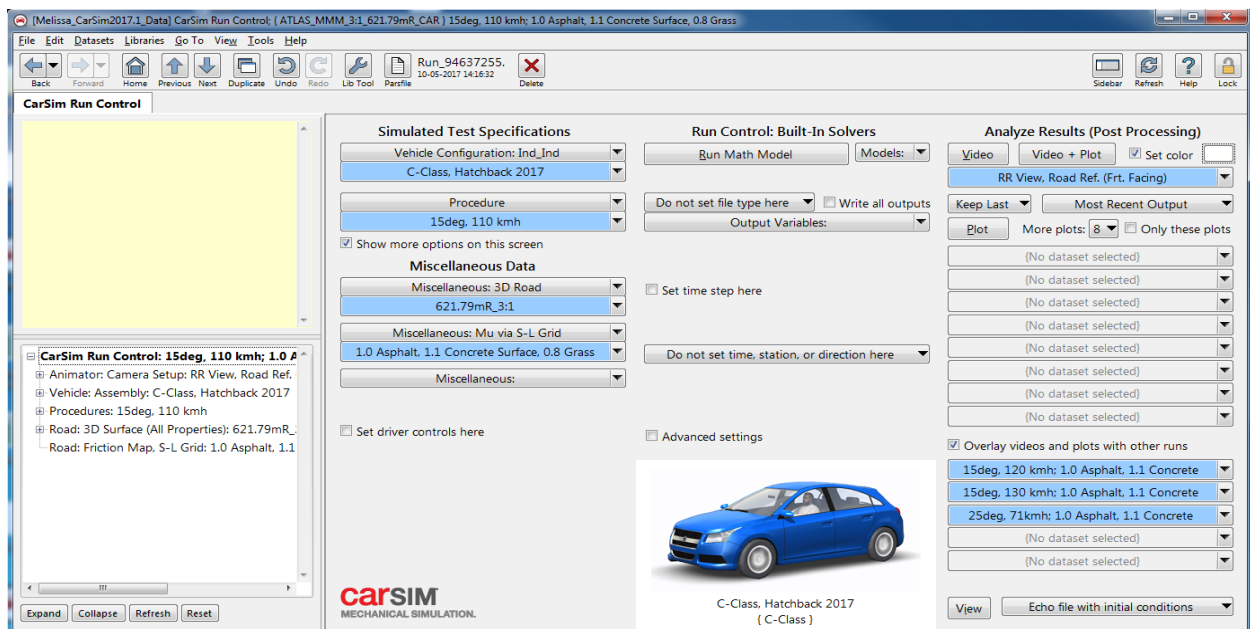


Figure 5. CarSim Run Control screen.

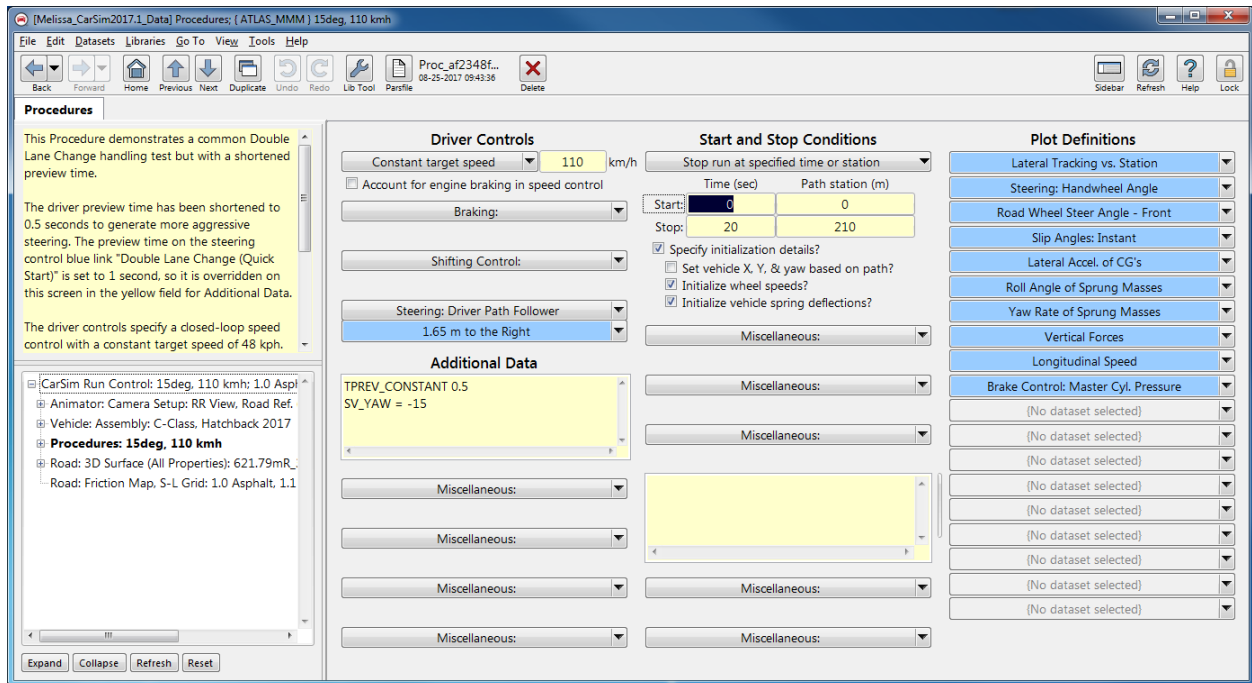


Figure 6. CarSim Procedures screen.



Figure 7. Class C hatchback.



Figure 8. Full-size SUV.



Figure 9. Full size pickup truck, 5.5 ft bed.



Figure 10. Class E sedan.



Figure 11. 621.79 m radius road with a 3:1 side-slope.



Figure 12. Straight road with a 3:1 side-slope.

Figure 13 and Figure 14 depict a profile of the roads. The side-slopes were intentionally created to be very long to be able to see how the side-slope affected the roll angle and not the ditch.

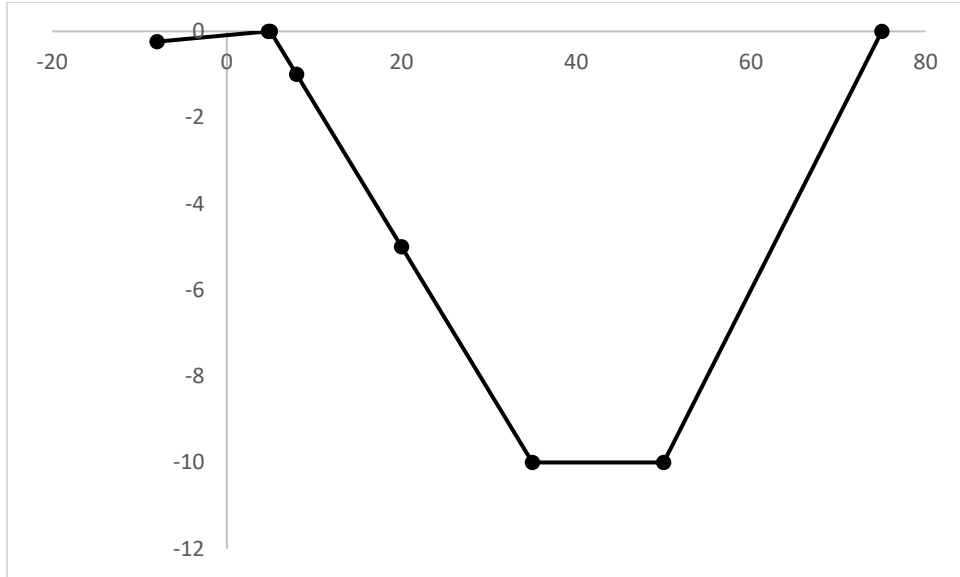


Figure 13. Road profile of the 3:1 side-slope.

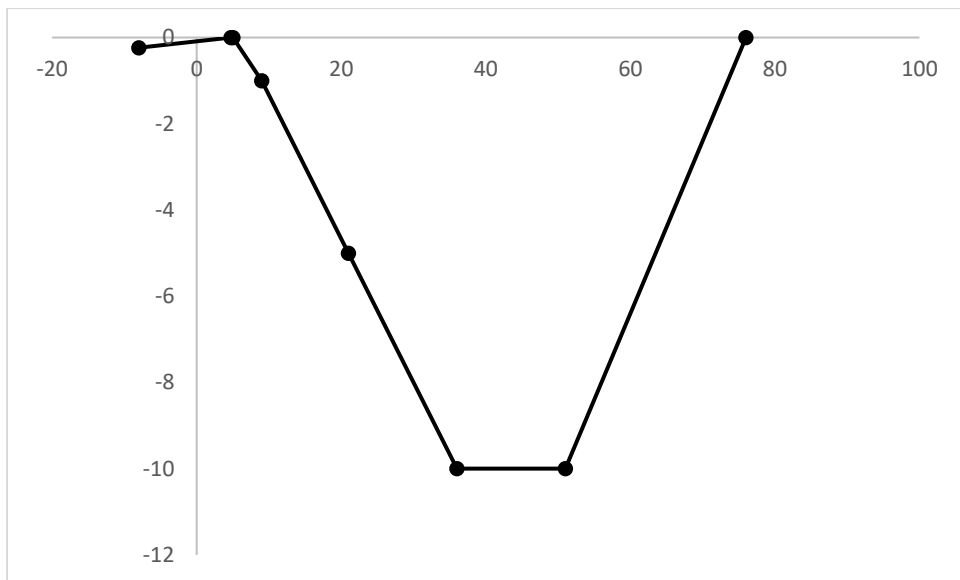


Figure 14. Road Profile of 4:1 side-slope.

Table 9. Vehicle dynamics simulation matrix.

Variables	Example Conditions
Ditch geometry	3:1, 4:1, 6:1
Vehicle speed (km/h)	65, 71, 80, 90, 110, 120, 130
Coefficient of frictions for tire-terrain friction (to represent soft soil conditions and various surface materials)	0.8, 0.9, 1.0, 1.5
Roadway curvature (m)	∞ , 253.8, 405.4, 621.79

All these parameters (vehicle, procedure, and roadway) are specified in the Run Control Screen pictured in Figure 5. After all parameters were specified, the math model was run. Plots were then analyzed, and data were gathered to be input into LS-OPT.

Data analytics tools have shown great advancement to address exponential growth of data in many fields including transportation. Researchers recommend using a data analytics utility to address meta-modeling, trends, and probability. LS-OPT allows the user to structure the design process, explore the design space, and compute optimal designs according to specified constraints and objectives. A total of 1040 rollover scenarios were created using CarSim. To use LS-OPT, the meta-model type must first be chosen. LS-OPT offers seven types of meta-models; polynomial, sensitivity, feedforward neural network, radial basis function network, kriging, support vector regression, and user defined. After several attempts, FeedForward Neural Network was chosen as the best meta-model for this study. Global sensitivities were also calculated. After the meta-model type was chosen and the data were imported, the model was run. Figure 15 shows a picture of the LS-OPT user interface.

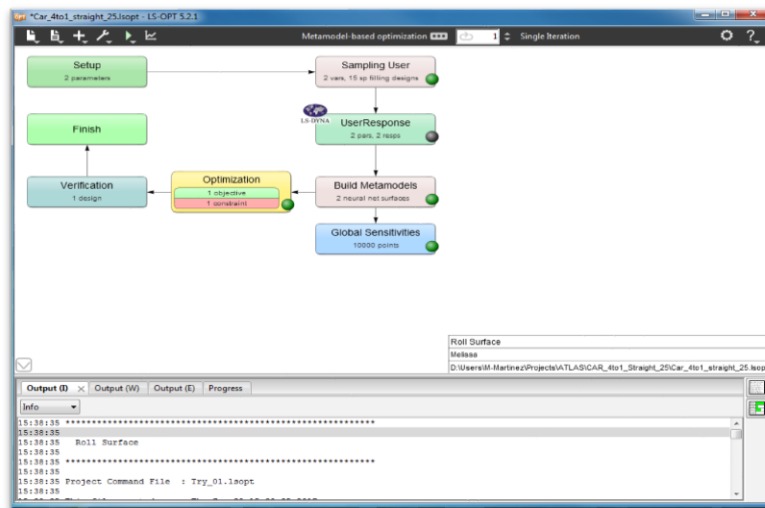


Figure 15. LS-OPT user interface.

The raw data from CarSim were input into 56 separate datasheets to be input into LS-OPT. Each data sheet has a vehicle type, a side-slope ratio, roadway curvature, and encroachment angle. Figure 17 is a flowchart of how the LS-OPT meta-models are categorized. The two meta-models discussed are the surface model and the sensitivity model. The two

variables discussed will be the vehicles' roll angle and the maximum deviation from the centerline of the right lane.

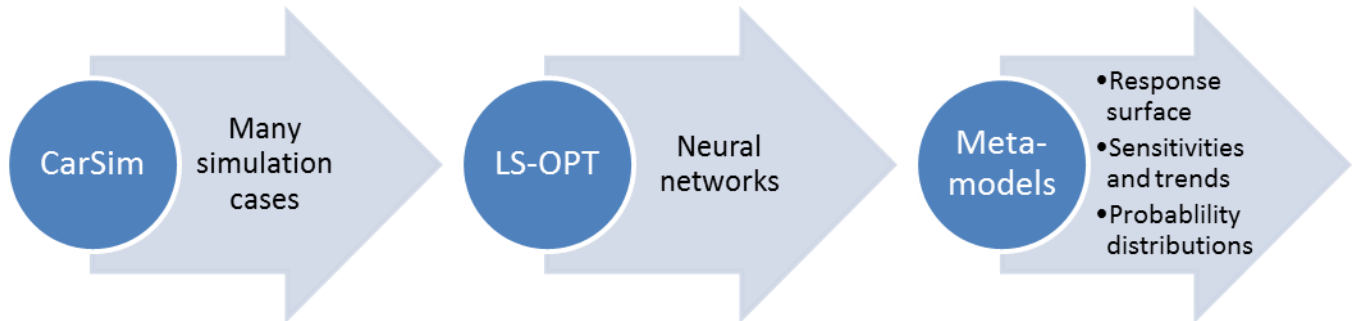


Figure 16. Data analytics.

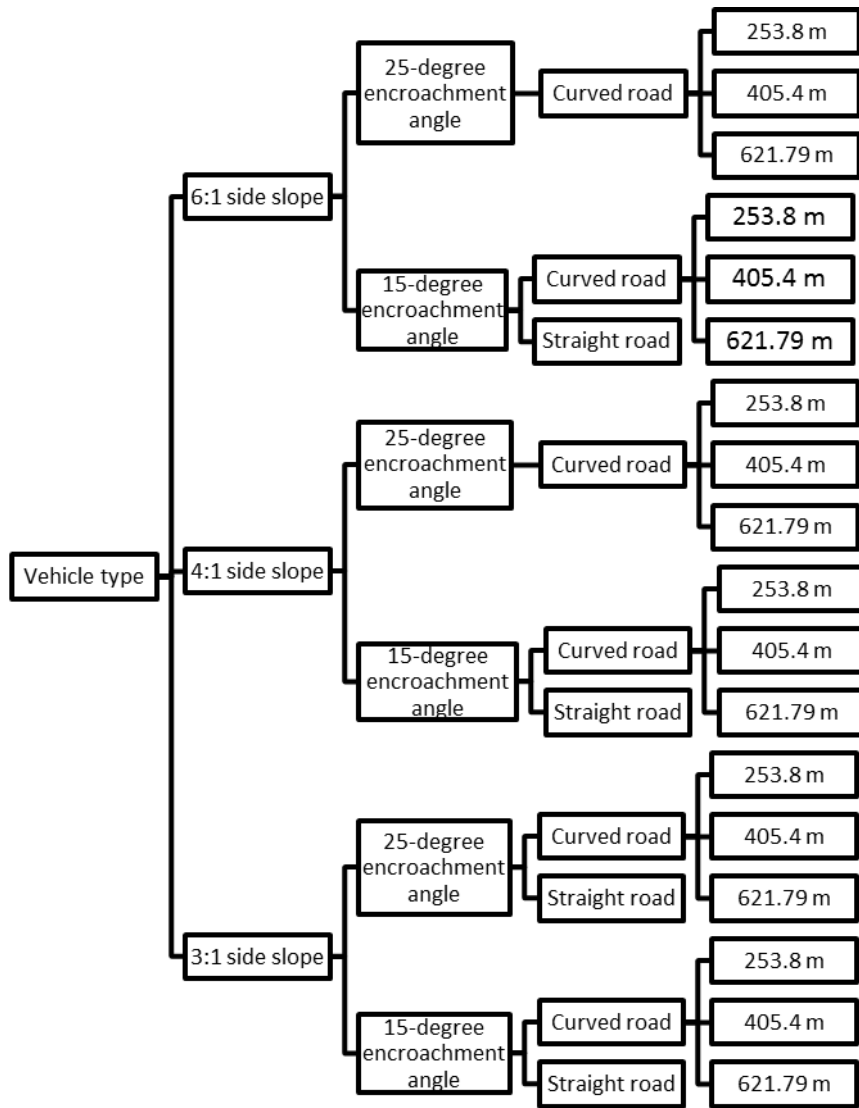


Figure 17. LS-OPT categories.

CHAPTER 4: RESULTS AND DISCUSSION

RESULTS

Vehicle Dynamics Simulations

A total of 882 scenarios was created using CarSim, 522 cases without driver perception-reaction (PR) time and 360 scenarios with driver PR time. The results include the number of rollover events on curved and straight roads, as well as the frequency of rollovers for each of the three observed friction forces (0.8, 1, and 1.5). Two other important factors analyzed were the number of rollovers that occurred at speeds greater than 110 km/h, and the number of vehicles unable to navigate back to the roadway after exiting. All results are shown in their respective tables below.

Without Driver Perception Reaction Time

The number of rollover events that occurred in scenarios without driver perception was 88 (16.9 percent) on curved roads and 64 (12.3 percent) on straight roads, for a total of 152 rollovers (29.1 percent). Of the 88 rollover events on curved roads, 21 (23.9 percent) were cars, 30 (34.1 percent) were SUVs, 17 (19.3 percent) were trucks, and 20 (22.7 percent) were sedans. Of the 64 rollover events on straight roads, 17 (26.6 percent) were cars, 28 (43.8 percent) were SUVs, 12 (18.9 percent) were trucks, and 7 (10.9 percent) were sedans. This shows that rollover was more likely to occur on curved roads. SUVs were most likely to rollover on both curved and straight roads. Sedans and trucks were almost equally as likely to rollover, but were least likely to rollover than the other vehicle types. The 3:1 slope resulted in only slightly fewer rollovers compared to the 4:1 slope.

Rollover events for all vehicles occurred more than twice as often when exiting the road at an encroachment angle of 25° as opposed to 15°, and in some cases nearly 12 times as often. This is shown by the 26 total rollovers as result of a 15° encroachment angle and the 126 total rollovers as result of a 25° encroachment angle. Rollovers with a 15° encroachment angle rarely occurred on straight roads; only 3 (1.97 percent) of the 152 total rollover events.

Vehicles traveling 110 km/h or greater were more susceptible to rollover than vehicles traveling at lower speeds. Of the 152 total rollovers, 119 (78.3 percent) scenarios involved a

speed of 110 km/h or greater. However, outliers do exist that show rollover at 71 km/h and 80 km/h.

In 21 (4.02 percent) of the 522 total cases, the vehicle was unable to navigate back to the road. This happened only once with an encroachment angle of 15°, suggesting that a higher encroachment angle decreases the likelihood of safely navigating back to the road. Sedans had the most cars unable to reach the road again, but was closely followed by SUVs and trucks. Only one of the cars was unable to navigate back to the roadway.

Table 10. Summary of vehicle dynamics simulations.

Vehicle Type		Car	SUV	Truck	Sedan	Total
Runs		120	162	120	120	522
Rollover	Curved	21	30	17	20	88
	Straight	17	28	12	7	64
	Total	38	58	29	27	152
15 encroachment	0.8	0	1	0	2	3
	1	1	2	2	2	7
	1.5	2	5	6	3	16
	Total	3	8	8	7	26
25 encroachment	0.8	11	12	1	2	26
	1	12	22	4	3	41
	1.5	12	16	16	15	59
	Total	35	50	21	20	126
≥ 110 km/h		38	39	20	22	119
Unable to navigate back to road		1	6	6	8	21

With Driver Perception Reaction Time

The number of rollover events that occurred in scenarios with driver perception was 66 (18.3 percent) on curved roads and 45 (12.5 percent) on straight roads, for a total of 111 rollovers (30.8 percent). Of the 66 rollover events on curved roads, 21 (31.8 percent) were cars, 27 (40.9 percent) were SUVs, and 18 (27.3 percent) were trucks. Of the 45 rollover events on straight roads, 17 (37.8 percent) were cars, 16 (35.6 percent) were SUVs, and 12 (26.7 percent) were trucks. Once again, rollover was more likely to occur on curved roads than straight roads. However, SUVs were only more likely to roll on curved roads. Whereas straight roads showed more rollover events in cars. When considering the driver perspective, it is much more obvious that rollover occurs more often on a 3:1 slope than a 4:1 slope.

Rollover events for all vehicles occurred more than twice as often when exiting the road at an encroachment angle of 25° as opposed to 15°, and in some cases nearly 12 times as often.

This is shown by the 19 total rollovers as result of a 15° encroachment angle and the 92 total rollovers as result of a 25° encroachment angle. Rollovers with a 15° encroachment angle rarely occurred on straight roads; only 3 (2.7 percent) of the 111 total rollover events.

Vehicles traveling 110 km/h or greater were more susceptible to rollover than vehicles traveling at lower speeds. Of the 111 total rollovers, 95 (85.6 percent) scenarios involved a speed of 110 km/h or greater. However, outliers do exist that show rollover at 71 km/h and 80 km/h.

None of the 111 observed scenarios involved a vehicle that was unable to navigate back to the roadway. This suggests that the driver perceptiveness allows better control of the vehicle.

Table 11. Summary of vehicle dynamics simulations: Driver perception reaction time.

Vehicle Type		Car	SUV	Truck	Total
Runs		120	120	120	360
Rollover	Curved	21	27	18	66
	Straight	17	16	12	45
	Total	38	43	30	111
15 encroachment	0.8	0	1	0	1
	1	1	2	2	5
	1.5	2	5	6	13
	Total	3	8	8	19
25 encroachment	0.8	11	7	1	19
	1	12	13	4	29
	1.5	12	15	17	44
	Total	35	35	22	92
≥ 110 km/h		35	39	21	95
Unable to navigate back to road		0	0	0	0

The results suggest that rollover is more likely to occur on curved roads than straight roads by 17.1 percent. SUVs were more likely to rollover than any other vehicle type and had the most rollover in every category except for cars that included the driver perception on straight roads. Increasing the encroachment angle had significant effects on vehicle behavior including the increase of rollover propensity and decreasing the likelihood of navigating back to the road. When driver perception was included, the likelihood of rollover did not improve, but stayed roughly the same. However, adding a driver did reduce the number of vehicles unable to navigate back to the road by 100 percent.

Four types of roadways (one straight and three curved with radii of 621.79 m, 405.4 m, and 253.8 m) were created for an SUV traveling at various speeds (70 km/h–130 km/h) and with three ditches with different side slopes (3:1, 4:1, and 6:1). Two different encroachment angles were tested (15° and 25°) with three different coefficients of friction (0.8, 1, and 1.5). Each combination of roadway and ditch slope included 30 scenarios with varying encroachment angle, friction, and speed. Results for all 360 scenarios can be seen in Table 12.

Of the 90 total scenarios created on a straight road, 18 (20 percent) SUVs were involved in a rollover. The ditches with side-slopes of 3:1 and 4:1 had roughly the same number of rollovers, 8 and 7, respectively. However, a side-slope of 6:1 decreased the rollover frequency by about 13 percent, with only 3 vehicles that rolled. The 15° encroachment angle only resulted in 1 rollover with friction of 1.5 on 3:1 side-slope, 1.11 percent of all scenarios, and 5.56 percent of all rollovers on straight roads. The 25° encroachment angle resulted in 17 rollovers, 18.89 percent of all scenarios and 94.44 percent of rollover events on straight roads. All but one rollover event occurred at speeds equal than or greater to 110 km/h. The one rollover that occurred at a lesser speed was at 80 km/h, with a 3:1 side-slope, 25° encroachment angle, and 1.5 friction. All scenarios that did not involve rollover were able to navigate back to road, indicated by the row for vehicles unable to navigate back (UNB) to road on Table 12.

Of the 90 total scenarios created on a curved road with radius 621.79 m, 30 (33 percent) SUVs were involved in a rollover. The ditches with side-slopes of 3:1 and 4:1 had 13 rollovers each, 14.4 percent of total scenarios each, and 43.3 percent each for all rollovers on this road type. However, a side-slope of 6:1 decreased the rollover frequency by over 30 percent, with only 4 vehicles that rolled. The 15° encroachment angle only resulted in 9 rollovers, 10 percent of all scenarios, and 30 percent of all rollovers on this road type. There is a clear trend that the steeper the slope, the greater the chance of rollover. For the 15° encroachment angle, five rollovers occurred on the 3:1 slope, three occurred on the 4:1 slope, and one occurred on the 6:1 slope. Likewise, the rollover frequency increased as the coefficient of friction increased. Again, 5 rollovers occurred at friction of 1.5, 3 at friction of 1.0, and 1 at friction of 0.8. The 25° encroachment angle resulted in 21 rollovers, 23.33 percent of all scenarios and 70 percent of rollover events on straight roads. The same trends in side-slope and friction occurred with 8, 10, and 3 rollovers for each side-slope, and 11, 6, and 4 for each friction. All but four rollover events occurred at speeds equal than or greater to 110 km/h. All of these rolls happened at 80 km/h,

three on a 3:1 side-slope with 25° encroachment, occurring at each friction coefficient. The fourth of which occurred on a 4:1 side-slope with a 25° encroachment angle and friction of 1.5. All scenarios that did not involve rollover were able to navigate back to road, indicated by the row for vehicles UNB to road on Table 12.

Of the 90 total scenarios created on a curved road, with curve radius of 405.4 m, 36 (40 percent) SUVs were involved in a rollover. The ditches with side-slopes of 3:1 and 4:1 had 15 rollovers each. However, a side-slope of 6:1 decreased the rollover frequency by 30 percent, with only six vehicles that rolled. The 15° encroachment angle only resulted in 14 rollovers, 15.56 percent of all scenarios and 16.67 percent of all rollovers on this road type. The same general trend mentioned previously occurs on this road type: rollovers for increasing side-slope were 7, 5, and 2, and rollover for increasing friction was 3, 4, and 7. The 25° encroachment angle resulted in 22 rollovers, 24.44 percent of all scenarios and 61.11 percent of rollover events on this road type. All but four rollover events occurred at speeds equal than or greater to 110 km/h. All of these rolls happened at 80 km/h, three on a 3:1 side-slope with 25° encroachment, occurring at each friction coefficient. The fourth of which occurred on a 4:1 side-slope with a 25° encroachment angle and friction of 1.5. All scenarios that did not involve rollover were able to navigate back to road, indicated by the row for vehicles UNB to road on Table 12.

Of the 90 total scenarios created on a curved road with curve radius of 253.8 m, 40 (44 percent) SUVs were involved in a rollover. The ditches with side-slopes of 3:1 and 4:1 had roughly the same number of rollovers, 15 and 17 respectively. However, a side-slope of 6:1 decreased the rollover frequency by over 23 percent, with only eight vehicles that rolled. The 15° encroachment angle resulted in 20 rollovers, 22.22 percent of all scenarios and 50 percent of all rollovers on this road type. The same general trends appear here, with rollovers on increasing side-slope occurring with frequencies of 9, 7, and 4 times, and rollover of increasing friction occurring at frequencies of 5, 6, and 9 times. The 25° encroachment angle resulted in 20 rollovers, 22.22 percent of all scenarios and 50 percent of rollover events on this road type. All but five rollover events occurred at speeds equal than or greater to 110 km/h. All of these rollovers occurred at 80 km/h and a 25° encroachment angle, two on the 3:1 side-slope with friction 0.8 and 1.0, two on the 4:1 side-slope with friction of 1.0 and 1.5, and on the 6:1 side-slope with friction of 1.5. All scenarios that did not involve rollover were able to navigate back to road, indicated by the row for vehicles UNB to road on Table 12.

The general trends to be noted from these results are as follows: rollover propensity increases as the degree of road curvature increases, as speed increases, as friction increases, and as side-slope decreases.

Table 12. General trends.

	Straight Road				621.79 m				405.4 m				253.8 m				
	3:1	4:1	6:1	Total	3:1	4:1	6:1	Total	3:1	4:1	6:1	Total	3:1	4:1	6:1	Total	
Rollover	8	7	3	18	13	13	4	30	15	15	6	36	15	17	8	40	
15°	0.8	0	0	0	1	0	0	1	2	1	0	3	3	2	0	5	
	1	0	0	0	2	1	0	3	2	2	0	4	3	2	1	6	
	1.5	1	0	0	1	2	2	5	3	2	2	7	3	3	3	9	
	Total	1	0	0	1	5	3	1	9	7	5	2	14	9	7	4	20
25°	0.8	1	1	0	2	1	3	0	4	1	3	0	4	1	2	0	3
	1	2	3	0	5	3	3	0	6	3	3	0	6	2	4	0	6
	1.5	4	3	3	10	4	4	3	11	4	4	4	12	3	4	4	11
	Total	7	7	3	17	8	10	3	21	8	10	4	22	6	10	4	20
≥ 110 km/h	7	7	3	17	10	12	4	26	12	14	6	32	13	15	7	35	
UNB	0	0	0	0	0	0	0	0	0	0	0	0	0	0	0	0	

A total of 1080 simulations was created with a fixed length to the side-slope. Half the simulations were with the Full-Size SUV while the other half were of the Class-C Hatchback. These simulations were used for data analytics.

Data Analytics

Using the 882 vehicle dynamics simulation scenarios created in CarSim, 56 categories were created to be input into the meta-modeling software. Each category had varying vehicle type, roadway curvature, side-slope, and encroachment angle. Fifty percent of the categories were at a 15° encroachment angle while the rest of the categories were at a 25° encroachment angle. Thirty-two categories were using scenarios without driver perception reaction time. Twenty-four of the categories were vehicle dynamics scenarios that included a driver perception reaction time of 1 second. The Class-C Hatchback, Full Size SUV, and Full Size Pickup Truck each had 16 categories while the Sedan had eight categories.

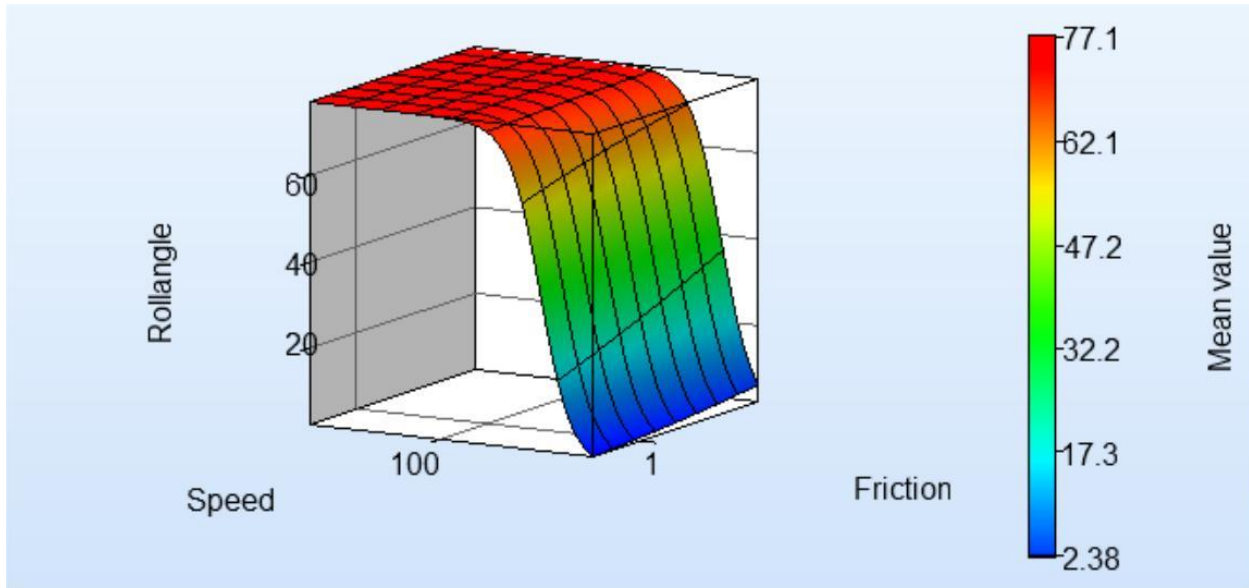
A total of 1080 runs was used in a data analytics run using all variables instead of categorizing them. The Full-Size SUV and Class-C Hatchback were used for these simulations. Table 13 shows all variables used for these data analytics run.

Table 13. Design variables for data analytics.

Design Variable	Range
Radius (m)	Infinite, 621.79, 405.4, 253.8
Side-Slope	3:1, 4:1, 6:1
Coefficient of friction	0.8, 1, 1.5
Encroachment angle (degree)	15, 20, 25
Encroachment speed (km/h)	71, 80, 110, 120, 130

DISCUSSION

The most prominent surface for the roll angle created on LS-OPT was one similar to Figure 18. For this surface at a speed less than 100 km/h, vehicles experienced a higher roll angle on a higher friction surface. Meta-models for the SUVs had a steeper transition into the higher roll angle than the meta-models for the Class C Hatchback. This indicates that SUVs are more likely to roll over than the class C hatchback. This may be due to the static stability factor mentioned in the background information under the fundamentals of vehicle dynamics section. The height of the CG for an SUV is usually higher than that of a car. A higher CG height yields a smaller static stability factor. The lower the stability factor, the more likely the vehicle is to rollover. Vehicles with a 15° encroachment angle were less likely to roll than those traveling at a 25° angle. Most vehicles departing the road at this angle were able to navigate back onto the road successfully. The vehicle were also more likely to roll over on a 3:1 slope than on the 4:1 or 6:1 side-slope. It is important to study factors of roadway design since these are factors that can be changed to create safer roadway conditions. One cannot control how drivers navigate the road but posted speeds, and other roadway characteristics such as side-slope and ditches are factors that can be modified for safer roads.



Global Sensitivities Plot for Rollangle
 Mean = 64.769, Total variance = 485.394, Noise variance = 2.96896e-006

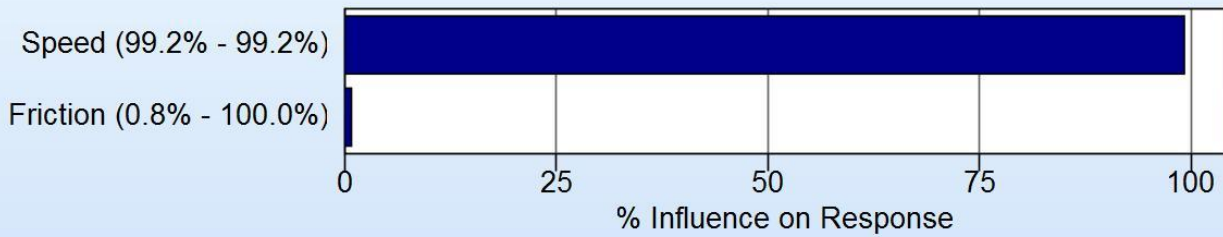


Figure 18. Response surface and global sensitivities for a full-size SUV.

Data analytics have shown great promise and usefulness in many sciences and industries where large amount of data (Big Data) has to be analyzed for trends, sensitivities, and probabilistic prediction of desired responses. Advanced algorithms, approaches, and tools have been developed in response to the exponential growth of data in many fields including transportation. Researchers recommend using a data analytics utility to address the desired vehicular responses as functions of roadway and roadside variables. The approach recommended is to construct extensive database of the desired responses, design variables, and encroachment conditions via massive simulation runs. Then, a higher order meta-model (response surface) is to be constructed. Subsequently, this constructed meta-model can be used for probabilistic analyses to develop sensitivities, trends, and probabilities via Monte Carlo simulation.

Meta-modeling (Response Surface)

A neural network is a computing architecture that consists of massively parallel interconnection of simple neurons. Engineers are interested in neural networks from problem solving. They can adapt to changes in data and learn the characteristics of input signals. Neural networks can perform filtering operations, which are beyond the capabilities of conventional linear filtering techniques due to its nonlinear nature. Neural networks may be used for pattern classification by defining nonlinear regions in the feature space. They are also able to overcome limitations of conventional computers due to their ability to learn and their parallel architecture.

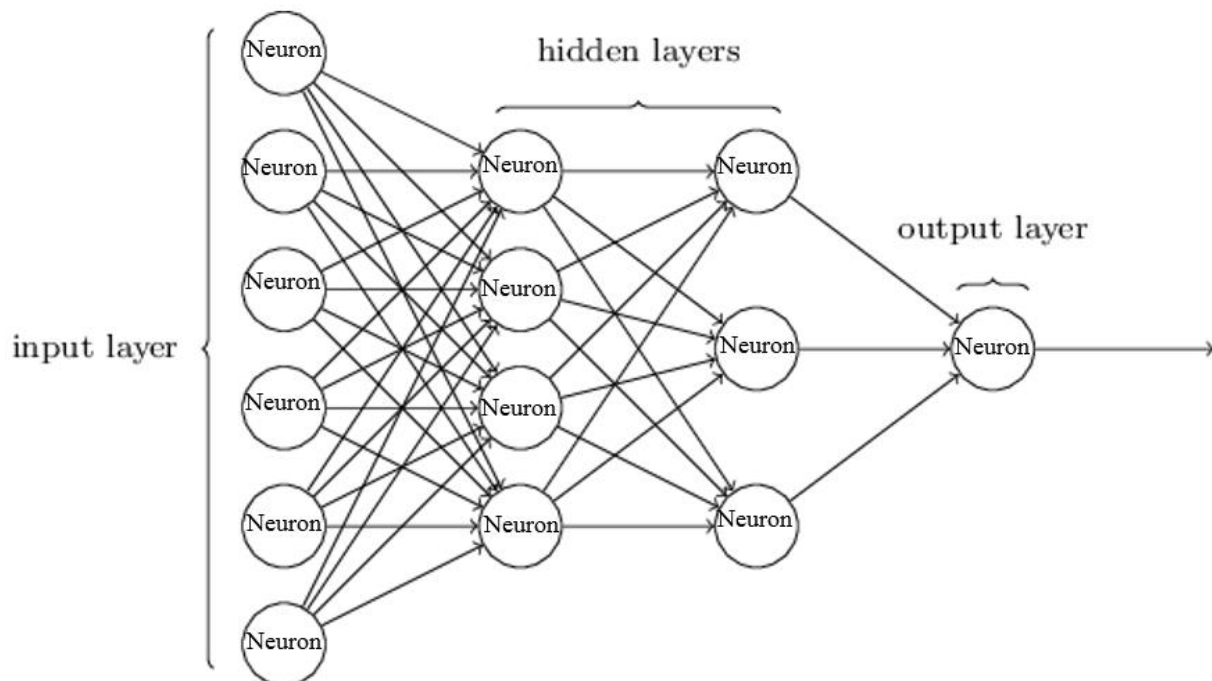


Figure 19. Neural network.

Neural networks can be divided into three basic categories: feed-forward, feed-back, and self-organizing (12). Each category is based on a different philosophy and obeys different principles, the characterization of a system by the term “neural network” implies an ability to learn. Feed-forward neural networks contain one or more layers of nonlinear processing elements or units. The elements belonging to neighboring layers are connected by sets of synaptic weights. These neural architectures are called feed-forward since the output of each layer feeds the next layer of elements. The Perceptron and the Adaline are the earliest feed-forward neural architectures. Multilayered neural networks include one or more layers of hidden elements

between the input and output layer. The feed-forward neural network may be seen as a system transforming a set of input patterns into a set of output patterns. This type of neural network can be trained to provide a desired response to a given input. The network achieves this by adapting its synaptic weights during the learning phase based on learning rules. The training of feed-forward neural networks requires the existence of a set of input and output patterns. This type of learning is called supervised learning.

Monte Carlo Simulation

The Monte Carlo method is a statistical approach to the study of differential equations, or more generally, of integral-differential equations that occur in various branches of the natural sciences (13). The Monte Carlo method provides approximate solutions to a variety of mathematical problems by performing statistical sampling experiments using extensive computational evaluations of such equations (14). This method applies to problems with no probabilistic content and to those with innate probabilistic structure.

Monte Carlo method uses random selection of independent variables (design variables) to select the point where the desired function or performance being evaluated. These evaluations give more accurate representation of the overall response once large number of evaluations are conducted to prevent clustering and bias. Simple example would be the number of coin flip experiments to obtain accurate probabilities of head or tail. Hence, the Monte Carlo method can be very expensive with the increase number of variables and the increase complexity of the function or the response being evaluated. Statistics, reliability information on all constraints, the number of times a specific constraint was violated during the simulation, probability of violating the bounds, the confidence region of probability, and the reliability analysis for each constraint can be computed for all responses. Therefore, the Monte Carlo method can be used to simulate the uncertainty of variables using random samples given the variable distribution. The approximation to the nominal value is:

$$E[f(X)] = \frac{1}{N} \sum f(X_i) \quad [8]$$

When X_i values are independent, the laws of large numbers gives higher degree of accuracy by increasing N values (9).

The overcome the cost of brute force Monte Carlo analysis using massive number of analyses , methods were developed where the Monte Carlo analyses would be performed on the Response Surface (Meta-model). This combined approach starts first by constructing the response surface using a sample set that are less than the massive samples needed for the brute force Monte Carlo approach. However, these samples need to be sufficient enough to construct a response surface with the desired accuracy. Next, Monte Carlo would sample randomly using generated the constructed response surface.

The process for incorporating the combined Monte Carlo and Response Surface approach is shown in Figure 20, which is the overall flow of the data analytics process. Existing codes such as CarSim and TTI Wrapper program are used to generate the outcomes (responses) of vehicular encroachments. Vehicle type, encroachment conditions such as speed and angle, and certain roadway and roadside design variables are considered. A total of 1080 of outcomes (samples) was generated for use in constructing the two different response surface. The response surface chosen is the Neural Network, which has more accuracy than other approximations. Roll angle probability and lateral travel responses are determined using Monte Carlo simulation of the constructed Neural Networks.

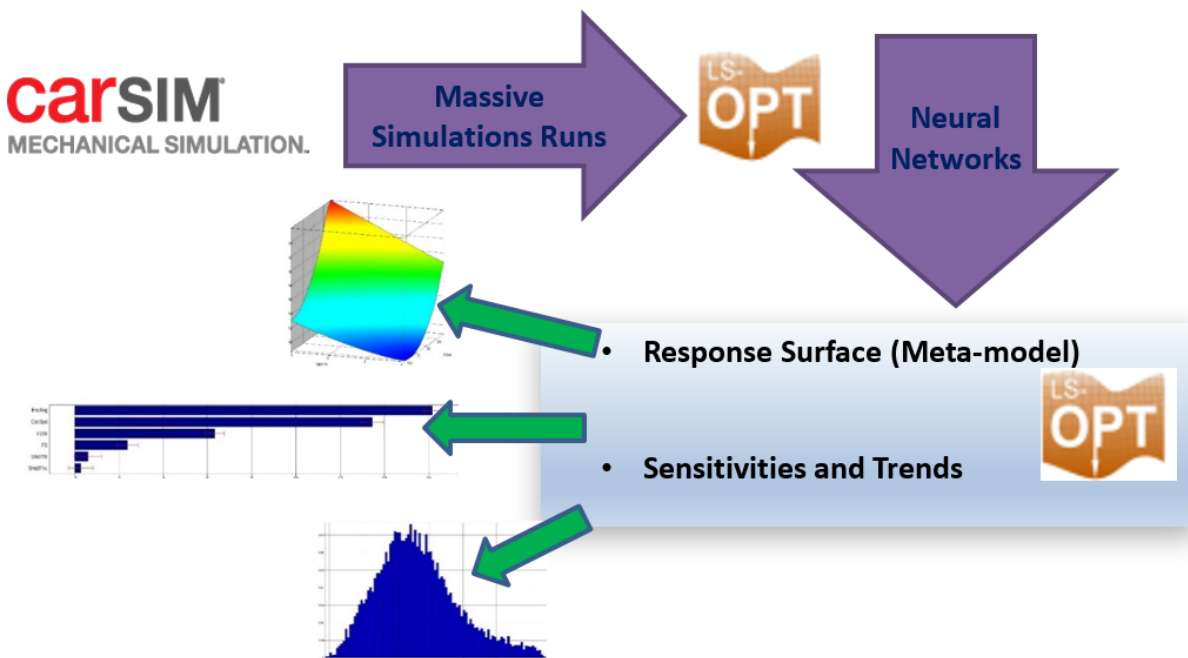


Figure 20. Data analytics.

The tool used for building the response surface and conducting the Monte Carlo simulation is LS-OPT. LS-OPT is a program that allows the user to define the design process, explore the design space, and compute optimal designs according to specified constraints and objectives. Additionally, LS-OPT offers 7 types of response surfaces: polynomial, sensitivity, feedforward neural network, radial basis function network, kriging, support vector regression, and user defined. LS-OPT has a built in Monte Carlo analysis tool that be used for both brute force Monte Carlo and combined Monte Carlo–Meta Model analysis. The research team investigated different response surfaces for this project and Feedforward Neural Network was chosen because it has the highest accuracy given the metrics discussed herewith.

The research team constructed two examples of using Data Analytics adapting the LS-OPT to the needs of this project. The example consists of five different design variables, four radii ranging from 253.8 to infinity meters, the friction of the shoulder ranging from 0.80 to 1.50, and a side-slope ranging from 3:1 to 6:1. The encroachment conditions consist of speed ranging from 71 to 130 km/h and an encroachment angle ranging from 15 to 25°. The vehicles used were a Full-Size SUV and a Class-C Hatchback.

Table 14. Range of variables.

Design Variable	Range
Radius (m)	Infinite, 621.79, 405.4, 253.8
Side slope	3:1, 4:1, 6:1
Coefficient of friction	0.8, 1, 1.5
Encroachment angle (degree)	15, 20, 25
Encroachment speed (km/h)	71, 80, 110, 120, 130

The response surfaces of the vehicular maximum roll and lateral travel for the Full-Size SUV is shown in Figure 21 and Figure 22. Only independent variables are shown for a given response to the higher dimensionality of the surface and the visually limitation of 3D surface to the human eye.

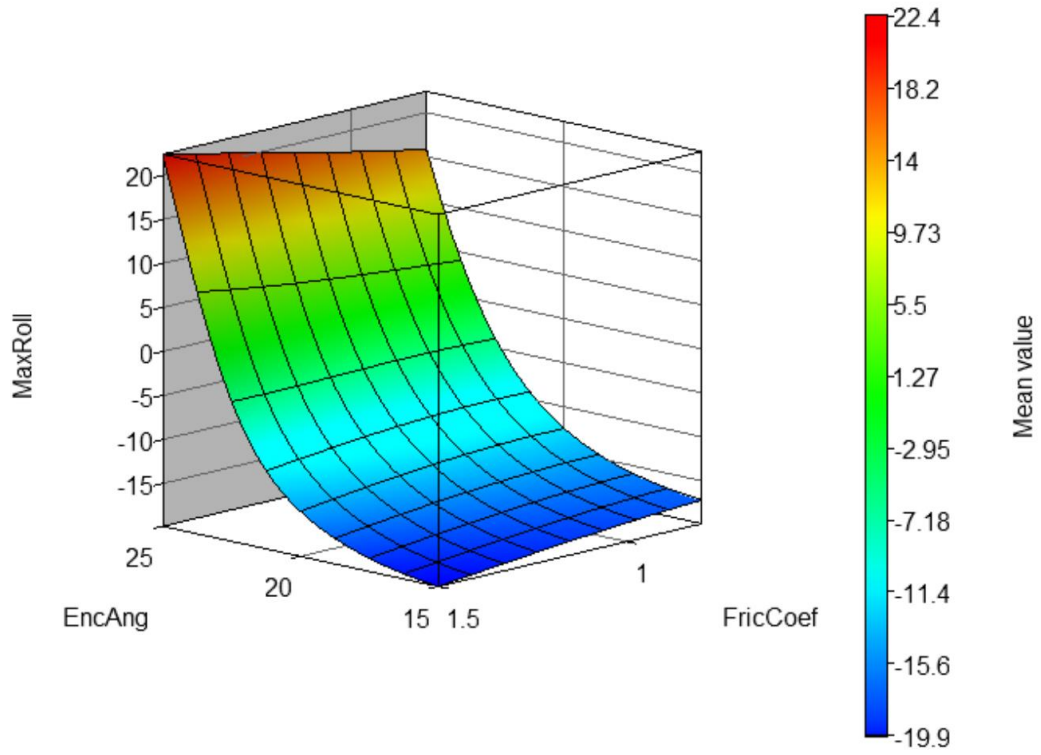


Figure 21. Maximum roll angle response surface as a function of the encroachment angle and friction coefficient.

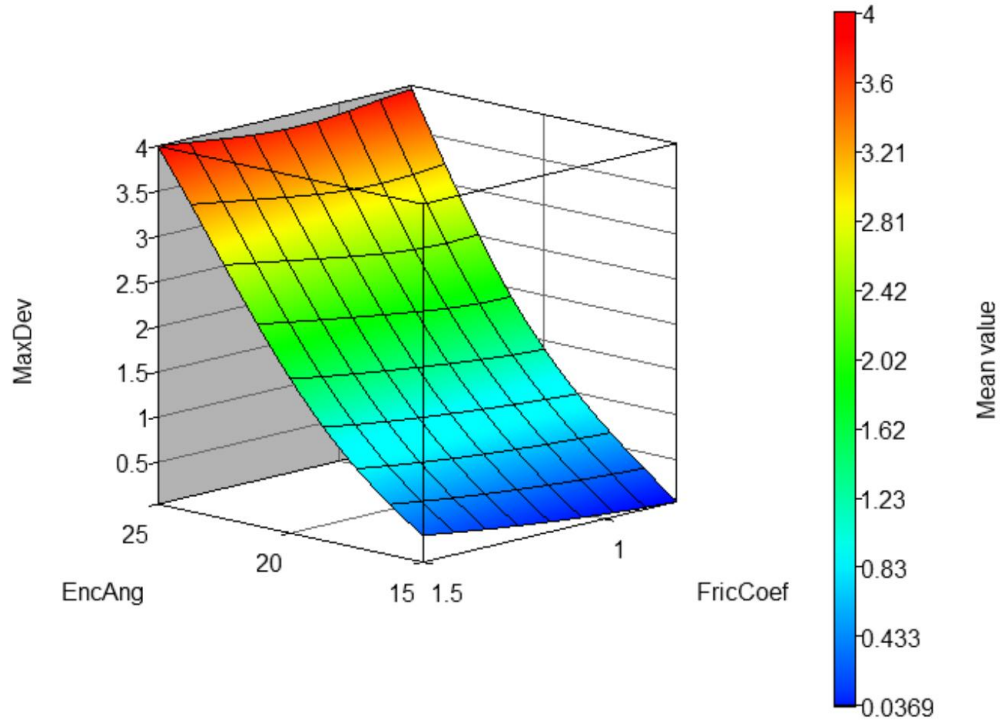


Figure 22. Lateral vehicular travel response surface as a function of encroachment angle and friction coefficient.

The quality of the maximum roll angle and vehicular lateral travel response surfaces are shown on Figure 21 and Figure 22, respectively. The metrics used for the quality of these surfaces are the RMS error and the coefficient of determination R^2 . The surface level of accuracy is improved with R^2 is valued at 1 or very close to 1 and RMS error is very small or closer to zero. Practical values are dependent on the problem at hand and the desired accuracy. The RMS error and R^2 values are calculated using the equations below.

The coefficient of determination R^2 and the RMS error are defined as:

$$R^2 = \frac{\sum_{i=1}^P (\hat{y}_i - \bar{y})^2}{\sum_{i=1}^P (y_i - \bar{y})^2} \quad [9]$$

$$\varepsilon_{RMS} = \sqrt{\frac{1}{P} \sum_{i=1}^P (y_i - \hat{y}_i)^2} \quad [10]$$

Where:

- P: number of design points.
- Y: predicted response.

- Y_i : mean of the responses.
- Y_i : the actual response.

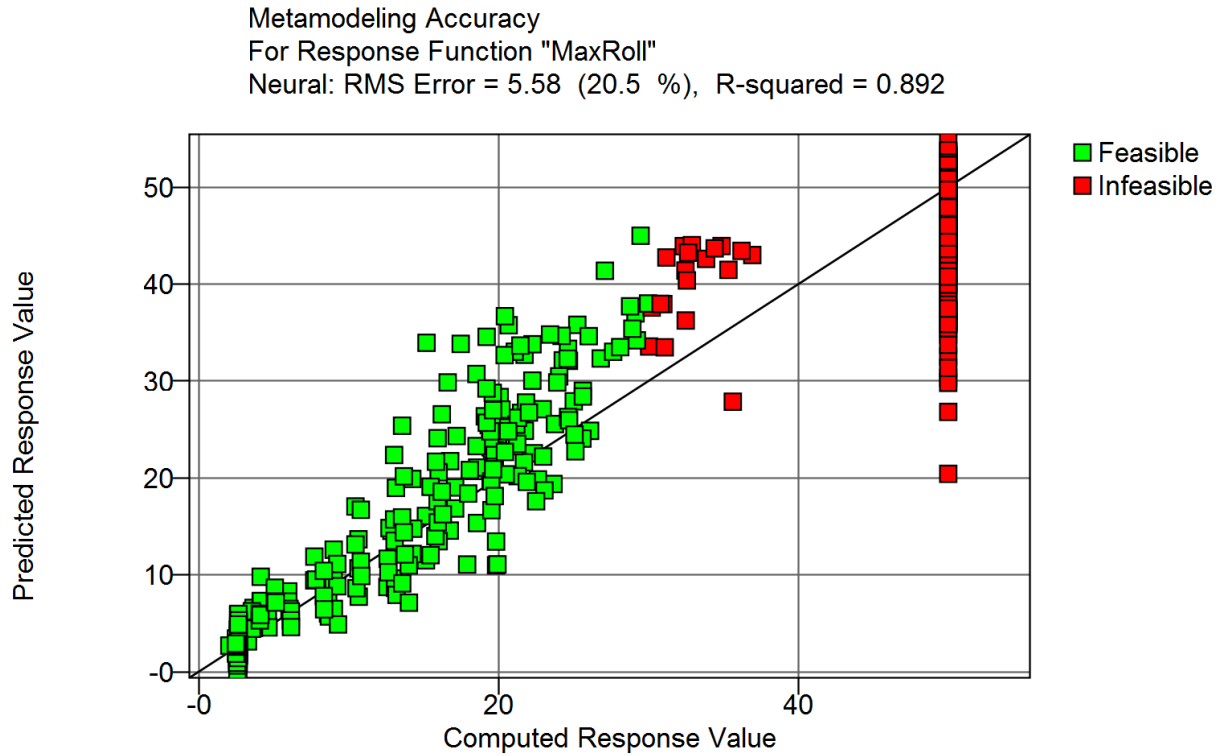


Figure 23. Quality of maximum roll angle response surface.

Metamodeling Accuracy
 For Response Function "MaxDev"
 Neural: RMS Error = 2.42 (29.9 %), R-squared = 0.901

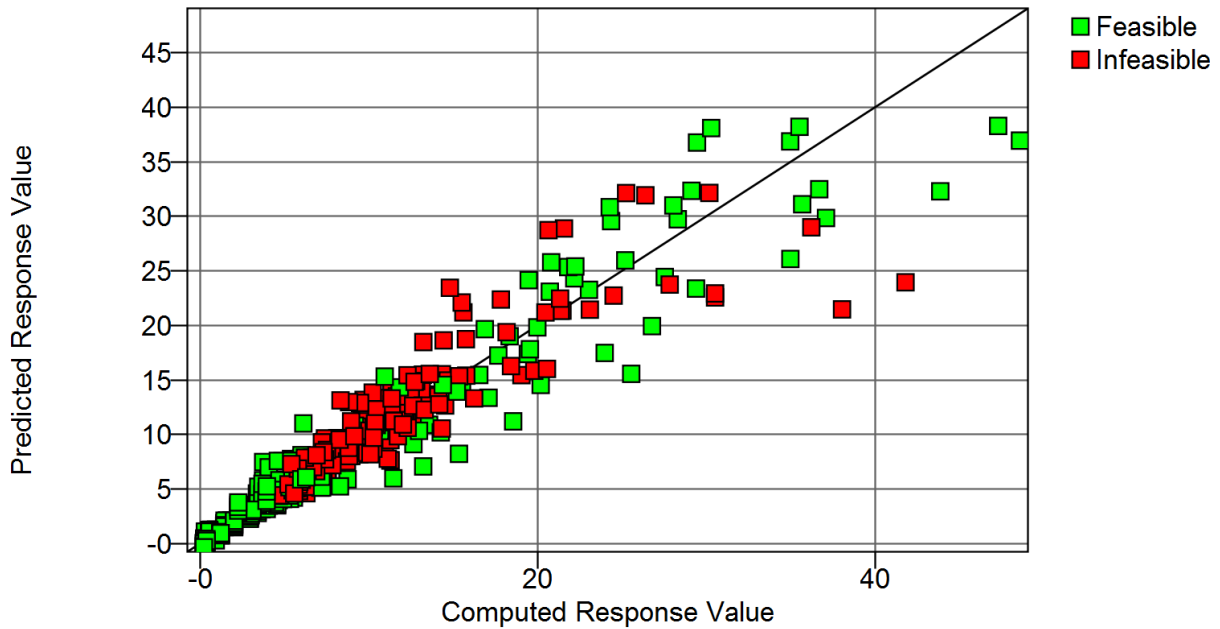


Figure 24. Quality of the lateral travel response surface.

A maximum 20° roll angle was set as a constraint therefore making points above 20° marked as infeasible. These points are shown as red squares as opposed the green square points.

Once Monte Carlos analyses are conducted on the response surfaces of interests, many useful measures that can be used in understanding the interrelationship between the design variables and the response of interest. Two entities are presented here, the ANOVA measure and the global sensitivity measure.

The analysis of variance (ANOVA) of the approximation to the experimental design is performed if a polynomial response surface method is selected.

The ANOVA results are viewed in bar chart format. Figure 25 shows ANOVA calculations for this study. The ANOVA bars show which design variable is important for the computation of the response. The ANOVA value is represented by the blue bar. The red bar indicates the confidence interval. When a red bar is too large, the value computed cannot be trusted. When the red bar is small, the confidence interval is small and the contribution of that variable is substantial. In this figure, the speed held the most substantial contribution. This

design variable also has a large confidence level. The radius of the roadway had both the smallest contribution and confidence level.

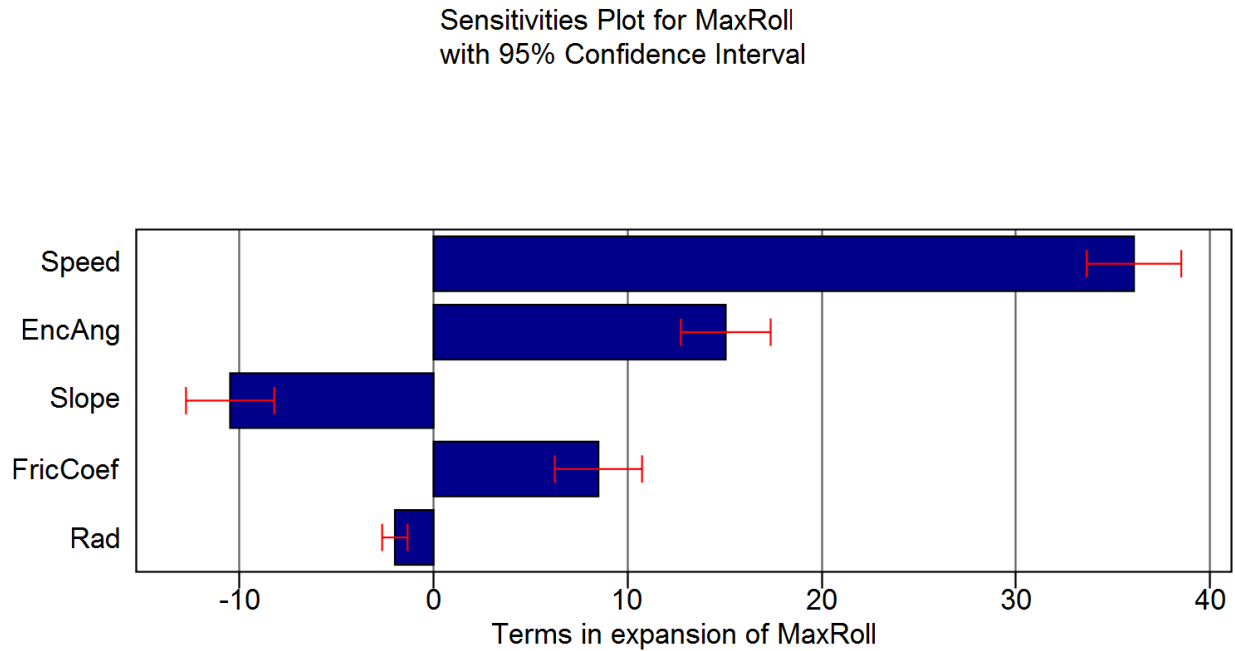


Figure 25. ANOVA bars for maximum roll angle.

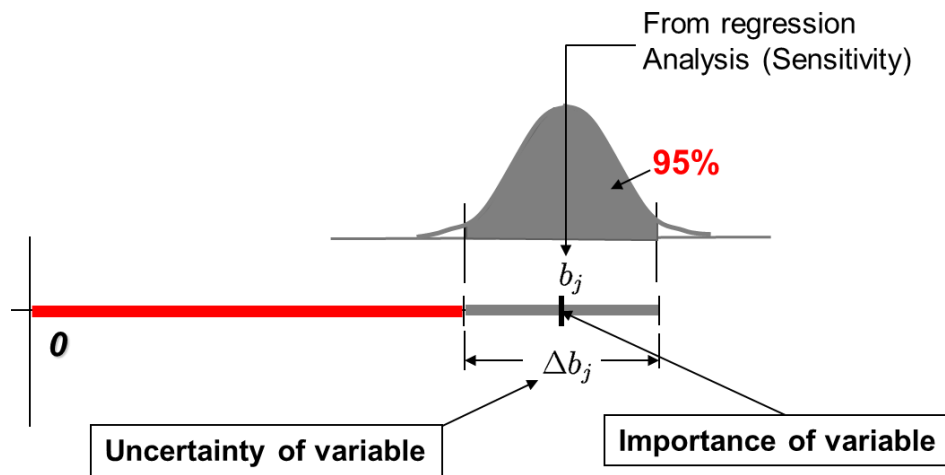


Figure 26. ANOVA value with 100(1-alpha)% confidence level.

Another measure is the global sensitivity measure. This measure is also known as the stochastic sensitivity analysis or Sobol's analysis. The variance of the response may be written using the Sobol's indices approach.

$$f(x_1, \dots, x_n) = f_0 + \sum_{i=1}^n f_i(x_i) + \sum_{i=1}^n \sum_{j=i+1}^n f_{ij}(x_i, x_j) + \dots + f_{1,2,\dots,n}(x_1, \dots, x_n) \quad [11]$$

Figure 27 shows the global sensitivities analysis. For the maximum roll angle, the speed has the greatest percentage of influence on the response. Encroachment angle holds the second largest influence for the maximum roll angle. For the maximum lateral travel, encroachment angle holds the greatest percentage of influence with the encroachment speed holding the second largest percentage.

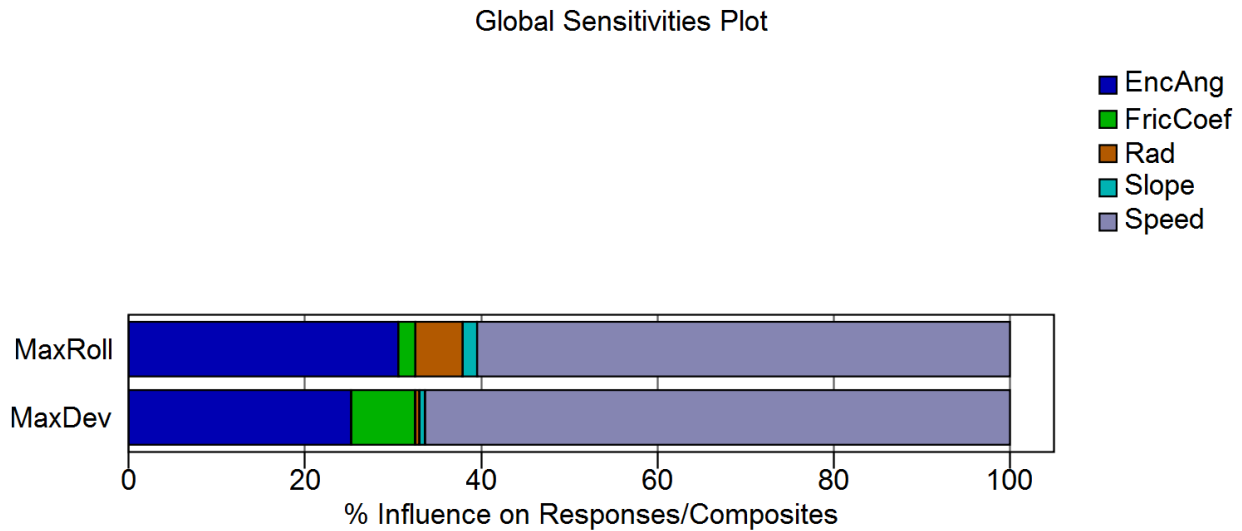


Figure 27. Sensitivity of the response on the design variables and encroachment conditions.

Higher accuracy of the response surface is desired for these measures. This may be achieved by:

- Adding statistically independent sampling points.
- Increasing the depth of the neural network learning layers.
- Including other meta-modeling methods.
- Combining the above steps.

CHAPTER 5: VERIFICATION AND COMPARISON OF VEHICLE DYNAMICS SIMULATIONS USING FINITE ELEMENT ANALYSIS

Researchers used varying levels of vehicle model complications ranging from lumped masses, springs, and dampers, to detailed finite element model representations using thousands of elements. All computer codes have limitations, and each considers different levels of assumptions. It is crucial that the codes selected are capable of accurately modeling relevant characteristics of the vehicle, terrain, and the interactions in a reasonable amount of time.

VEHICLE, TERRAIN, AND INTERACTIONS

The inertia of the vehicle and the mass moments of inertia play a major role in the behavior of the vehicle and must therefore be accurately quantified and modeled. This is due to the fact the inertial forces are key factors in any dynamic vehicle maneuver. Moreover, the suspension of the vehicle that links the sprung and unsprung mass needs to be modeled accurately to present the realistic behavior of the vehicle's dynamic response to a given maneuver such as traversing a slope or ditch.

Tires are the connection between the vehicle and the ground through the suspension system. Despite the simple functional description of them, their interaction mechanism with the ground is quite complicated. Finally, a model must account for steering of the vehicle to accurately capture the vehicle motion during the slope traversal. Driver's reaction is one of the most significant factors that can affect the vehicle's roll angle. The code selected for the simulation must have the capability to define driver's reaction in terms of steering angle, braking force, and acceleration.

The selected code must have capability of implementing the terrain conditions such as roadway, shoulders, back-, and foreslopes appropriately. Tire-terrain friction should be accurately defined based on the ground material/type to provide a realistic dynamic behavior during the slope traversal.

Vehicle body contact with terrain can also influence vehicle dynamics for roadside encroachments. The vehicle body to terrain contact may not be as crucial while the vehicle is traversing the foreslope; however, once the vehicle reaches the bottom of the slope, it is expected to encounter a sudden change in slope, which may result in vehicle body to terrain contact.

Ability of the selected solver to model this contact will be useful in evaluating the effect of height of fill to vehicle stability.

Following available code categories are briefly investigated in this study:

1. Multirigid-body dynamics codes (e.g., CarSim).
2. Non-linear finite element analysis codes (e.g., LS-DYNA) (16).

COMPUTATIONAL TIME AND ACCURACY

In addition to the specific simulation code to construct a realistic model of the vehicle, terrain, and interactions, it is important to evaluate the computational resources necessary to provide minimum acceptable accuracy of the model. Considering the detailed nature of finite element modeling methods, they require significantly large computation time to complete each simulation. For example, a simple 3–5 seconds driving maneuver simulated in a finite element code may require several days to finish; however, a similar simulation using vehicle dynamics code typically completes in less than 5 seconds. This is due to the large number of degrees of freedom involved in a finite element model like LS-DYNA as opposed to a multirigid-body vehicle dynamics code like CarSim.

Because of the considerably larger degrees of freedom in a finite element model, the code is capable of calculating stresses and deformations in the structure with great deal of accuracy. This feature is not available in vehicle dynamics codes, and hence finite element codes are extremely popular in crash simulations and other types of analyses requiring determination of loads and deformations.

Using finite element code does not necessarily provide better accuracy for recording vehicle dynamics maneuver. Earlier research compared use of LS-DYNA and CarSim in encroachment simulation of a 2000P Chevrolet C2500 and an 820C Geo Metro car on a 6H:1V foreslope (15). Figure 28 illustrates that the trajectory of the vehicles obtained from CarSim closely matched the trajectory of the vehicles obtained from LS-DYNA. The same simulation that required 16 hours run time with LS-DYNA, only needed 0.8 sec to complete using CarSim (both single core processor). Therefore, use of a multirigid-body dynamics code like CarSim was considered to be more feasible.

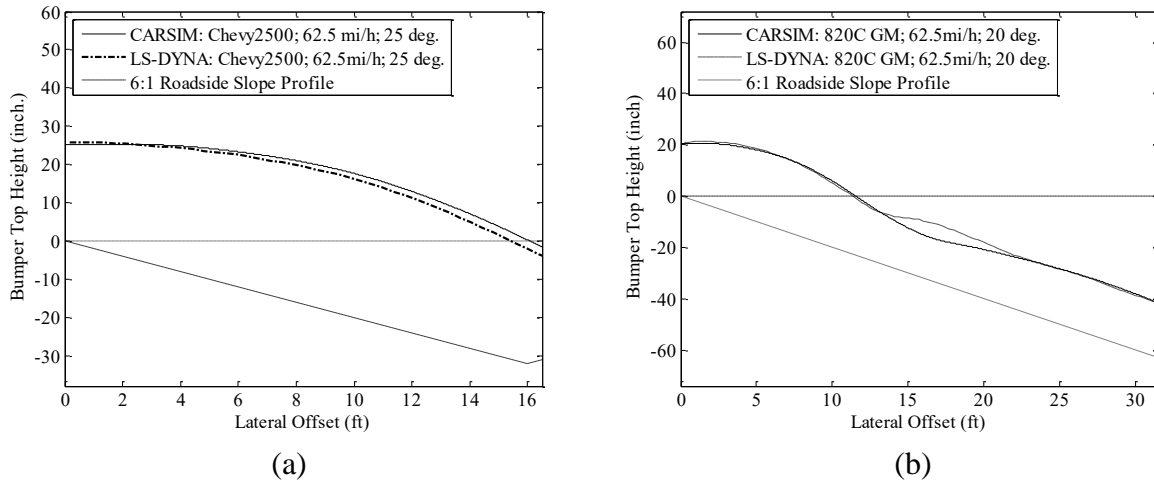


Figure 28. Comparisons of two codes, CarSim and LS-DYNA, in simulating vehicle encroachment events on slope (a) pickup truck encroachment and (b) passenger car encroachment.

Of the 1080 rollover scenarios in the data analytics database, four cases were modeled in LS-DYNA to compare the vehicle’s roll angle. A positive roll angle is a roll toward the passenger side of the vehicle. A negative roll is a roll toward the drivers’ side of the vehicle. Table 15 summarizes the vehicle dynamics simulation cases chosen to be modeled in LS-DYNA. The table includes vehicle type, mass of the vehicle, the speed, and the vehicle’s encroachment angle. For all cases, a straight road with a 3:1 ditch was used and a friction factor of 0.8. Driver inputs for all case were a constant target speed defined in the table below, no braking or shifting, a defined path set to 1.65 m to the right of the centerline of the road. A driver preview time of 1.5 seconds is set as well as a Maximum steering wheel angle of 720° and a maximum steering wheel angle rate of 1200 deg/s.

The finite element analysis models were set up as either one of two vehicles, small car or pickup truck, at specified velocities and encroachment angles to a 3:1 rigid slope. The vehicles used were a Toyota Yaris for the small car and a Chevrolet Silverado for the pickup. The roadway was modeled a flat horizontal sheet of shell elements at about 4.6 m wide by 38 m long. Connected to the edge of the roadway is the slop itself, which is another sheet of shell elements that drops down from the edge of the road way at an angle of 18.43° from the horizontal plane. The total distance of the slope in this direction is about 6.3 m (negative in z-direction 2 m by positive in y-direction 6 m). Then, the ground continues as a horizontal base of the slope for

50 m. The main contact resides between the vehicle of the simulation and the rigid ground surface. This contact is defined as an automatic surface to surface through LS-PrePost for the part sets of these two entities, and it includes all parts of the vehicles.

Table 15. Summary of simulation cases used in FEA.

Design Variable	Vehicle Dynamics Simulation				Finite Element Modeling			
	Case 1	Case 2	Case 3	Case 4	Case 1	Case 2	Case 3	Case 4
Vehicle type	Pickup Truck	Pickup Truck	Class C Hatchback	Class C Hatchback	Chevrolet Silverado	Chevrolet Silverado	Toyota Yaris	Toyota Yaris
Mass (kg)	1998	1998	1270	1270	2225	2225	1048	1048
Speed (km/h)	110	80	110	120	110	80	110	120
Encroachment angle (deg.)	15	25	15	25	15	25	15	25

Case 1 is a Pickup Truck encroaching at a 15° angle at a speed of 110 km/h. Figure 29 shows the results of the vehicle dynamics simulation. A positive roll angle is a roll toward the passenger side of the vehicle. A negative roll is a roll toward the drivers' side of the vehicle. The truck experiences a maximum roll angle of 25.62° when navigating back to the road. The truck is able to successfully navigate back to the path. In the first case, the vehicle being used is the Chevrolet Silverado with the intent of mimicking the no-roll full-size SUV situation from CarSim. This situation includes the standard ground model with a 3:1 rigid slope and a coefficient of both static and dynamic friction being 0.8. The initial velocity of the truck is set at 110 km/h (68.35 mph) with an encroachment angle of 15° on the roadway. The truck does not roll in this scenario, which is the result CarSim calculated as well. Figure 30 shows the results from the simulation. However, there is no steering imparted into either vehicle used in the finite element simulations. Steering is imparted into the vehicles in CarSim to act as a driver would as the slope were encountered. The addition of steering into the models and simulations would change the friction experienced when the leading tire (passenger front tire) comes into contact with the ground. A corrective steering measure toward the left side (driver's side direction) of the vehicle would force the tire to slide parallel to its rotation axis as opposed to promoting the rolling of the wheel. This is one component of the simulation that has the potential to increase the chance of rolling if this were used. Figure 33 and Figure 34 show the roll angle and lateral tracking history for this case. The roll rate in Figure 33 is in radians per seconds.

Figure 31 and Figure 32 show the results of the Pickup Trucks' roll angle for both modeling methods. The maximum roll angle for the finite element modeling was about 26° while

the maximum for the vehicle dynamics simulations was about 23°. Figure 33 and Figure 34 show the results for the lateral displacement. In Figure 33, the target line refers the vehicle's path that is user specified.



Figure 29. Pickup truck encroaching at a 15° angle at a speed of 110 km/h (CarSim).

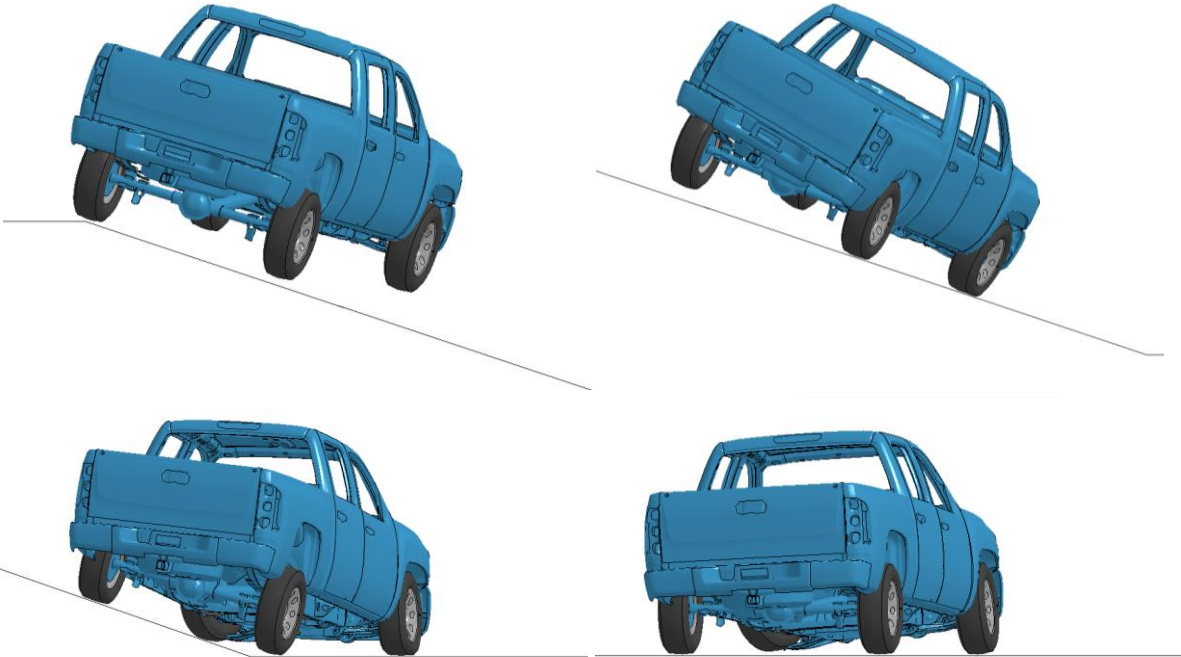


Figure 30. Pickup truck encroaching at a 15° angle at a speed of 110 km/h (FEA).

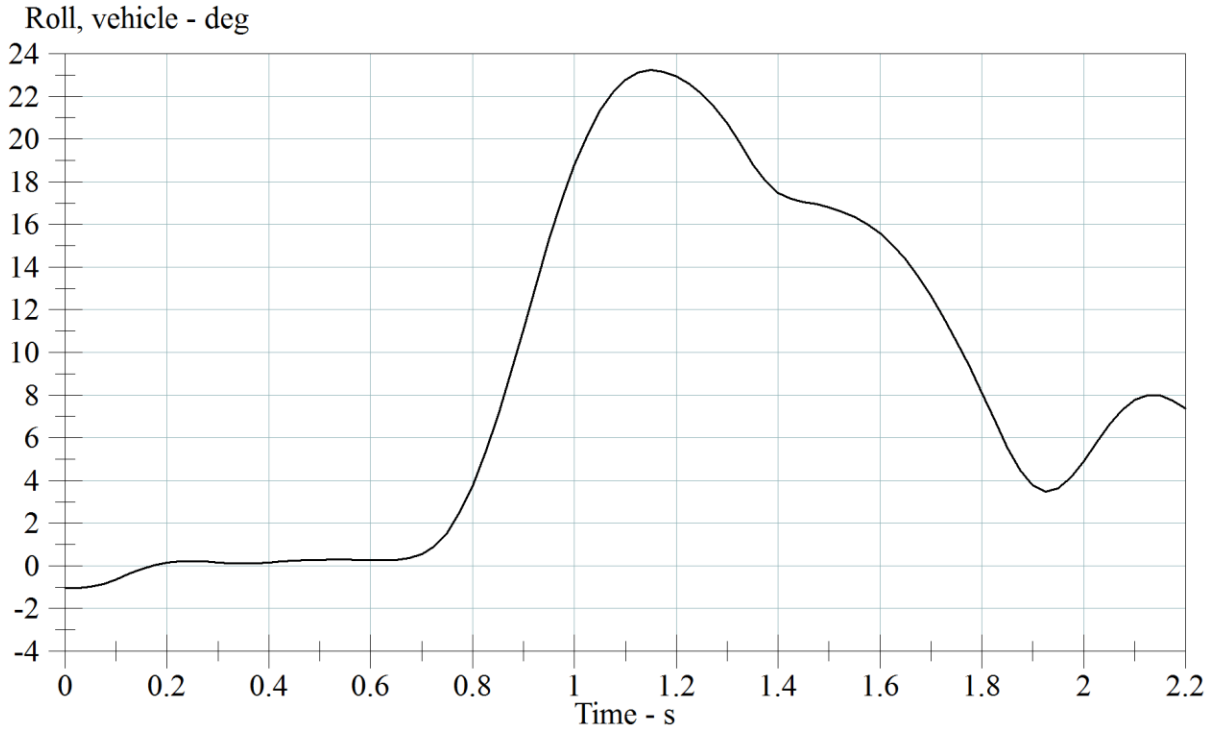


Figure 31. Roll angle results—Case 1 (CarSim).

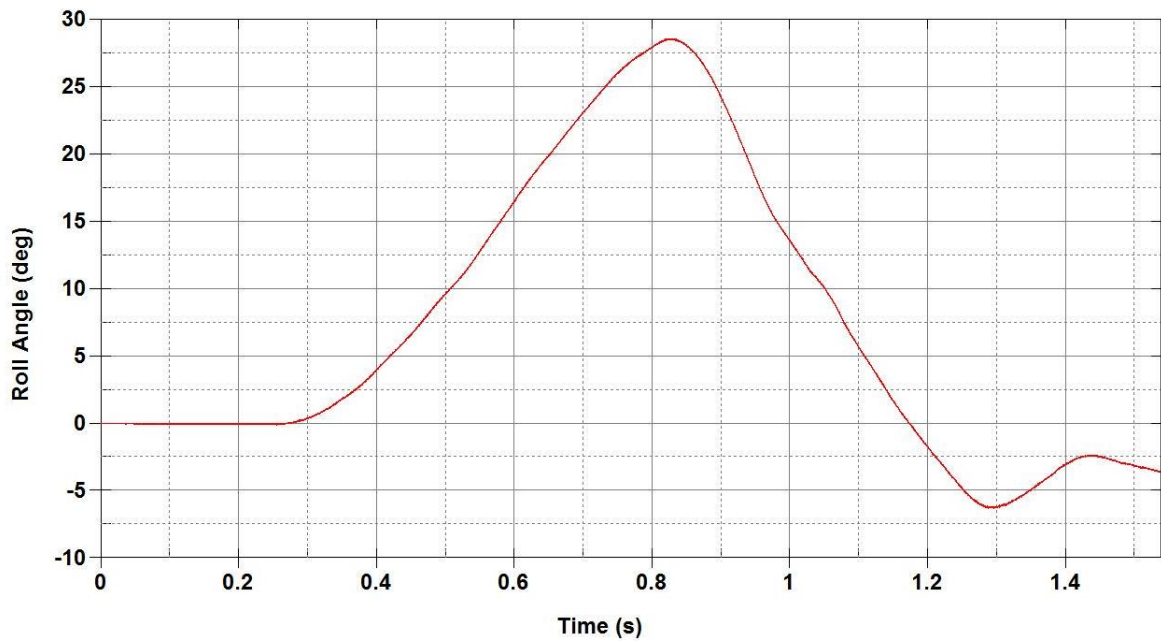


Figure 32. Roll angle results—Case 1 (FEA).

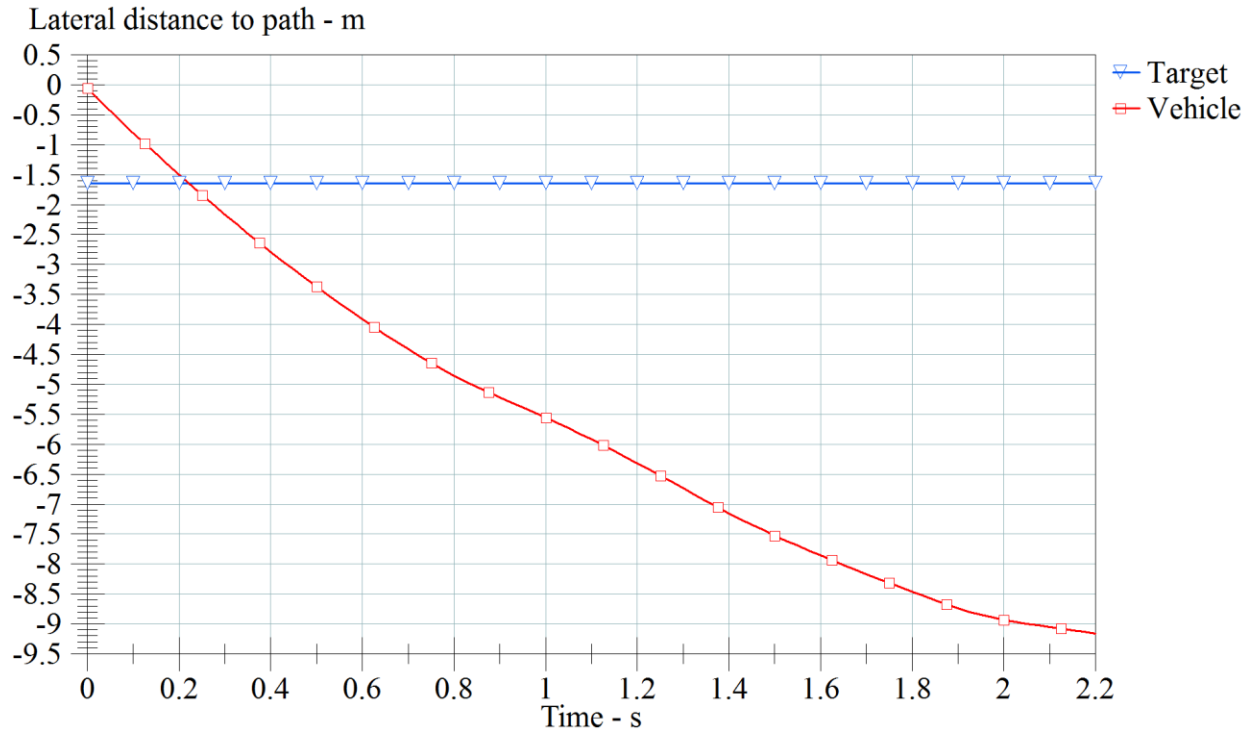


Figure 33. Lateral displacement—Case 1 (CarSim).

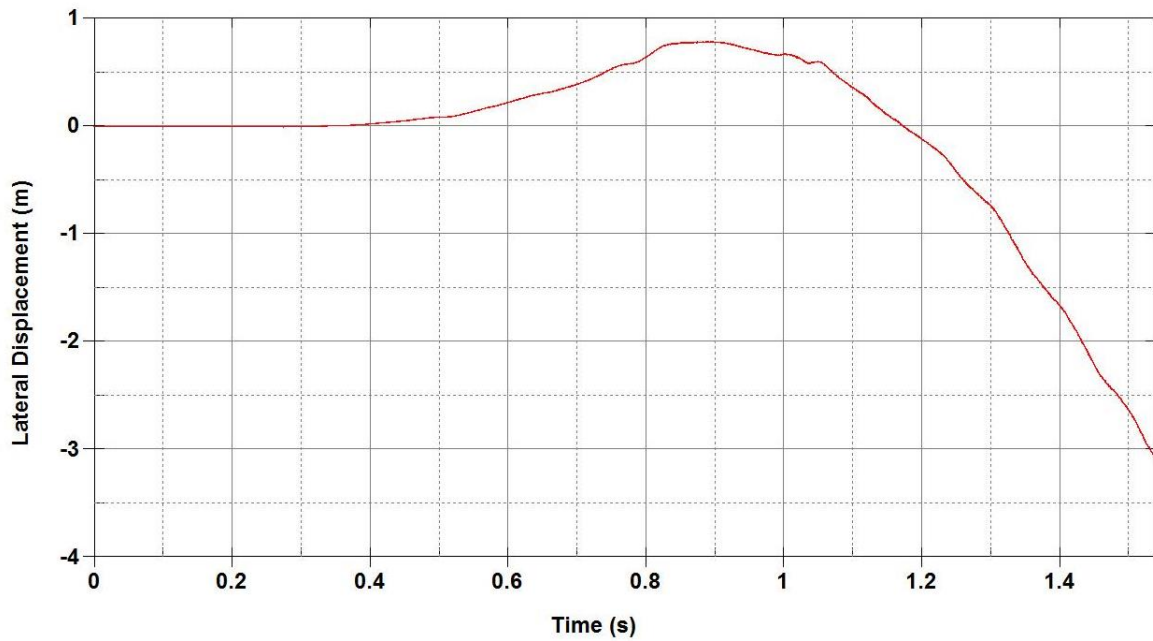


Figure 34. Lateral displacement—Case 1 (FEA).

Case 2 is also a Pickup Truck traveling on a straight road. The Pickup Truck experiences a maximum roll angle of 31° when navigating back to the road. The vehicles roll angle is in degrees while the lateral tracking is in meters. The steering would more closely make an impact

in the simulation of the second case. Figure 36 shows the results of the simulation in CarSim. The second case involves the same truck, slope, and friction attempting to model the rolling full-size SUV scenario from CarSim. The truck in this scenario is heading at 80 km/h (49.71 mph) with an encroachment angle of 25° . Despite the lower speed, the larger encroachment angle increases the amount of pitch the vehicle experiences as it flies through the air. This causes the vehicle to favor rolling over in the CarSim simulation, but this same result is not experienced in the finite element analysis model. The simulation results are shown in the lack of steering in the finite element analysis simulation may be a factor in this situation. Figure 36 shows the results of the analysis. Figure 38 and Figure 37 show the results of the roll angle for the vehicle dynamics simulation and finite element modeling, respectively. Figure 39 and Figure 40 show the lateral displacement in meters of both modeling methods.



Figure 35. Pickup truck encroaching at a 25° angle at a speed of 80 km/h.

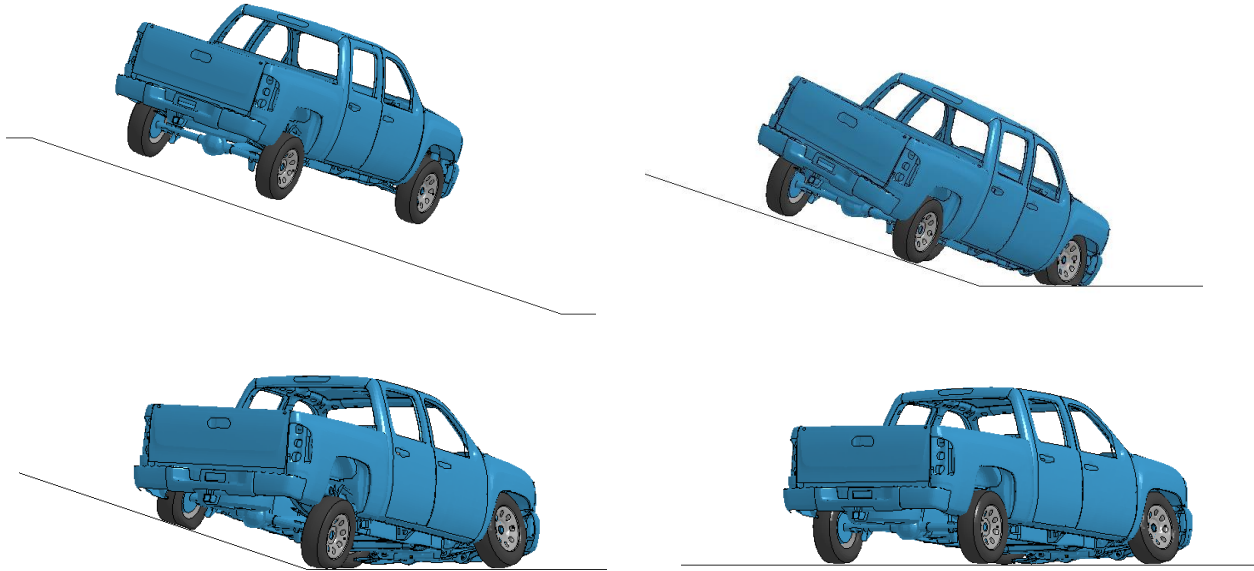


Figure 36. Pickup truck encroaching at a 25° angle at a speed of 80 km/h.

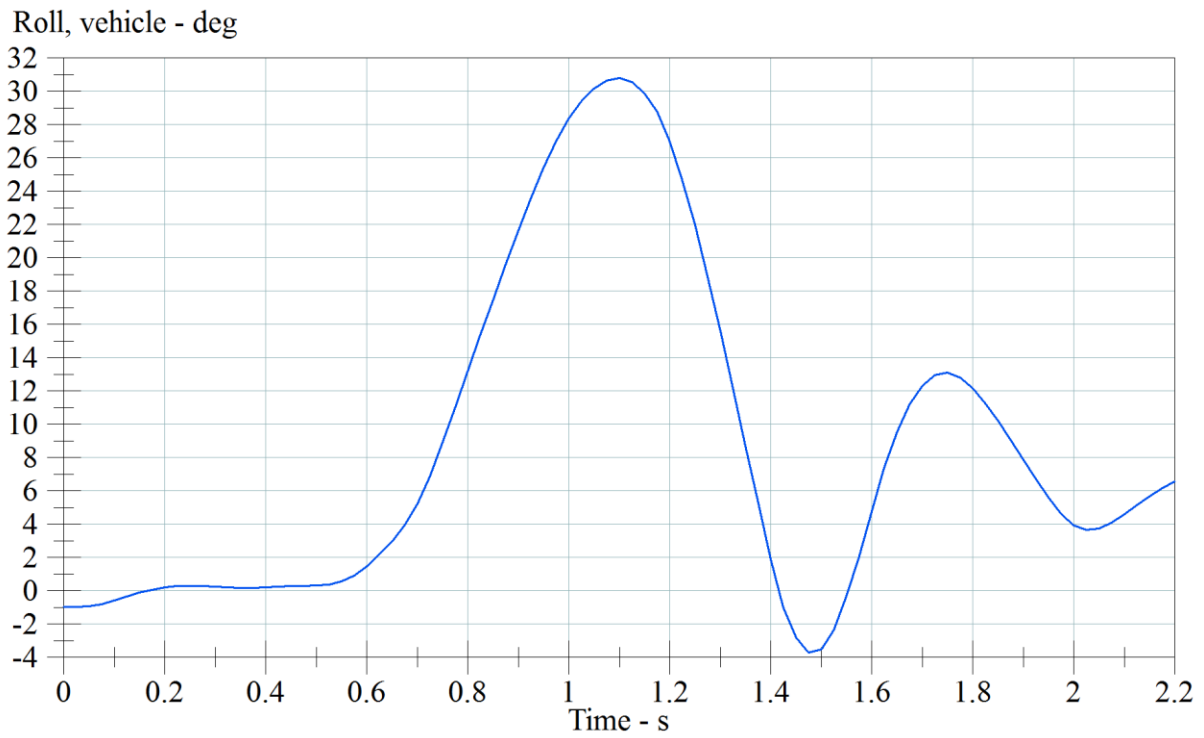


Figure 37. Roll angle results—Case 2 (FEA).

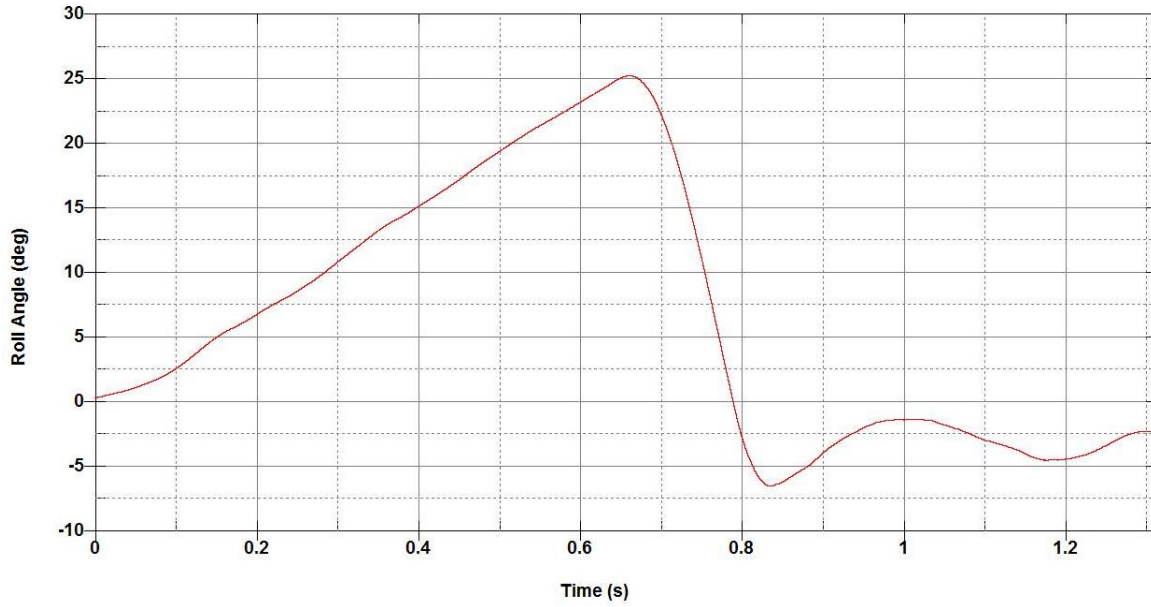


Figure 38. Roll angle results—Case 2 (CarSim).

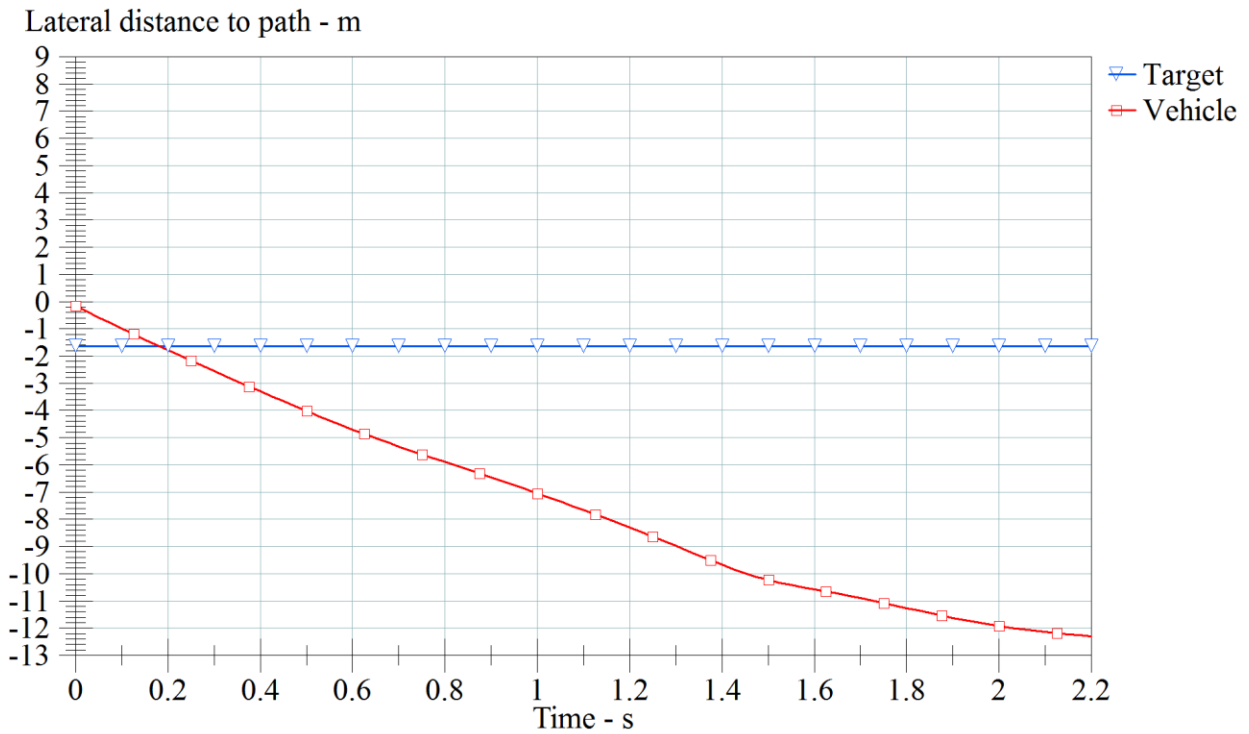


Figure 39. Lateral displacement—Case 2 (CarSim).

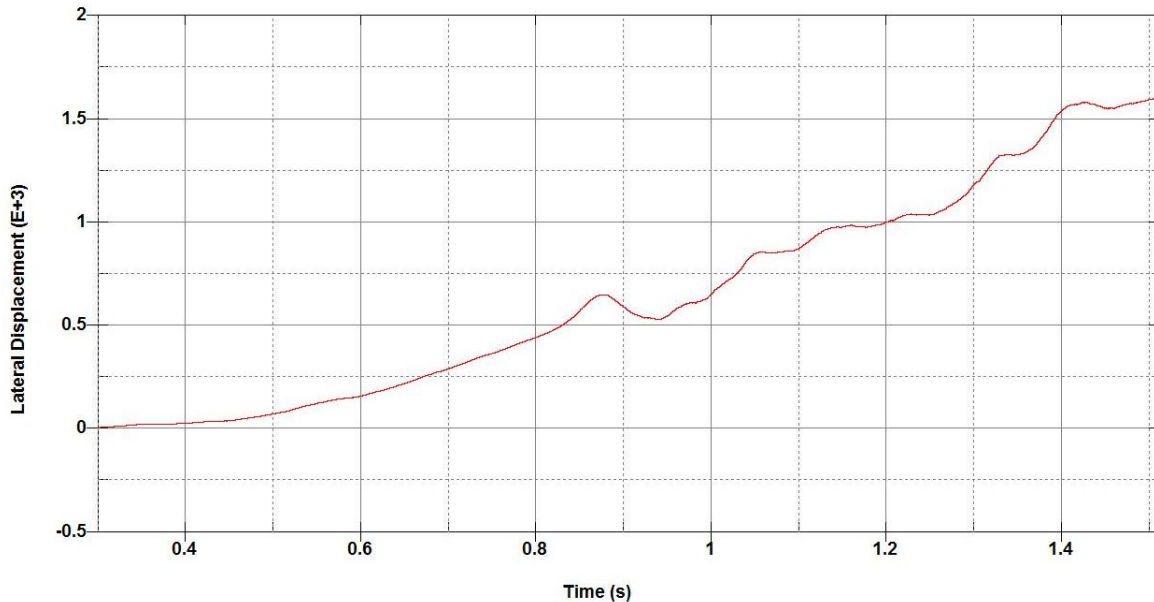


Figure 40. Lateral displacement—Case 2 (FEA).

Case 3 is Class C hatchback with a 15° encroachment angle traveling on a straight road with a side-slope ratio of 3:1 with a low roll angle. Figure 41 shows the results of the vehicle dynamics simulation using CarSim. The car experiences a maximum roll angle of 22° when navigating back to the road. The third case involved the use of the smaller car model, the Toyota Yaris, on the same 3 to 1 rigid slope and coefficient of friction being 0.8. This is to model the no-roll scenario for the small car as resulted from CarSim. The car has an initial velocity of 110 km/h (68.35 mph) with an encroachment angle of 15° to the edge of the roadway. The car in this case shares the same CG with the CarSim model, but there does not exist any steering correction, as stated before. The vehicle does not roll but simply flies in the air over the slope and later lands on the ditch. Figure 42 shows the results of the finite elements simulations using LS-DYNA. Figure 43 shows the time history of the vehicular roll angle using CarSim. The car was able to successfully navigate back to the designated path. The roll angle is in degrees while the lateral tracking is in meters. Figure 44 shows the time history of the vehicular roll angle using LS-DYNA. Figure 45 and Figure 46 show the lateral tracking history for CarSim and LS-DYNA respectively.



Figure 41. Class C hatchback departing at a 15° encroachment angle at a speed of 110 km/h.

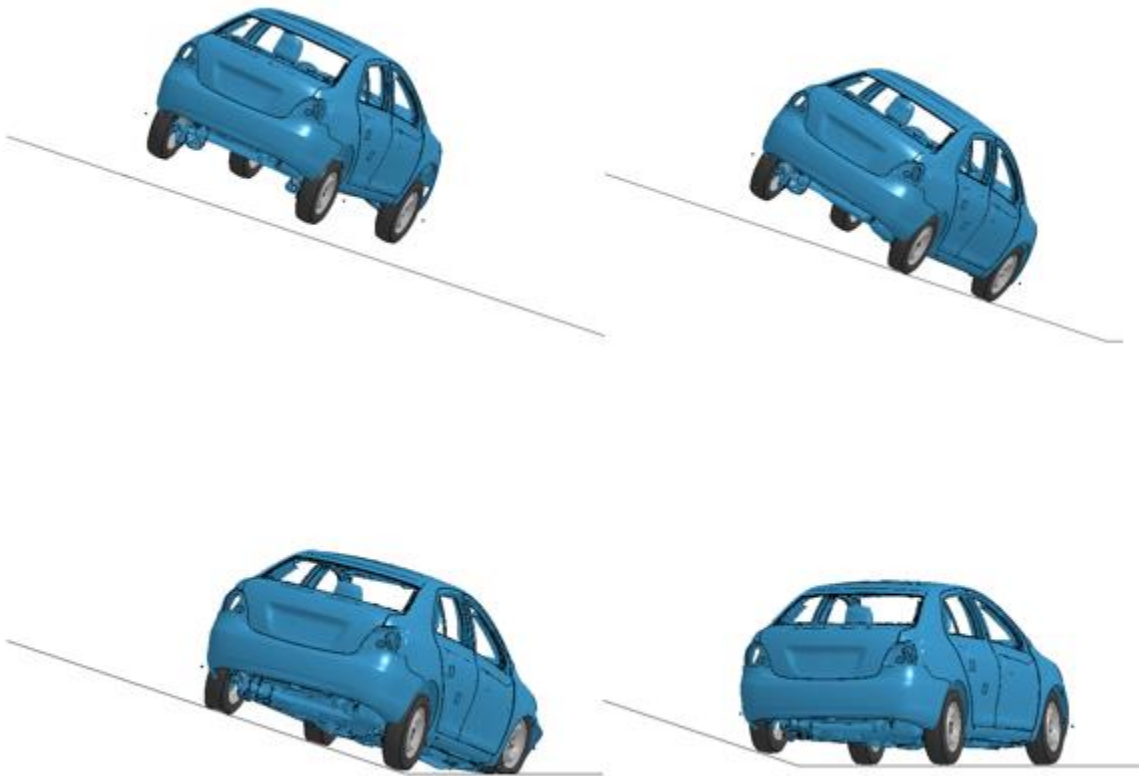


Figure 42. Toyota Yaris encroaching at a 15° angle at a speed of 110 km/h.

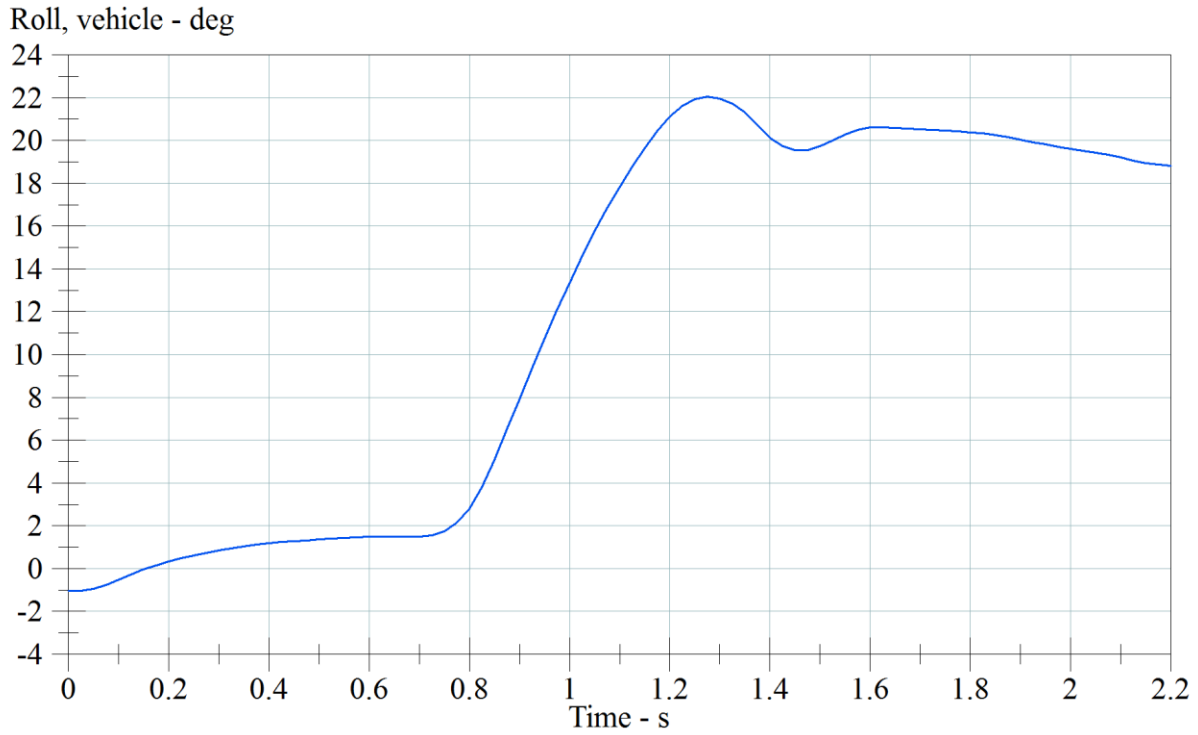


Figure 43. Roll angle results—Case 3 (CarSim).

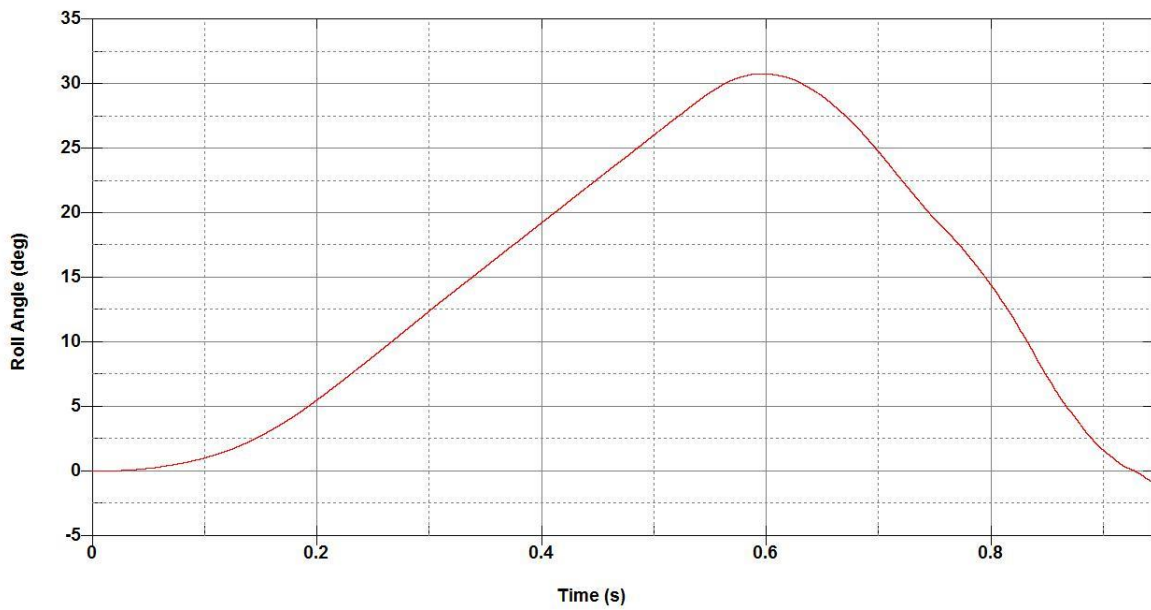


Figure 44. Roll angle results—Case 3 (FEA).

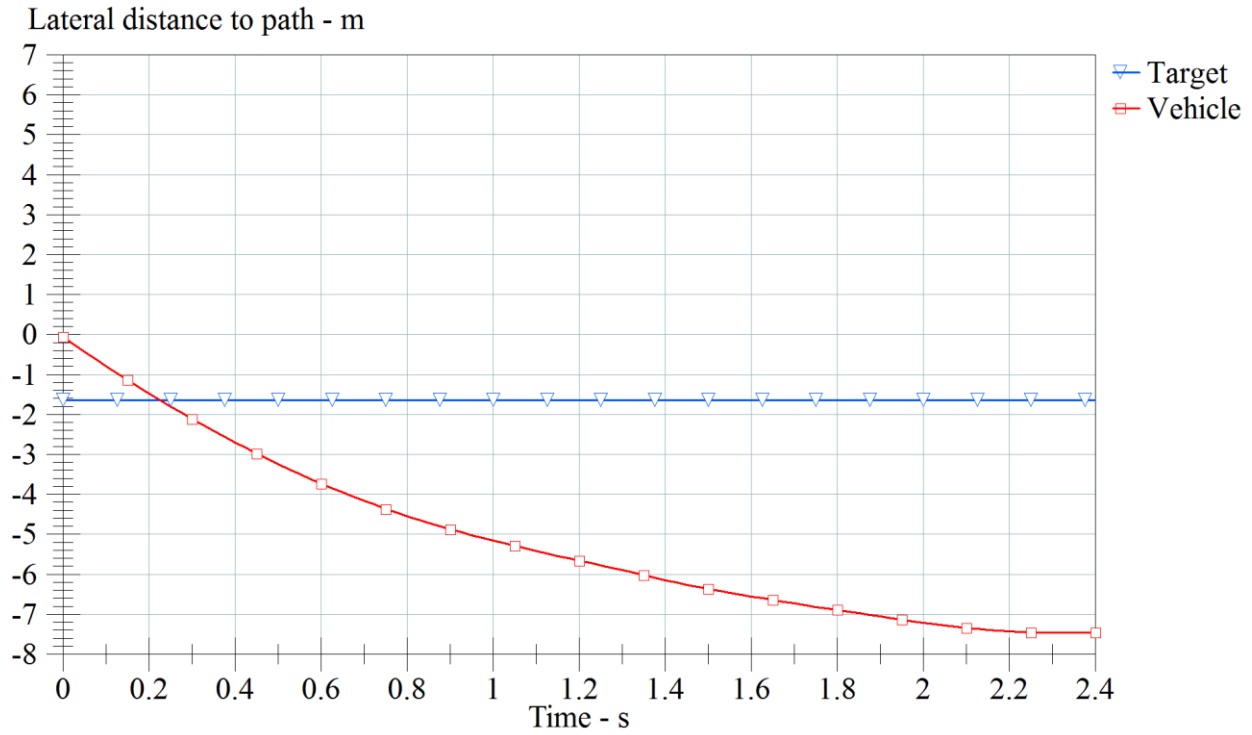


Figure 45. Lateral displacement results—Case 3 (CarSim).

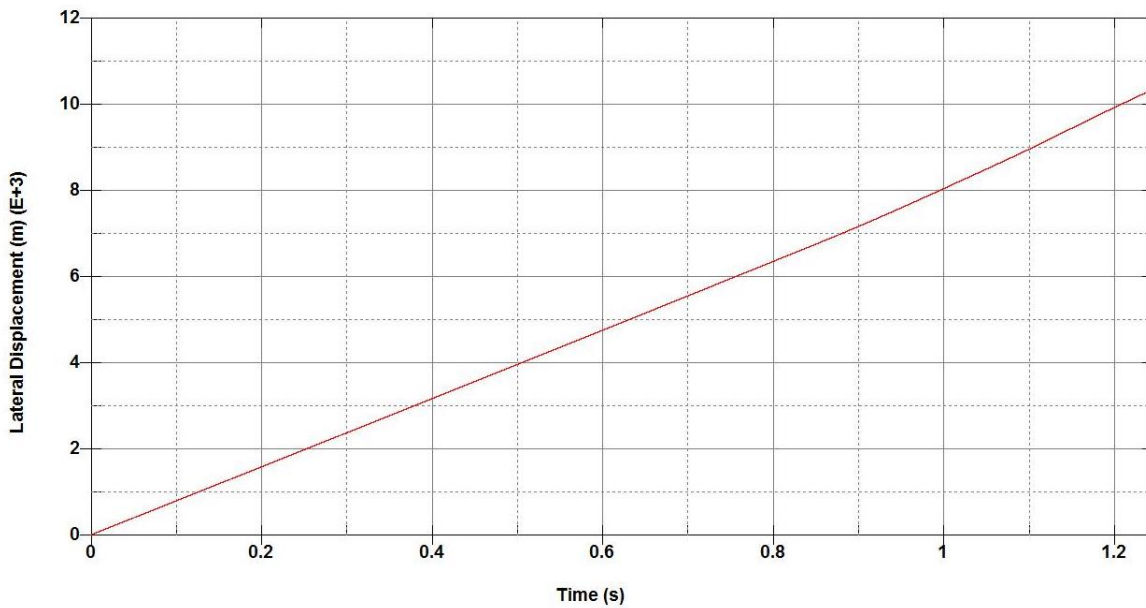


Figure 46. Lateral displacement results—Case 3 (FEA).

Case 4 is a Class C hatchback with a 25° encroachment angle traveling on a straight road with a side-slope ratio of 3:1 with a high roll angle. Figure 49 and Figure 50 show the roll angle and lateral tracking history for case 4. Figure 47 shows the results of the vehicle dynamics

simulation. The car experiences a maximum roll angle of 28° when navigating back to the road. The vehicle was successful in navigating back onto the path. Figure 49 and Figure 51 show the roll angle and lateral tracking results from this modeling method. The last case is for the same car to replicate the rolling car situation from CarSim. The car is traversing the same rigid slope model with the same coefficient of friction. The car has an initial velocity of 120 km/h (74.56 mph) and approaches the roadside at an encroachment angle of 25° . In this case, the car also does not roll, but the results of this case show the highest amount of rolling angle experienced by any of the cases. The vehicle impacts the ground dragging its front bumper and passenger side wheel, but does not roll over itself and rocks back to all four wheels on the ground. Figure 48 shows the results of the simulation. The suspension then forces another rolling motion onto the vehicle, and after all four wheels are on the ground, the driver's side of the vehicle begins to lift up again in a rolling motion. This rolling motion was not anticipated mainly because it was expected that any chance of rolling would occur immediately after the vehicle reached the base of the slope or when the vehicles' wheels impacted the ground.



Figure 47. Class C hatchback encroaching at a 25° angle at a speed of 120 km/h.

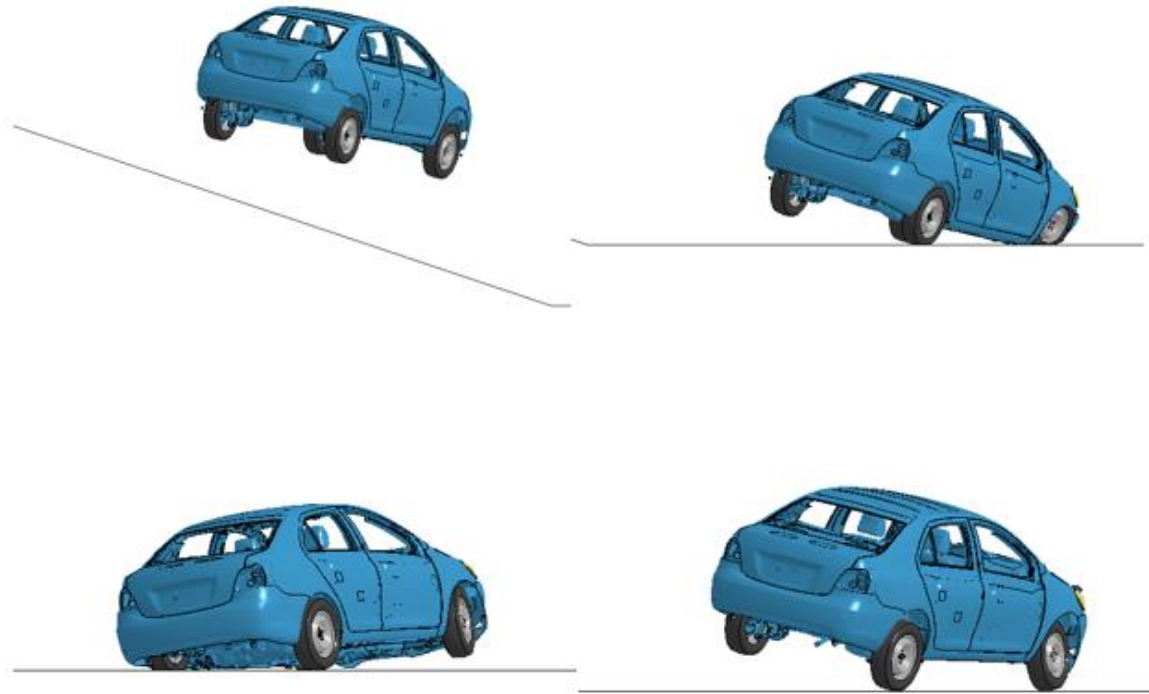


Figure 48. Toyota Yaris encroaching at a 25° angle at a speed of 120 km/h.

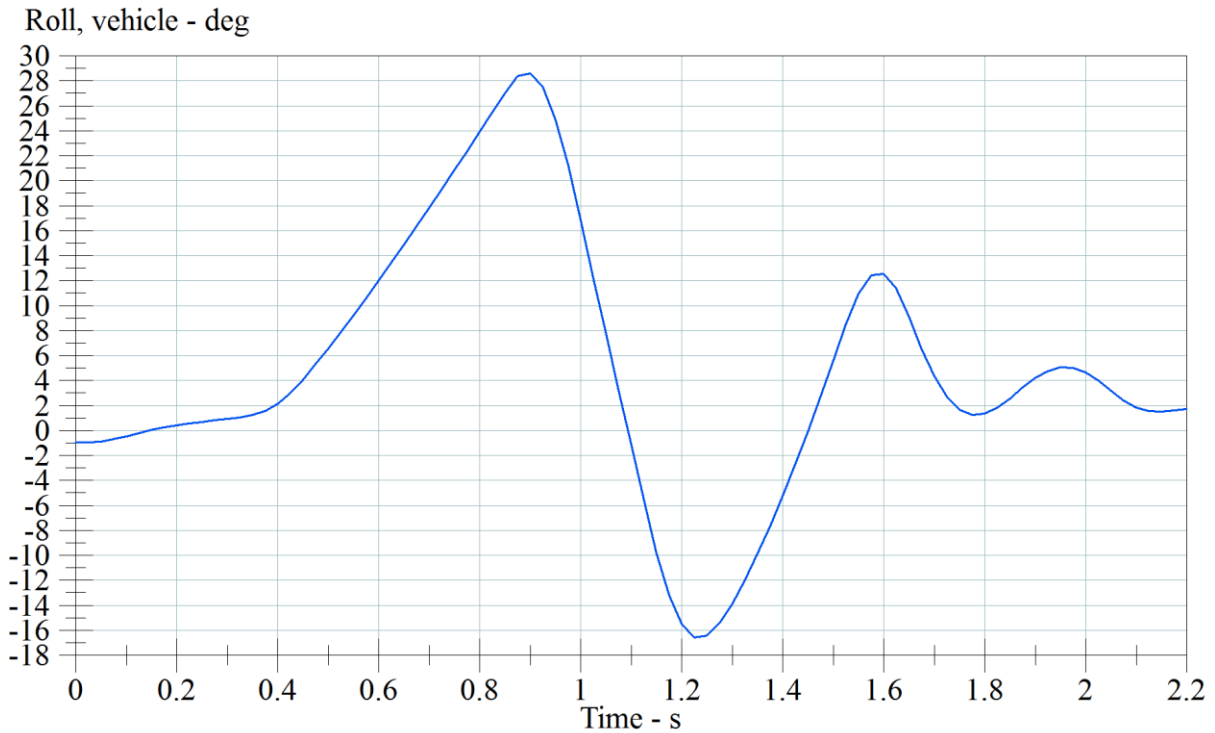


Figure 49. Roll angle results—Case 4 (Carsim).

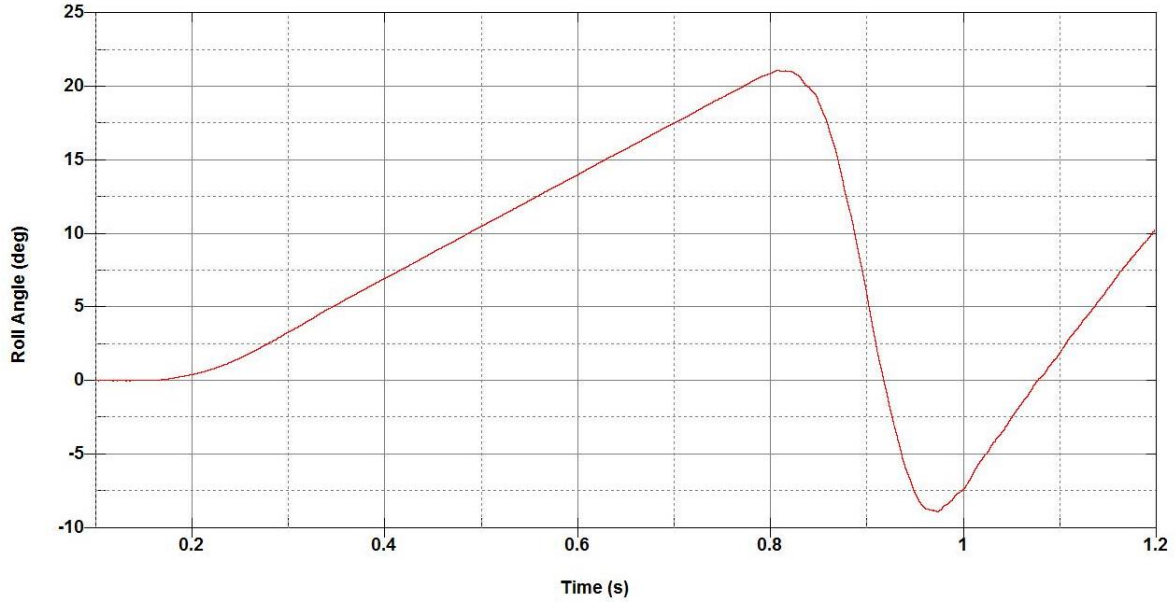


Figure 50. Roll angle results—Case 4 (FEA).

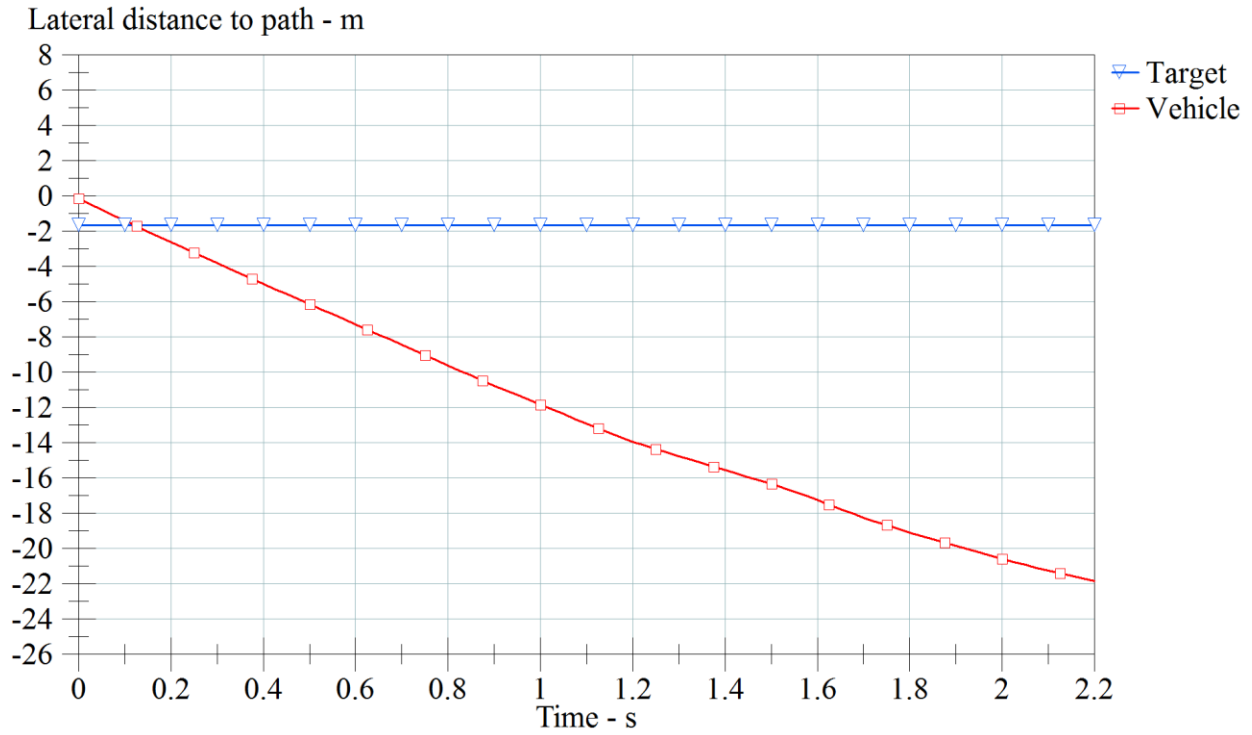


Figure 51. Lateral displacement results—Case 4 (CarSim).

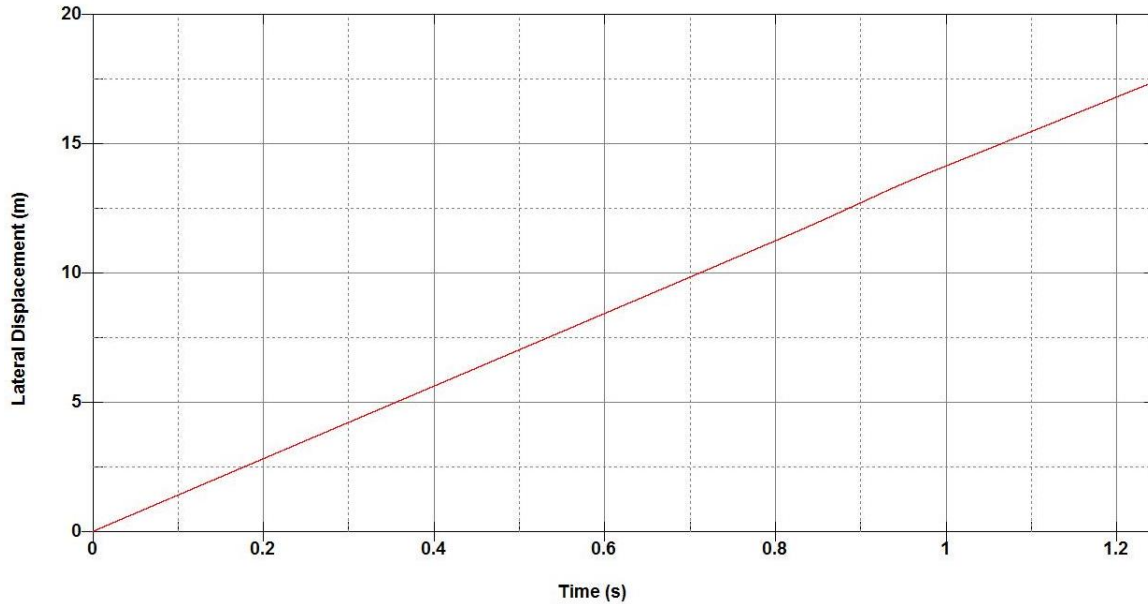


Figure 52. Lateral displacement results—Case 4 (FEA).

All vehicles in the finite element simulations had higher airborne time than the CarSim models. This would lead one to think that rolling is favored in all scenarios as it allows the vehicle to roll and change in pitch as it travels through the air. Another noteworthy feature of the finite element analysis situations is that the computer runtime involved with carrying out the LS-DYNA computations is many magnitudes larger than the computational runtime and effort required by the CarSim program. This favors the use of CarSim for its computational efficiency and its design for these vehicle dynamics simulations.

CHAPTER 6: CONCLUSIONS AND RECOMMENDATIONS

The main goal of this research was to enhance our understanding of a vehicle's propensity to rollover using vehicle dynamics simulations instead of crash data. The rollover crash is one of the most fatal forms of crashes among passenger vehicles. In 2015, they accounted for one third of all occupant fatalities. Forty-eight percent of crashes occurred on rural roads and 45 percent occurred on urban roads. The percentage of fatalities in rollover crashes was highest for SUVs, followed by pickup trucks, vans, and passenger cars. Although there are many vehicular technical innovations that act as a preventative or protective improvement, rollover crashes and subsequent loss of life are still highly represented in crash statistics. Limited studies investigated the initiating mechanisms contributing to a vehicle's propensity to roll over. Expanding the knowledge on initiating factors would enhance our understanding of roadway, vehicular, and human factors affecting rollover events. Side-slopes and ditches have been identified as the primary tripping mechanisms in single vehicle ran-off road rollovers. Researchers used varying levels of vehicle model complications ranging from lumped masses, springs, and dampers to detailed finite element model representations using thousands of elements. All computer codes have limitations, and each considers different levels of assumptions. It is crucial that the codes selected are capable of accurately modeling relevant characteristics of the vehicle, terrain, and the interactions in a reasonable amount of time.

Using CarSim and LS-OPT, vehicle rollover scenarios and meta-models for data analytics were built. For vehicle simulations, a fixed superelevation of 6 percent was assumed. Four road curvatures, three side-slopes, seven different speeds and three encroachment angles were used to create the simulations. A total of 1602 rollover scenarios was created on CarSim using four different vehicles. It was deduced that:

- The Full Size SUV was more likely to rollover than the Class C Hatchback due to its static stability factor.
- For both the roll angle and lateral displacement, speed held the greatest influence on the vehicle's propensity to rollover followed by encroachment angle.
- Vehicles traveling at a higher encroachment angle are more likely to roll over.

Rollover scenarios created in CarSim showed that the Full Size SUV was more likely to rollover than the Class C Hatchback. This is similar to data from NCHRP 17-22 showing that light trucks are more likely to rollover than cars. These scenarios were used as raw data to be input into LS-OPT. For meta-model building, the vehicle rollover scenarios were first divided into categories. For both roll angle and lateral displacement, speed had the greatest influence on the vehicle's propensity to rollover followed by the encroachment angle. The SUV was more likely to roll over due to its static stability factor. The vehicles traveling at a 25° encroachment angle were more likely to roll over than those traveling at a 20° or 15° angle.

Researchers used 1080 of the vehicle simulations in data analytics. These simulations were used to create a neural network response surface, which was then used in the Monte Carlo analyses. The Monte Carlo analysis provides a useful measure to understand the interrelationship between the design variables and the response surface. For both the maximum roll angle and lateral tracking, speed had the greatest influence on the variables with encroachment angle having the second greatest influence. It is important to study factors of roadway design since these are factors that can be changed to create safer roadway conditions. One cannot control how drivers navigate the road, but posted speeds and other roadway characteristics such as side-slope and ditches are factors that can be modified to ensure drivers are using the safest road possible.

For future work, more variables could be implemented into the vehicle dynamics simulations within a Machine Learning (ML) architecture. Ditches, roadway shoulders, and tire-soil interaction are a just a few that can be implemented into the data analytics. Automating vehicle dynamics simulations for improvement of the quality of the response surface may also be considered for future work. Figure 53 shows how this additional step may be implemented. A massive number of runs would be input into the ML to create a response surface, sensitivities, and trends. The quality of the ML quality shall be analyzed using the RMS error and the coefficient of determination. Improvement of quality may be achieved using the following steps or a combination thereof:

- Adding statistically independent sampling points.
- Increasing the depth of the neural network learning layers.
- Including other meta-modeling methods.

This cycle will continue until the desired quality of the response surface is achieved.

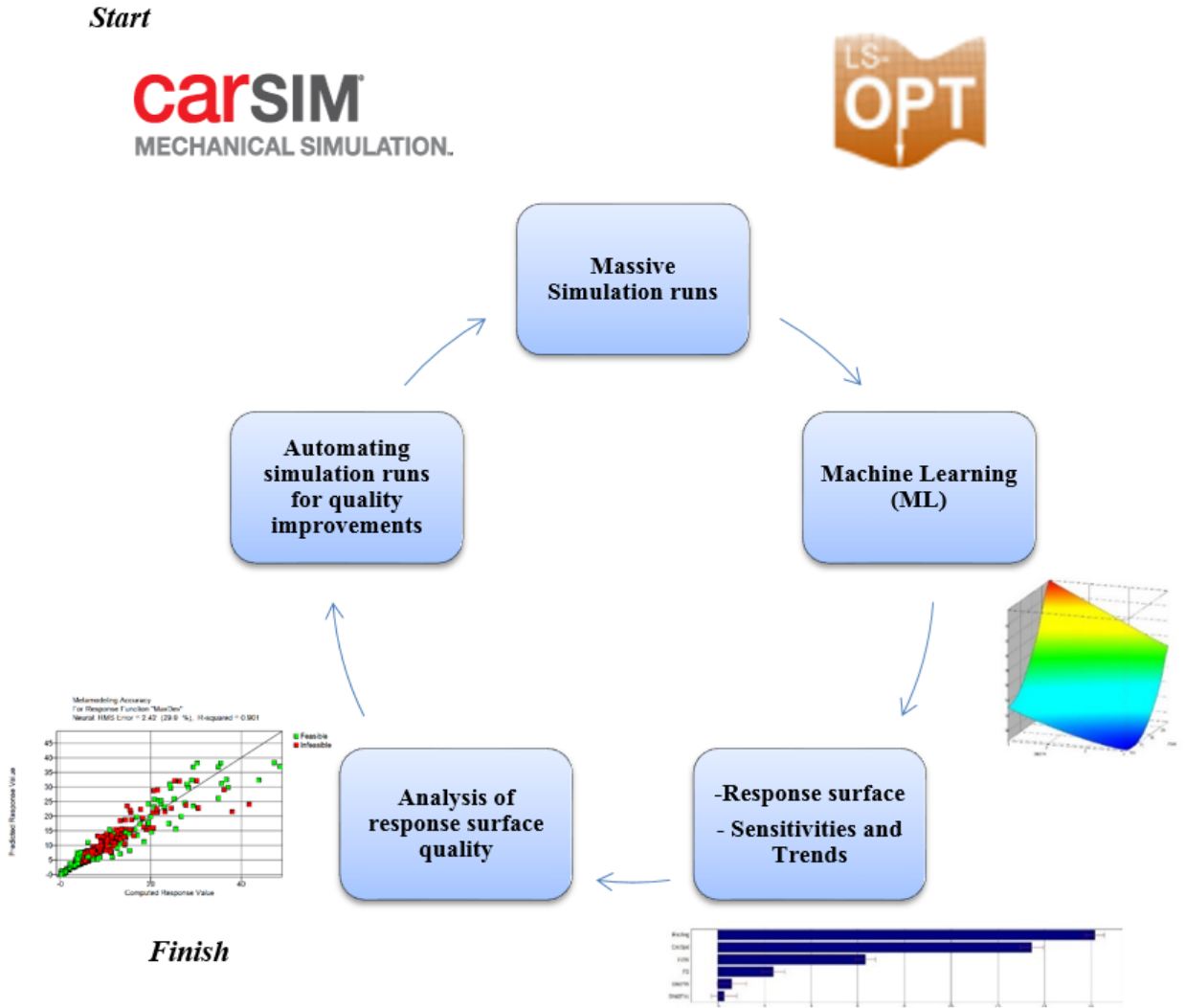



Figure 53. Data analytics: Recommended future work.

The proposed ML technology has several visionary features that advance highway safety models into an adaptable, more accurate and self-correcting realm. At the core of the technology is an open source ML architecture. The ML can be trained via feeding it with massive simulations from vehicle dynamics. These codes allow the use of almost any roadway and roadside features (roadway curvature, friction, shoulders, roadside slopes, and other features as well as vehicle class). Additionally, existing crash analysis such as NCHRP Project 17-22 and NCHRP Project 17-43 can be used to provide encroachment conditions such as encroachment speed and encroachment angle distributions. Moreover, current vehicle dynamics codes have connected vehicle simulation capabilities that allow the model to use these various technologies

to account for their response in creating a metric for a safety outcome. The recommended use of Monte Carlo method of analyzing the ML meta-models is based on a random selection of values and hence a risk-based outcome is presented, which is a much better presentation of a desired safety metrics.

REFERENCES

1. National Highway Traffic Safety Administration. "Rural/Urban Comparison of Traffic Fatalities." April 2017. <https://crashstats.nhtsa.dot.gov/Api/Public/ViewPublication/812393>. Accessed Jul. 31, 2017.
2. American Association of State Highway and Transportation Officials. *A Policy on Geometric Design of Highways and Streets*. Washington, DC. 2011.
3. American Association of State Highway and Transportation Officials. *Roadside Design Guide*. Washington, DC. 2011.
4. Viner, J. G. 1995. "Rollovers on Sideslopes and Ditches," *Accident Analysis & Prevention* 27(4): 483–491.
5. Gillespie, T. D. *Fundamentals of Vehicle Dynamics*. Thomas D. Gillespie. Warrendale, PA : Society of Automotive Engineers, [1992], 1992.
6. Brewer, M.A., et al. "Effects of Cross-Slope Break on Roadway Departure Recovery for Trucks on Horizontal Curves." vol. 2588, National Research Council, 01 Jan. 2016. Transportation Research Record.
7. Kim, J.-H., S. Hayakawa, T. Suzuki, K. Hayashi, S. Okuma, N. Tsuchida. "Modeling of Driver's Collision Avoidance Maneuver Base on Controller Switching Model." *IEEE Transactions on Systems, Man, and Cybernetics, Part B: Cybernetics*, 35 (6), 1131-1143. IEEE Systems, Man, and Cybernetics Society. New York, NY. 2005.
8. Allen, R. and Rosenthal, T., "Requirements for Vehicle Dynamics Simulation Models," SAE Technical Paper 940175, 1994, <https://doi.org/10.4271/940175>.
9. LS-OPT User's Manual Version 5.2, Livermore Software Technology Corporation, Livermore, 2015.
10. Mak, K., D. Sicking, B. Coon, and F. de Albuquerque, "Identification of vehicular impact conditions associated with serious ran-off-road crashes," Final Report, NCHRP Project 17-22, National Cooperative Highway Research Program, Transportation Research Board, Washington, D.C., May 2009. 
11. CarSim, Mechanical Simulation Corporation, <http://www.carsim.com>.
12. Karayiannis N.B., Venetsanopoulos A.N. (1993) Neural Network Architectures and Learning Schemes. In: Artificial Neural Networks. The Springer International Series in Engineering and Computer Science, vol 209. Springer, Boston, MA

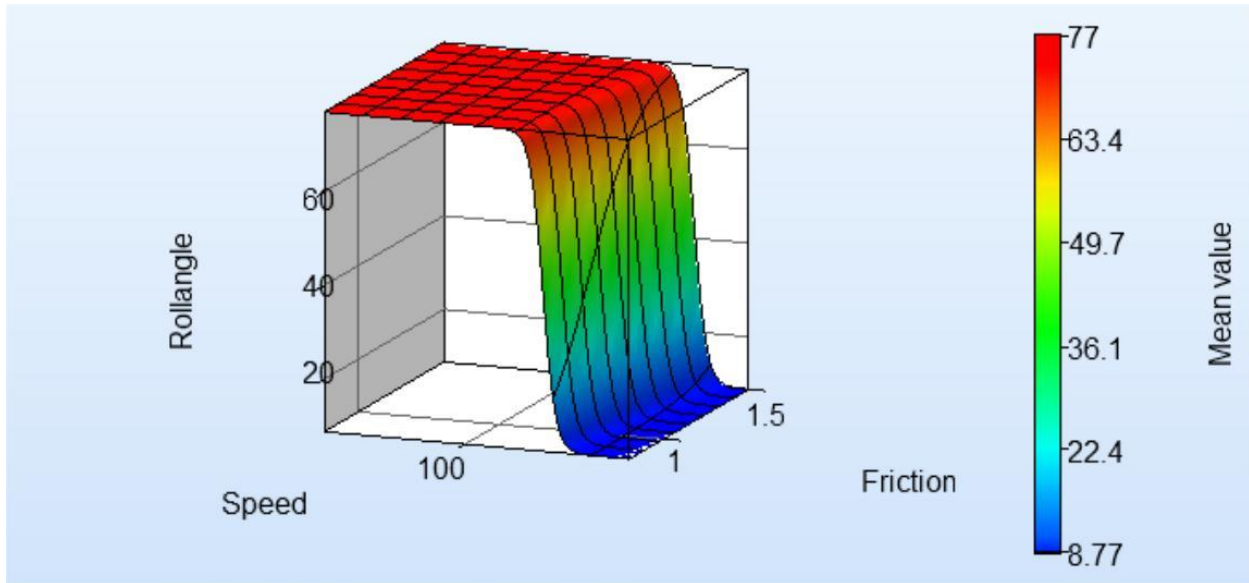
13. Metropolis, Nicholas, and S. Ulam. "The Monte Carlo Method." *Journal of the American Statistical Association*, vol. 44, no. 247, 1949, pp. 335–341. *JSTOR*, JSTOR, www.jstor.org/stable/2280232.
14. Fishman G.S. (1996) Introduction. In: Monte Carlo. Springer Series in Operations Research. Springer, New York, NY
15. Ferdous M.R., "Placement of Traffic Barriers on Roadside and Median Slopes. Department of Civil Engineering," Texas A&M University, College Station, TX, 2011.
16. LS-DYNA User Manual Version 10.0, Livermore Software Technology Corporation, Livermore, 2017.

SUPPLEMENTAL SOURCES CONSULTED

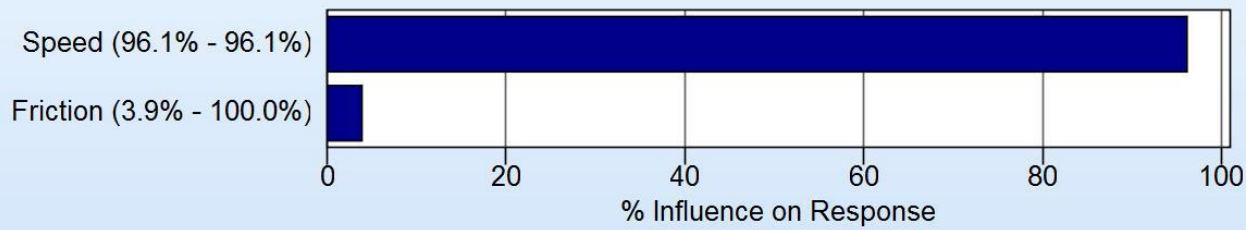
- Kahane, C.J. 2012. "Relationships between fatality risk, mass, and footprint in model year 2000-2007 passenger cars and LTVs — final report." Report no. DOT HS-811-665. Washington, DC: National Highway Traffic Safety Administration.
- Deutermann, W. 2002. "Characteristics of fatal rollover crashes." Report no. DOT HS-809-438. Washington, DC: National Highway Traffic Safety Administration.
- Lave, Charles, and Patrick Elias. "Did the 65 mph speed limit save lives?." *Accident analysis and prevention* 26.1 (1994):49-62. Web.
- Farmer, Charles M, Richard A Retting, and Adrian K Lund. "Changes in motor vehicle occupant fatalities after repeal of the national maximum speed limit." *Accident analysis and prevention* 31.5 (1999):537-543. Web.
- Renski, Henry, Asad Khattak, and Forrest Council. "Effect of Speed Limit Increases on Crash Injury Severity: Analysis of Single-Vehicle Crashes on North Carolina Interstate Highways." *Transportation research record* 1665(1999):100-108. Web.
- Aarts, L., and van Schagen, I., "Driving speed and the risk of road crashes: A review." *Accident analysis and prevention* 38.2 (2006):215-224. Web.
- Alvarez, A., et al. "Vehicle Dynamics Simulation at Commercial Vehicle Development." SAE technical paper series *Vehicle Dynamics Simulation at Commercial Vehicle Development*. 1. Web.
- Garcia, R., October 2014, *Roadway Design Manual*.
<http://onlinemanuals.txdot.gov/txdotmanuals/rdw/rdw.pdf>. Accessed July 31, 2017.

- Kimley-Horn and Associates, May 2013, "Traffic Safety Evaluation for SR 147 MP 7 to MP 14." <http://www.zerofatalitiesnv.com/wp-content/uploads/2015/10/SR-147-Lake-Mead-Report.pdf>. Accessed July 31, 2017.
- Whitehead, R., et al. "A Study of the Effect of Various Vehicle Properties on Rollover Propensity." *SAE Conference Proceedings P*, vol. 386, 2004, pp. 205-212.
- Zhen-Feng Wang, et al. "Influence of Road Excitation and Steering Wheel Input on Vehicle System Dynamic Responses." *Applied Sciences (2076-3417)*, vol. 7, no. 6, June 2017, pp. 1-23.
- Rice, R.S. and F. Dell'Amico. "An Experimental Study of Automobile Driver Characteristics and Capabilities." Calspan Report No. ZS-5208-K-1. Calspan Corporation. Buffalo, NY. March 1974.
- Maeda, T., N. Irie, K. Hidaka, and H. Nishimura. "Performance of Driver-Vehicle System in Emergency Avoidance." International Automotive Engineering Congress and Exposition. Society of Automotive Engineers. Detroit, MI. 1977.
- Huston, R.L. and F.A. Kelly. "Another Look at the Static Stability Factor (SSF) in Predicting Vehicle Rollover." *International Journal of Crashworthiness*, vol. 19, no. 6, 01 Nov. 2014, p. 567-575. EBSCOhost, doi:10.1080/13588265.2014.919730.
- Viano, D. C., and Parenteau, C., *Occupant and Vehicle Responses in Rollovers*. Warrendale, PA, Society of Automotive Engineers, 2004.
- NCHRP Project 17-11, "Recovery-Area Distance Relationships for Highway Roadsides," ongoing study conducted by Texas Transportation Institute, Texas A&M University System, College Station, Texas.
- Mak, K. K., and D. L. Sicking, "Rollover Caused by Concrete Safety Shaped Barrier," Final report, prepared for Federal Highway Administration, U. S. Department of Transportation, Washington, D.C., September 1988.

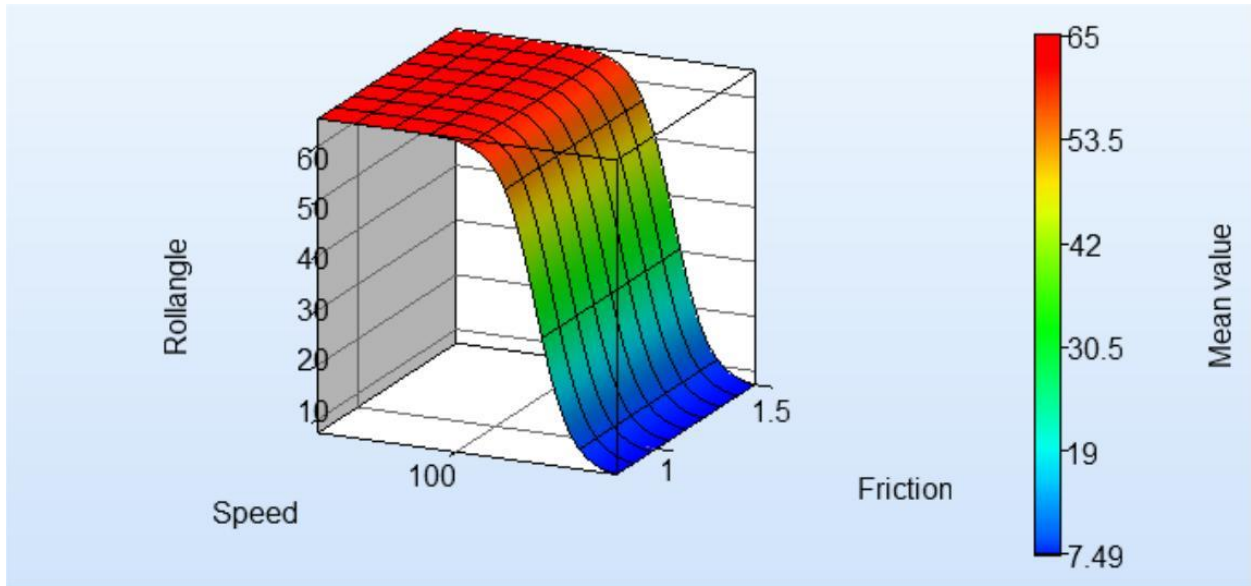
APPENDIX: META-MODELS CASES



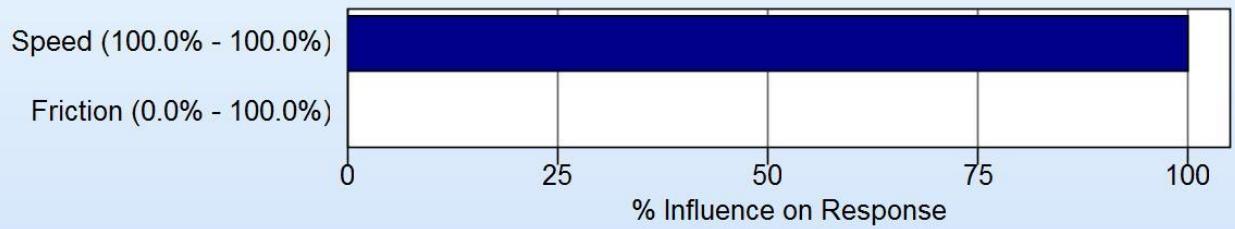
Global Sensitivities Plot for Rollangle
Mean = 61.3045, Total variance = 729.029, Noise variance = 7.93493e-008



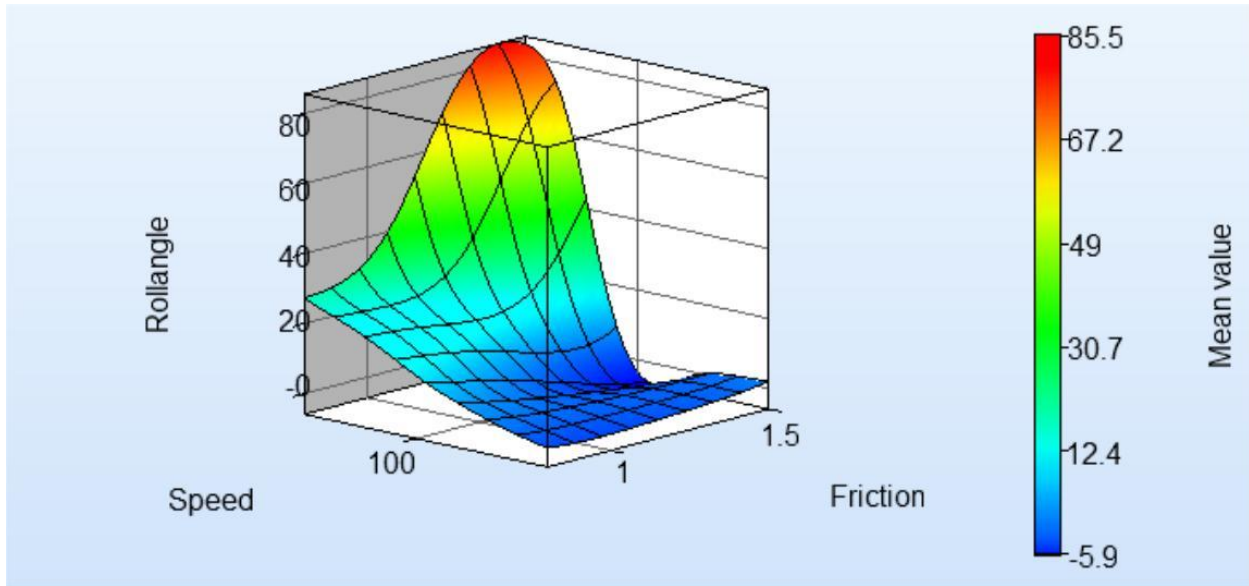
Full-size SUV traveling on a straight road with a 3:1 side-slope at a 25° encroachment angle.



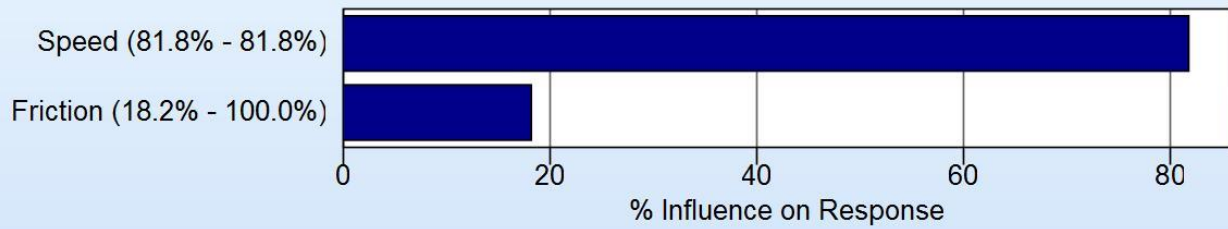
Global Sensitivities Plot for Rollangle
 Mean = 49.1902, Total variance = 472.949, Noise variance = 0.00012074



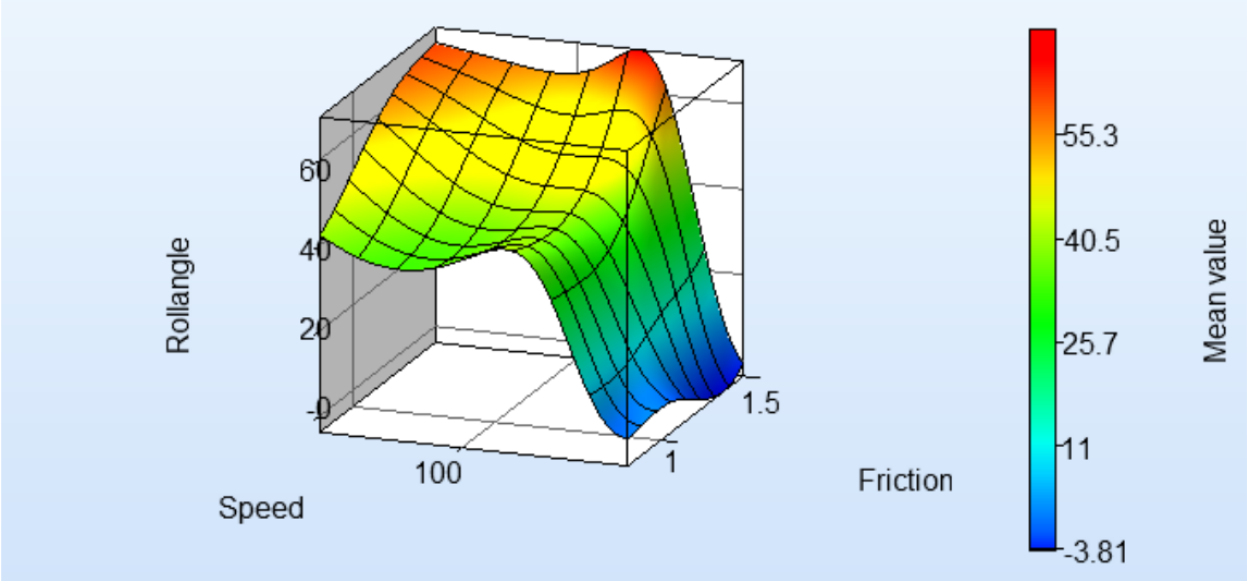
Class C hatchback traveling on a curved road with a 4:1 side-slope at a 25° encroachment angle.



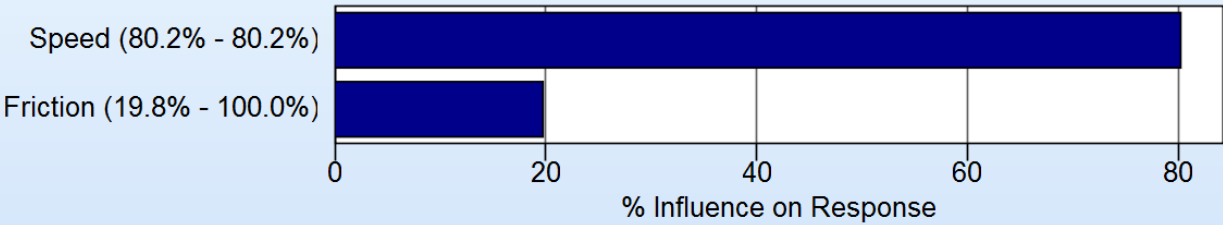
Global Sensitivities Plot for Rollangle
 Mean = 12.229, Total variance = 333.06, Noise variance = 196.73



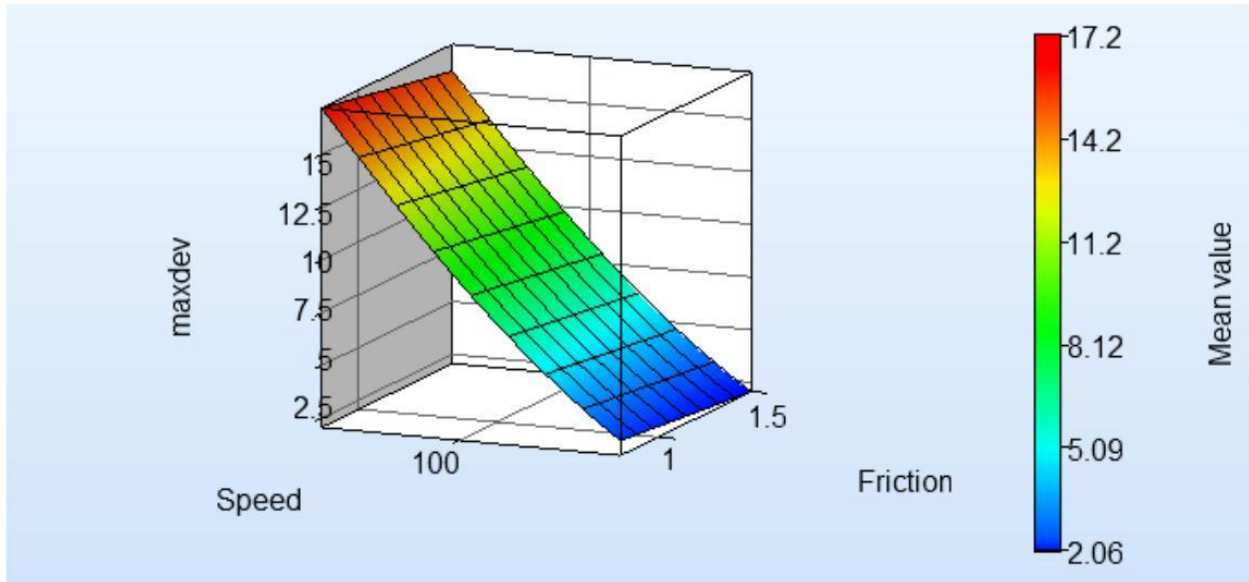
Full size pickup truck traveling on a straight road with a 4:1 side-slope at a 15° encroachment angle.



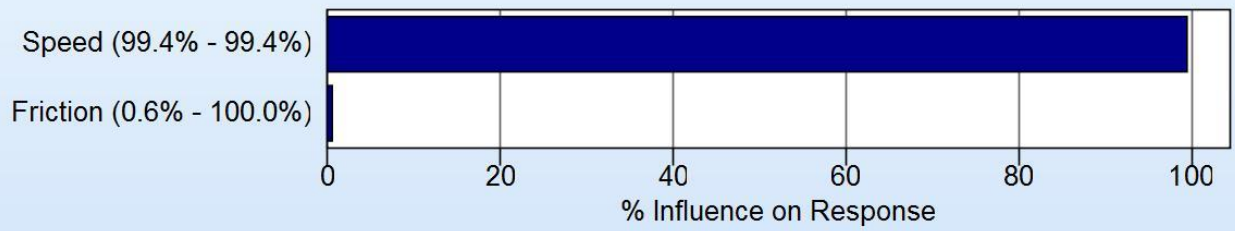
Global Sensitivities Plot for Rollangle
 Mean = 40.1243, Total variance = 269.82, Noise variance = 14.1592



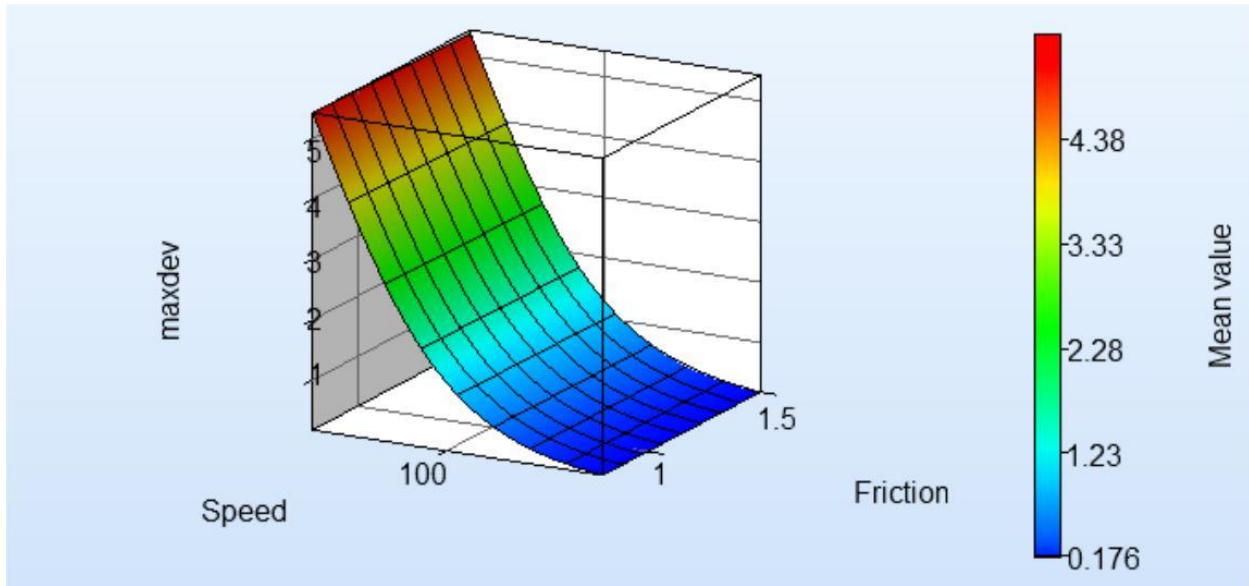
Sedan traveling on a straight road with a 3:1 side-slope at a 15° encroachment angle.



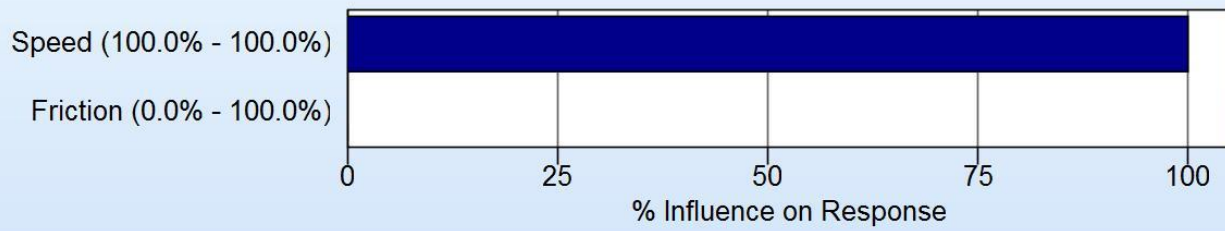
Global Sensitivities Plot for maxdev
 Mean = 8.78146, Total variance = 16.9808, Noise variance = 0.000731363



Class C hatchback traveling on a curved road with a 3:1 side-slope at a 25° encroachment angle.



Global Sensitivities Plot for maxdev
 Mean = 1.70025, Total variance = 2.29976, Noise variance = 7.0409e-010



Full-size SUV traveling on a straight road with a 4:1 side-slope at a 15° encroachment angle.